# DEVELOPMENT OF A BATTERY OPERATED ELECTROSTATIC SPRAYER

**by**

**DIPAK S. KHATAWKAR**


**DEPARTMENT OF FARM MACHINERY AND POWER ENGINEERING**

**KELAPPAJI COLLEGE OF AGRICULTURAL ENGINEERING AND TECHNOLOGY, TAVANUR – 679 573**

**KERALA, INDIA**

**2019**

# DEVELOPMENT OF A BATTERY OPERATED ELECTROSTATIC SPRAYER

**by**

**DIPAK S. KHATAWKAR**

**(2016-28-002)**

**THESIS**

**Submitted in partial fulfilment of the requirement for the degree of**

**DOCTOR OF PHILOSOPHY**
**IN**
**AGRICULTURAL ENGINEERING**

**(Farm Power and Machinery)**

**Faculty of Agricultural Engineering and Technology**
**Kerala Agricultural University**


**DEPARTMENT OF FARM MACHINERY AND POWER ENGINEERING**

**KELAPPAJI COLLEGE OF AGRICULTURAL ENGINEERING AND TECHNOLOGY, TAVANUR – 679 573**

**KERALA, INDIA**

**2019**

# DECLARATION

I hereby declare that this thesis entitled **'DEVELOPMENT OF A BATTERY OPERATED ELECTROSTATIC SPRAYER'** is a bonafide record of research work done by me during the course of research and that the thesis has not previously formed the basis for the award to me of any degree, diploma, fellowship or associateship or other similar title of any other University or Society.

**DIPAK S. KHATAWKAR**
**(2016-28-002)**

Place: Tavanur
Date: 03.10.2019

# CERTIFICATE

Certified that this thesis entitled **'DEVELOPMENT OF A BATTERY OPERATED ELECTROSTATIC SPRAYER'** is a record of research work done independently by **Er. DIPAK S. KHATAWKAR (2016-28-002)** under my guidance and supervision and that it has not previously formed the basis for the award of any degree, diploma, fellowship or associateship to him.

**Dr. SHAJI JAMES P.**
Chairman, Advisory Committee,
Professor (FPME),
Agricultural Research Station, Mannuthy.

Place: Tavanur
Date: 03.10.2019

# CERTIFICATE

We undersigned, members of the advisory committee of **Er. DIPAK S. KHATAWKAR (2016-28-002)**, a candidate for the degree of Doctor of Philosophy in Agricultural Engineering, majoring in Farm Power and Machinery, agree that the thesis entitled **'DEVELOPMENT OF A BATTERY OPERATED ELECTROSTATIC SPRAYER'** may be submitted by Er. Dipak S. Khatawkar, in partial fulfilment of the requirement for the degree.

**Dr. SHAJI JAMES P.**
Chairman, Advisory Committee,
Professor (FPME),
Agricultural Research Station, Mannuthy.

**Dr. Dhalin D.**
**(Member)**
Assistant Professor,
Dept. of Agril. Engg. CoA, Vellayani,

**Dr. Jayan P. R.**
**(Member)**
Professor and Head,
Dept. of FMPE, KCAET, Tavanur.

**Dr. Berin Pathrose**
**(Member)**
Assistant Professor,
College of Horticulture, Vellanikkara

**Er. Shivaji K. P.**
**(Member)**
Assistant Professor,
Dept. of FMPE KCAET, Tavanur.

Date : 10.10.2019
Place : Tavanur

**External Examiner**

# ACKNOWLEDGEMENT

## ACKNOWLEDGEMENT

*With due respect, I record my gratitude and utmost indebtedness to* ***Dr. Shaji James P.****, Professor (Farm Power, Machinery and Energy), Agricultural Research Station – Mannuthy and Chairman of the Advisory Committee for his avuncular advice, guidance, encouragement and creative criticism during the course of this research work and in the preparation of the thesis. His unending support and attentiveness during the course of this research work was one of the greatest inspirational force behind my accomplishment.*

*It is my greatest pleasure to acknowledge the sincere guidance and valuable help rendered to me by* ***Dr. Sathian K. K.,*** *Dean, Kelappaji College of Agricultural Engineering and Technology, Tavanur.*

*I express my immense gratitude towards* ***Dr. Jayan P. R,*** *Professor and Head, Department of Farm Machinery and Power Engineering, Kelappaji College of Agricultural Engineering and Technology, Tavanur and member of Advisory Committee for his valuable critics and help during preparation of the thesis.*

*It is my privilege to express heartfelt thanks to* ***Dr. Dhalin D.,*** *Assistant Professor, Department of Agricultural Engineering, College of Agriculture, Vellayani and member of Advisory Committee for his excellent advice and help during each step of this research work as well as ingenious criticism during preparation of the thesis.*

*I express my sincere thanks to* ***Dr. Berin Pathrose,*** *Assistant Professor, Department of Plant Pathology, College of Horticulture, Vellanikkara and member of Advisory Committee for his exceptional guidance and support during the phase of field performance evaluation of the developed prototype and analysis of the results as well as inventive criticism during preparation of the thesis.*

*It is my pleasure to express heartfelt reverence to* ***Er. Shivaji K. P.*** *Assistant Professor, Department of Farm of Farm Machinery and Power*

*Engineering, Kelappaji College of Agricultural Engineering and Technology, Tavanur and member of Advisory Committee for his kind guidance and help during this research work.*

*The award of* ***Senior Research Fellowship (SRF)*** *for this research work by* ***CSIR, New Delhi*** *is also greatly acknowledged.*

*I am truly grateful towards my post graduate colleagues Er. Basavaraj Patil, Naveen B. V., Er. Venkata Reddy, Er. Uday Bhanu Prakash, Er. Chetan, Er. Venkatsai, Er. Sai Krishna and Er. Majeed Pasha for their help at every step of this research work.*

*It is my enormous pleasure to recall the kind help and support extended to me by junior colleagues Er. Sandeep, Er. Shivendra, Er. Amit, Er. Rohit and Praneet during this research work.*

*I also extend my sincere thanks to my near and dear ones for their warm blessings and unfailing support which enabled me to have everything at reach.*

*Above all, I bow my head to* ***The God Almighty****, whose blessings filled me with all the power to bring this work to the success.*

*At last but not the least, I am short of words to express my gratitude towards my beloved parents* ***Mr. Suresh N. Khatawkar*** *and* ***Mrs. Kalpana S. Khatawkar*** *as well as my beloved elder sisters* ***Mrs. Neha Namit Pandharkame*** *and* ***Miss Tejashri S. Khatawkar*** *for their endless love, blessings, inspiration and such a great support.*

*Dipak S. Khatawkar*

# ***DEDICATION***

*This research work is dedicated to my guide* ***Prof. Shaji James P.*** *and* ***my beloved parents****, who sacrificed greatly to bring me up to this level of success.*

# LIST OF TABLES

# LIST OF FIGURES

# SYMBOLS AND ABBREVIATIONS

| | | |
|---|---|---|
| $\alpha$ | : | Alpha, Level of significance |
| @ | : | At the rate of |
| $^{o}$ | : | Degree |
| $^{o}C$ | : | Degree Celsius |
| $\varepsilon_0$ | : | Permittivity of air |
| $\kappa$ | : | Dielectric constant of spray liquid |
| $\varrho$ | : | Resistivity of spray liquid |
| $\Gamma$ | : | Surface tension of spray liquid |
| $\tau$ | : | Charge transfer time |
| $\tau_f$ | : | Droplet formation time |
| % | : | Percentage |
| $\pm$ | : | plus or minus |
| $\mu A$ | : | micro ampere |
| $\mu C$ | : | micro coulomb |
| $\mu C.kg^{-1}$ | : | micro coulomb per kilogram |
| $\mu F$ | : | micro farads |
| $\mu g\text{-}mL^{-1}$ | : | micro gram per milli litre |

| | | |
|---|---|---|
| µm | : | micro meter |
| µs | : | micro second |
| µV | : | micro volt |
| Ω-m | : | ohm meter |
| A | : | Ampere |
| ABS | : | Acrylonitrile Butadiene Styrene |
| AC | : | Alternating Current |
| Ah | : | Ampere-hour |
| a. i. | : | Active Ingredient |
| ANOVA | : | Analysis of variance |
| AOAC | : | Association of Analytical Communities |
| AP | : | Action Potential |
| AS | : | Ideal deposition |
| $A_s$ | : | Spot area |
| BMS | : | Battery Management System |
| C | : | Coulomb |
| CCD | : | Charge Coupled Device Camera |
| $mC.kg^{-1}$ | : | milli coulomb per kilogram |
| $(CH_3)_2CO$ | : | Acetone |

| | | |
|---|---|---|
| CMR | : | Charge to Mass Ratio |
| $CMR_{theoretic}$ | : | Theoretical Charge to Mass Ratio |
| $CMR_{Rayleigh\ limit}$ | : | Charge to Mass Ratio at Rayleigh charge limit |
| cm | : | centimeter |
| $cm^3$ | : | cubic centimeter |
| CRD | : | Completely Randomized Design |
| CRT | : | Cathode Ray Tube |
| C-W | : | Cockroft-Walton |
| CWVM | : | Cockroft-Walton Voltage Multiplier |
| DC | : | Direct Current |
| DMM | : | Digital Multimeter |
| EHD | : | Electro-Hydro dynamics |
| EIC | : | Electrostatic Induction Charging |
| ESS | : | Electrostatic Spraying Systems |
| Govt. | : | Government |
| HV | : | High Voltage |
| HVDC | : | High Voltage Direct Current |
| HP | : | Horse Power |
| IC | : | Integrated Circuit |

| | | |
|---|---|---|
| kPa | : | kilo-Pascal |
| HP | : | Horse Power |
| IC | : | Integrated Circuit |
| kPa | : | kilo-Pascal |
| kV | : | kilo-volt |
| LAI | : | Leaf Area Index |
| LD-HP | : | Low Discharge High Pressure |
| lpm | : | Litre per minute |
| $m^3$ | : | cubic meter |
| MΩ | : | Mega-ohm |
| mA | : | milli ampere |
| mm | : | millimeter |
| NMD | : | Number median diameter |
| No. | : | Number |
| ppm | : | parts per million |
| SS | : | Stainless steel |
| VMD | : | Volume mean diameter |
| VP | : | Variation Potential |
| WSP | : | Water Sensitive Paper |

# CONTENTS

# INTRODUCTION

# CHAPTER I

# INTRODUCTION

Plant protection is inevitable in agriculture for its economic sustainability, produce food at an affordable cost and for maintaining adequate food supply for the ever increasing population. Without pest and disease management, crop losses could be as high as 50 per cent for field crops and 100 per cent for fruit crops and greenhouse ornamentals (Oerke, 2006). In India, annual agricultural production losses due to pests were estimated to be 42.66 million USD (Sushil, 2016).

Pest and disease management in commercial agriculture is mostly achieved by application of chemical in various forms like spray, dust and fog. Majority of these chemicals are generally applied through aqueous spray formulations. Though, chemical pesticides are well recognized for their biological efficacy in the pest and disease control, their adverse consequences on the environment (mainly soil and water resources) is a major concern. Moreover, the presence of residual chemical contents in the agricultural products is raising many questions from the perspective of human health.

According to statistical database (2019) of the Directorate of Plant Protection, Quarantine and Storage (DPPQS), Ministry of Agriculture and Farmers Welfare, Govt. of India, the annual pesticide consumption in India has increased tremendously by 41.77 per cent in the last decade. The total plant protection chemical consumption reported during year 2017-18 was 62183 MT compared to 43860 MT during 2008-09. Maharashtra (15568 MT) and Uttar Pradesh (10824 MT) were the top most pesticide consuming states contributed 42.44 per cent of the total pesticide consumption during 2017-18. Especially, Kerala state has shown an overwhelming 4 folds increment in the pesticide usage from 2008-09 (273 MT) to 2017-18 (1067 MT).

On the other hand, demand for plant protection machinery in India is increasing every year. In India, the knapsack sprayers are the most popular and versatile pesticide application equipment because of their simplicity, ease of

operation and low cost. However, these sprayers must overcome the problems of poor deposition efficiency, uneven distribution and less penetration into the plant canopies to enhance pesticide use efficiency. Environmental contamination associated with the pesticides arising from over application and off-target movement of toxic pesticides through an inefficient spray application is the another matter of global concern.

Recently, the climate change induced occurrences of pest outbreaks, especially of sucking insects have been on the rise in many parts of our country. One of the major problem being faced in vegetable cultivation is the invasive pest called Neotropical solanum whitefly (*Aleurothrixus trachoides*) and is spreading fast in South India (Sundararaj, 2018). The peculiarity of the pest was its leaf underneath habitat on the host crop mainly brinjal, chilli and tomato. The conventional application methods are capable of depositing the pesticide on the top surface of plant leaves only and found to be obsolete in controlling invasive pests like whitefly. Whereas the electrostatic spray technique is well known for its wrap-around effect which could effectively deposit the pesticide spray on the leaf above as well as leaf underneath surfaces where the target pest inhabits.

The Indian agriculture census (Phase-I) 2015-16 revealed that the total number of agricultural land holdings have increased from 138.35 million in 2010-11 to 146.45 million in 2015-16 resulting an increase of 5.86 per cent. On contrary, the total cultivated area in the country has decreased from 159.59 million ha in 2010-11 to 157.82 million ha in 2015-16 showing a decrease of 1.11 per cent. The small (< 1.00 ha) and marginal (≥ 1.00 and < 2.00 ha) land holdings together constituted 86.08 per cent of the total holdings in 2015-16 against 85.01 per cent in 2010-11. The semi-medium (≥ 2.00 and < 4.00 ha) and medium (≥ 4.00 and < 10.00) holdings in 2015-16 were only 13.35 per cent with 43.99 per cent operated area. The corresponding figures for 2010-11 census were 14.29 per cent and 44.82 per cent. The large holdings (≥ 10.00 ha) were merely 0.57 per cent of total number of holdings in 2015-16 and had a share of 9.07 per cent in the operated area as against 0.70 per cent and 10.59 per cent respectively for 2010-11 census. As a

result, the average size of operational holding in India has dropped to 1.08 ha in 2015-16 as compared to 1.15 ha in 2010-11 (Anonymous, 2019).

Particularly in Kerala, the net cultivated area has declined to 1.36 million ha (2015-16) against 1.51 million ha in 2010-11. On the other hand, the total number of land holdings have increased by 11.02 per cent (7.58 million in 2015-16) compared to 6.83 million in 2010-11. This has resulted a sharp decline of 18.18 per cent in the average size of operational holding from 0.22 to 0.18 ha (Anonymous, 2019). It is evident that the per capita agricultural land holdings are being fragmented day by day.

The introduction of electrostatically charged spray for agricultural application can provide greater control of droplet transport with impending reduction in wastage (Lane and Law, 1982). The electrostatic spraying can increase the deposition efficiency by about 80 per cent with 50 per cent or lesser spray chemicals. At present, a number of electrostatic spraying systems are commercially available worldwide and mainly manufactured by US (ESS®-MaxCharge™), Italy (Martignani Inc.) and China (Henan Yugong Machinery Pvt. Ltd.) based companies. However, their high prices (above 1 lakh) make the marginal farmer community in India reluctant to own such a technologically advanced plant protection equipment due to its expensiveness. In our country, only a few attempts have been made so far in developing and testing indigenous electrostatic spraying systems. Moreover, the development of an affordable battery powered electrostatic sprayer will be an advantage to the Indian farmers especially the small and medium land holders, as it may conveniently be used even in remote areas by providing solar photo-voltaic charging facilities.

Particularly, the three methods which could be adopted to charge the airborne liquid particles were ‘Conduction charging’, ‘Corona charging’ and ‘Induction charging’. Conduction charging involves direct application of high voltage potential to the spray fluid by direct contact i.e. by conduction. Since this technique involves high voltage high power supply, the hazard of a lethal electric shock to the operator makes it redundant. Corona charging uses the corona

discharge field to charge the spray particles passing through it, which also has drawbacks of life hazard and may cause chemical changes to the subjected spray material. The method of 'Electrostatic Induction Charging' (EIC) generates non-contact charge induction on the spray fluid passing through the high voltage electrical field. As the high voltage electrode has no direct contact with the working fluid, the probabilities of receiving high voltage shock to the operator are negligible. Moreover, the accidental human contact with the high voltage electrode would not be leading any fatalities, since the low DC power output is well within safe limits. Thus, the electrostatic induction charging is considered as the best method for charging aqueous spray formulations for plant protection.

Hence, the development of a low cost battery operated air assisted electrostatic induction charging sprayer was envisaged with the following specific objectives:

1. To develop an electrostatic induction charging system compatible to a DC power source.
2. To develop a DC electric powered liquid atomizer suitable to a blower to aid electrostatic spraying.
3. To evaluate the performance of the developed system.

# REVIEW OF LITERATURE

# CHAPTER II

# REVIEW OF LITERATURE

In this chapter, a brief review of research works carried out in the context of the development and evaluation of electrostatic charging systems for agricultural sprays are presented.

## 2.1 ELECTROSTATIC CHARGING OF AGRICULTURAL SPRAY FORMULATIONS

Smith *et al.* (1977) conducted study on AC charging of agricultural sprays and its effectiveness. A controllable DC voltage supply unit and three different charging annuli were used with charging voltage stepped in 4.3, 8.2, 12.5 and 16.5 kV with frequency range of 1040 to 1975 Hz. The spray nozzle was operated at three constant pressures viz. 173, 276 and 380 kPa at three charging potentials of 0.8, 11.5 and 15 kV used in a square wave form. The 15 kV square wave form AC charging produced more number of small droplets under 50, 20 and 10 µm, so that the charge per droplet could be higher and droplet voltage was measured with Keithley 614B Electrometer which showed values in the range of 50 mV to 175 mV for charging voltage 5 kV to 15 kV.

Anantheswaran and Law (1979) developed an electrostatic spray charging nozzle for charging pesticide spray droplets by induction. The charging unit was operated by 12V DC battery, which gave an output voltage of -30 kV. For experimental analysis voltage given to the metal plate electrode varied from 0 to -30 kV, in steps of 10 kV. Dielectric barrier type precipitator made of polythene sheet stretched over a square plexi-glass was also evaluated. There was an accumulation of negative charges on its surface and later these charges repelled spray droplets downward towards the turf grass. The deposition was found to be increased significantly on increasing the inclination angle. In conjunction with the dielectric barrier, deposition increased by 3.6 folds compared to the uncharged spray.

Carlton and Bouse (1980) developed and evaluated an electrostatic spray charging spinning nozzle for aircraft. By regulating the motor voltage, the rotational speed of the spinner was varied which in turn altered the droplet size. Spray charging efficiency increased with increase in spinner speed and CMR about 2 x $10^{-2}$ C.$kg^{-1}$. The experiments showed that electrostatically charged spray deposition could exceed that of uncharged spray by 800 per cent.

Gupta *et al.* (1994) designed and developed a knapsack type electrostatic spinning disc sprayer. The charging system consisted of a 12 V dc wet cell rechargeable battery with a HVDC power supply (Model-C30, Venus Scientific Inc., NY). Field studies were conducted with 1.2 kV charging potential, 50 ml.$min^{-1}$ liquid flow rate and 2000 to 3000 rpm spinning disc speed. The results gave CMR from the charging system in the range of 1.0 to 1.2 mC.$kg^{-1}$ with 169 µm mean droplet size.

Luciana and Cramariuc (2009) conducted experiments on an electro-hydrodynamic (EHD) spray injector. The studies included direct injector conduction charging, direct charging through open electrode and charging by induction with insulated electrode and grounded injector. DC high voltages ranging from 0 to 6 kV was used to charge the spray particles with liquid flow rate between 0.1 to 0.4 ml·$s^{-1}$. A two-stage Faraday cage and collector were used to measure the cloud current. They found induction charging as the most efficient method which could give an optimum charge to mass ratio of 5 µC·$g^{-1}$ at 3 kV at a spray liquid flow rate of 0.3 ml·$s^{-1}$. They claimed that there were no electrical hazards or power loss with induction charging system.

Maynagh *et al.* (2009) evaluated an electrostatic induction charging sprayer fitted with ultrasonic (30 kHz) nozzle for various design parameters such as electrode radius, voltage level, air velocity and electrode placement. The tests were performed with varying flow rate (5 to 25 ml·$min^{-1}$), voltage levels (1.5 to 7 kV), airflow speeds, electrode radius (10 and 15 mm) and its horizontal position (1 to 10 mm) from nozzle tip. They found optimum CMR of 1.032 µC·$g^{-1}$ at 7 kV

voltage and 23 $m \cdot s^{-1}$airflow speed, when the electrode of radius 15 mm was placed 10 mm from the nozzle tip. The liquid flow rate was kept at 5 $ml \cdot min^{-1}$ to reduce electrode wetting.

Yu *et al.* (2011) developed an axial flow air assisted ultra-low volume electrostatic sprayer with high voltage (20 kV) corona charging device. The sprayer was evaluated in laboratory as well as in field for parameters like CMR corresponding to different voltage levels, droplet size, deposition uniformity and pest mortality against *micro-melalopha troglodyte fungi* on roadside forestry trees. Spraying was performed with charge as well as without charge on both sides of the row in a 10 km stretch. Performance of electrostatic spray reported in terms of pest mortality was observed to be higher (95.40 %) over non-electrostatic spray (74.80 %). The CMR value was observed to be 2.35 $mC \cdot kg^{-1}$ with 80.80 µm droplet size at a charging voltage of 20 kV.

Mamidi *et al.* (2012) developed an electrostatic hand pressure swirl nozzle knapsack sprayer for small crop growers and evaluated different parameters as electrode position, charge to mass ratio, spray deposition and effect of applied pressure on droplet size and breakup length. Twin hole swirl disc with 0.8 mm orifice and copper ring electrode connected to programmable 10W HVDC module (EMCO-F101) was used. The voltage ranged from 0 to 10 kV where as the placement of ring electrode was varied from 1 to 6 mm. A manual hand pressure knapsack pump with output pressure ranging from 0 to 2.82 $kg \cdot cm^{-2}$ was used to drive the swirl nozzle. Cloud current (A) and mass flow rate ($kg \cdot s^{-1}$) were measured at 2.11 $kg \cdot cm^{-2}$ pressure and 3.3 kV voltage from which they found the optimum CMR value and droplet size as 0.37 $mC \cdot kg^{-1}$ and 100 µm, respectively, when the electrode was placed at 4.5 mm from orifice.

Patel *et al.* (2015) developed and analyzed an air assisted electrostatic spray charging nozzle for agricultural pesticide application in liquid form. Experiments were conducted to assess the parameters viz. charge to mass ratio (CMR), spray pattern, uniformity of deposition and coverage by using Water

Sensitive Paper (WSP) method. Chargeability was tested with Faraday cage and digital multimeter under +20 kV High Voltage DC power supply. Plants were sprayed electrostatically as well as non-electrostatically under all other identical conditions with WSPs mounted on front and back side of leaves at random locations in canopy. After 20 minutes of spraying, WSP samples were collected and analyzed with IMAGE-J Scanner based system. Analysis showed that 2 to 3 times increase in leaf top deposition in electrostatic spray over non-electrostatic spraying whereas under leaf deposition enhanced by 4 to 5 times.

## 2.2 HIGH VOLTAGE GENERATION TECHNIQUES

Santelmann (1986) invented the method and apparatus for efficient high voltage generation by resonant fly-back transformer. He employed the high voltage, low-current, high impedance power source circuits i.e. CRT (Cathode Ray Tube) anode fly-back HV supply to improve the efficiency and reliability over a wide input voltage ranges. The other advantages included small size and lesser weight. He used 160 V DC power supply as a source and employed FET (Field Effect Transistor) for switching the input to the primary of CRT (Model - TL494, Make - Texas Instruments Inc.) fly-back transformer at a frequency of 15.75 kHz. The invented circuitry was capable of generating 24 kV output voltage using four-stage cascade voltage multiplier with the no load maximum output current of 24 µA.

Petersen (1989) invented the high power fly-back, variable input-output voltage, decoupled power supply circuit. The system consisted of input voltage regulators, three-phase isolated secondary transformer and high frequency transistors and was capable of generating lower or higher voltages than the source dc voltage. Transistor phase-out at variable angles on the secondary side made possible to vary the output power and also to use the secondary coils either in series or parallel topology as per the application requirements.

Howard (1989) invented the power supply having combined forward converter and flyback action for high efficiency conversion from low to high

voltage. In a switching power supply including a step-up transformer, wherein in each successive cycle of operation, during a first period of time a voltage pulse was applied across the primary winding. This induced the forward current in the secondary to flow through a shuttle capacitor and output capacitor connected in series with the secondary winding. The shuttle capacitor forwarded its charge, in order to charge the output capacitor in an immediately following second period of time. At the moment of termination of the voltage pulse across the primary winding, the flyback energy stored in the secondary winding charged the shuttle capacitor again for transfer to the output capacitor during the next cycle of operation. This novel technique gave the combined effect and improved the operating efficiency approaching to 90 per cent.

Kuriyama *et al.* (1997) developed a DC-DC high voltage converter using fly-back transformer. The 12 V DC battery as an input source was coupled to high frequency MOS (Metal Oxide Semi-conductor) switch. The primary of the fly-back transformer was energized when the switch turned ON and as soon as the switch turned OFF, the voltage across the primary fallen to zero, which caused a rapid high voltage spike across the secondary winding. The energy stored in the secondary during first half-cycle was taken up by the low pass filter circuit consisting of diode and capacitor which gave a stacking effect on successive pulse train of the fly-back. The invented circuit was portable, light-weight and boosted the voltage from 12 V DC to 100 V DC.

Copple (1999) patented the high efficiency dc step-up voltage converter, invented especially for aircraft primary power supply. The functional prototype consisted of a FET (Field Effect Transistor), a snubber circuit comprised of high voltage diode with a 1000 pF capacitor, a rectifier circuit and a centre tapped inductor. The inductor was energized using FET switched 28 V DC voltage, with which there was a primary voltage rise up to 149 V DC and snubber voltage to 121 V DC to get a constant output of 270 V DC.

Almuhanna and Maghirang (2010) developed and evaluated a charge measuring device for measuring the net CMR induced on the filter with an electrometer. The device was tested using different kinds of airborne particles viz. corn starch, sodium bicarbonate, positively and negatively charged water spray and uncharged water spray. The device consisted of two conducting enclosures, one enclosed and insulated from another. It was electrically connected to the electrometer input (Keithley Instru. Inc., OH) and having particle filter with backup metal screen (Filter type – AE, SKC84-PA). Calibration circuit was made and used to generate known charges with variable DC voltage supply (B.K. Precision Triple, Max Tech Instru. Corp., Chicago) with 1, 2, 3 V DC fixed voltages and three different capacitors of 0.1µf, 0.01µf and 0.001µf. System provided by 'Electrostatic Spraying Systems' (ESS, Watkinsville) was used to charge the water spray. The device had shown reliable readings with good repeatability. With induction charging, significantly large CMR values (i.e. -6.5 mC $kg^{-1}$ for negatively charged water spray and +7.2 mC $kg^{-1}$ for positively charged water spray) were observed by the developed CMR measuring device, which were close to CMR value (-6 mC $kg^{-1}$) specified by the manufacturer (ESS, Watkinsville, GA).

Dwivedi and Daigavane (2011) designed and established a 60 kV high voltage DC power generation unit using epoxy molded high voltage transformer and CWVM circuit. The high voltage transformer was capable of stepping up the input voltage of 230V AC into 5 kV with 50 mA maximum output current. The stepped up voltage from the transformer was applied across the 6-stage CWVM network (G10-FS 10 kV diodes and 110 nF capacitors), which amplified open circuit output voltage up to 59.7 kV measured using voltage divider of 600 MΩ.

In a novel solid state Marx generator topology, higher pulse repetition rate and higher efficiency were achieved by replacing the sphere gap assembly of conventional Marx generator with solid state conventional Marx generator with solid state switches like MOSFETs (Patel *et al.*, 2014). Each Marx stage included a capacitor or pulse forming network, and a high voltage switches. The proposed

topology was capable of controlling the output pulse frequency and magnitude without using any a pulse transformer. The operation and performance of the developed generator was evaluated with simulation results of PSCAD software. They verified that the proposed PSCAD circuit was capable to produce a reliable output and there was possibility for its use in practical application.

Sharma *et al.* (2015) designed and fabricated a low cost direct current high voltage generator circuit using Cockroft-Walton Voltage Multiplier (CWVM) based on Grienacher Voltage Doubler (GVD) circuit. The seven stage CWVM circuit was fabricated using 100 nF capacitors and supply mains of 230 V AC at 50 Hz, in order to get a dc high voltage of 10 kV output. They suggested that the ripple voltage significantly depended on the lowest end capacitor size and advised to incorporate identically sized capacitors in the multiplier circuit. They also designed and simulated the voltage multiplier circuit for 100 kV using the MATLAB software.

Waluyo *et al.* (2015) developed the miniature prototype of modified voltage multiplier in which, the regulated AC single phase supply of 0 - 220V at 50 Hz was fed to the low voltage isolating transformer. The transformer was used as isolation between the source circuit and the main rectifier and cascade multiplier circuit, which also functioned as a voltage step up transformer. The secondary voltage from transformer was then magnified by using the modified Cockroft-Walton cascade multiplier up to four stages. These voltages were measured and recorded by using a precise digital storage oscilloscope through a voltage divider circuit under load and no-load conditions.

Choi *et al.* (2016) designed, simulated and developed a high voltage module for electrostatic industrial painting robot. The high voltage module consisted of four major components *viz.* rectifier unit, DC-DC boost converter, a resonant high voltage converter and a cascade voltage multiplier network. The 220 V AC power supply was converted into DC voltage using diode rectifier and forwarded to the cascade CWVM network via boost converter and resonant high

voltage transformer. The simulations of the circuitry were made in order to generate sufficient high voltage i.e. 100 kV for electrostatic paint application onto a conductive target. On the basis of simulation results obtained from PSIM software, the experimental prototype was fabricated and verified for its desired functioning. The developed prototype was able to generate 100 kV DC (200 µA max.) at the end of twelve-stage cascade multiplier network at 25 kHz pulsed frequency.

Chaudhari *et al.* (2017) developed a diode-capacitor pump to amplify the input AC voltage to DC high voltage. The sinusoidal AC power supply of 230 V at 50 Hz was used as input to the four stage voltage multiplier circuit consisting of 1N4007 diodes and 100 µF 400 V capacitors. The developed circuit could amplify the voltage up to 1.8 kV DC and was measured using a digital multimeter via potential divider network having 10:1 attenuation ratio. The electronic system simulation was done using CIRCUITLAB software to predict the output voltage levels with respect to the stages of the multiplier circuit.

Changqi (2018) developed an isolated high voltage high frequency pulsed power converter for plasma generation. The input voltage of 300 V DC was fed to the DC-DC boost converter (45 kHz operating frequency) to gain the boosted dc voltage of 500 V. The dual SiC (silicon carbide) MOSFET based oscillator circuit was employed for booster voltage (500 V) switching with high frequency range of 500 kHz to 15 MHz. This high frequency switched voltage was applied across the resonant transformer and filter capacitor (200 nF) which gave the secondary high voltage pulsed output of -12 kV at 1.6 µs pulse duration.

## 2.3 MEASUREMENT OF CHARGED SPRAY CLOUD CURRENT

Law (1975) conducted study on charge measurement of airborne liquid particles and developed an electrostatic induction instrument for tracking and charge measurement of airborne particles. Water held in a variable head glass reservoir was allowed to slowly drip from the blunt end of the hypothermic needle at the rate of 1 drop per 5 seconds. A negative charge was imparted on droplets by

maintaining the needle at selected negative high voltage potential. A smooth induction electrode of 14 mm inner diameter and 3 mm thickness was positioned 6 mm below the tip of the needle. Keithley Model-600B (Keithley Instru. Inc., OH) electrometer was used for charge measurement, which was connected with a vertical deflection oscilloscope. A small Faraday's cage was positioned in a Teflon insulator at the base of the apparatus. The average charge (- q) was determined experimentally by collecting and counting the number of drops acquired by Faraday's cage. Particle charges as high as (-) $4.25\times10^{-10}$ and (-) $2.45\times10^{-10}$ coulombs were attained which corresponded to the CMR values of (-) $2.5\times10^{-5}$ C.kg$^{-1}$ and (-) $6\times10^{-10}$ C.kg$^{-1}$ at (-) 2.5 kV charging potential.

Bode and Bowen (1991) studied spray distribution and charge-mass ratio of electrostatically charged agricultural sprays. Spray droplet size was analyzed with Fleming Particle Size Analyzer at flow rates of 25, 50 and 75 ml.min$^{-1}$ and spinner disc speed of 2000, 3000, 4000 and 5000 rpm for both charged and uncharged particles. For charged application a positive (0.5 to 3.0 kV) high voltage (HV) potential from HV power supply Model H-30 Ferrant Int., N.Y. was used. An Aluminium cup with 75 cm diameter and 50 cm height was used to intercept all the spray. Charged spray imparted an equal and opposite charge on the cup and was measured by Keithley 614 Electrometer. The measured droplet size was in the range of 115 to 203 µm without charging and 109 to 183 µm with charging. At all conditions studied, droplet size reduced by 1 to 10 per cent due to charging. At peak level of charging from 0.5 kV to 3.0 kV, CMR was achieved in the range of 1.0 mC.kg$^{-1}$to 2.5 mC.kg$^{-1}$ at spinner speed 3000 to 4000 rpm. The spray deposition efficiency was in the range of 55 to 94 per cent and relative increase due to charging was observed to be 1.6 to 2.0 fold over uncharged spray.

Kihm *et al.* (1991) conducted both laboratory as well as field experiments on charged aircraft sprays in order to assess the deposition characteristics with DC motor driven serrated cup atomizers with induction charging ring electrode. Laboratory experimental set-up consisted of a 40 hp motor driven blower at 175 km.h$^{-1}$ air velocity, 55 mm diameter serrated cup atomizer with ring electrode

having outer diameter of 63 mm and thickness of 1.6 mm. The clearance between Aluminium ring electrode and spinning cup edge was 2 mm axially and 2.4 mm radially. Malvern 2600D Aerosol sizer and charge collector Faraday's cage comprising of needle, plane mesh and concave mesh collector were used for droplet size analysis and spray cloud charge measurement respectively. The field apparatus consisted of 60 m long movable stand with 40 WSPs and Cessna Model P206B agricultural aircraft with 10 atomizers at a cruising altitude of 3 m at 175 $km.h^{-1}$ speed. CMR values were observed at 9000 and 12000 spinner rpm as 0.008 $C.kg^{-1}$ and 0.01 $C.kg^{-1}$ respectively. Field experiments showed increase of 45 percent in charged spray. However, the droplet size with bipolarly charged spray showed higher value than uncharged one.

Carlton *et al.* (1995) investigated an electrostatic charging of aerial spray to determine its depositional advantages. The three spray charging treatments studied were bi-polar charging, low frequency alternating direct current charging and no charging, maintaining all other parameters identical. The spray deposition data was obtained by using the Leaf-wash method with fluorescence tracer. Statistical analysis indicated bi-polar charging to be superior over other two treatments, enhancing the spray deposits. The plant canopy penetration was achieved by horizontal drift forces. The research established that a level of Q/M = 2.64 $mC.kg^{-1}$ (CMR) was required to achieve expected improvement in spray deposition on targets.

Law and Scherm (2005) experimented on electrostatic application of plant disease bio-control agent against fungal infection on Blueberry. Electric characters of plant flower were determined in terms of resistance and resistivity. Application tests were carried for three setups as, hydraulic nozzle, electrostatic nozzle with charge-off and electrostatic nozzle with charge-on. The applied induction voltage for spray charging was set at 1.09 kV corresponding to a CMR of -7.8 $mC.kg^{-1}$. Electrostatic charged spray application showed 4.5 times more deposition on target than the other two methods.

Robson *et al.* (2013) conducted a study on charge to mass ratio and liquid deposition efficiency of electrostatic spraying method. ESS-MBP 4.0 induction charging sprayer model was used for the experiment and Faraday cage equipped with digital multi-meter was used for chargeability analysis. The sprayings were done at distances 0, 1, 2, 3, 4 and 5 m from the Faraday cage and charge readings were obtained from digital multimeter. Liquid discharge rate was measured with graduated cylinder with precision of 5 mL. The highest charge-to-mass ratio was found to be 4.11 $mC \cdot kg^{-1}$ for the closest distance and it gradually decreased to 1.38, 0.64, 0.31, 0.017 and 0.005 $mC \cdot kg^{-1}$ for the corresponding distances 1, 2, 3, 4 and 5 m respectively.

## 2.4 DETERMINATION OF SPRAY DROPLET SPECTRUM

Derksen and Bode (1986) conducted study on droplet size analysis to determine suitable sampling techniques and atomization characteristics of selected rotary atomizers. Measurements of drop size and the size distribution were done using OAP-260X Laser Imaging Probe by Particle Measuring Systems, Inc. The atomizers were operated at rotational speeds 1000 to 5000 rpm and flow rates from 0.07 to 2.95 L $min^{-1}$. The data was analyzed using computer program DROPSZ. The drift potential of the sprays produced by all atomizers at 2000 rpm was very low over entire range of flow rates and the resultant droplet size was in the range of 100 to 345 µm.

Krause and Derksen (1991) conducted comparative assessment of Hand-gun type electrostatic sprayer with Cold-fog sprayer in a production greenhouse. Spray distribution characteristics and penetration data were assessed and analyzed under cold-field emission scanning electron microscope (CFESEM) with energy dispersive X-ray analysis system. The spray treatment was done on 2 month old Fucshia spp. randomly placed in a commercial greenhouse. The spray applied by ESS's electrostatic sprayer was 9 litres, while it was 20 litres for the same greenhouse by cold-fog sprayer. Droplet size observed for the electrostatic sprayer was in the range of 5 – 80 µm and 50 – 200 µm for cold-fog sprayer respectively. As compared to the cold-fog sprayer, electrostatic sprayer showed more

deposition with better uniformity, better canopy penetration and uniform droplet size.

Almekinder *et al.* (1992) investigated spray deposition patterns of an electrostatic atomizer, primarily on electrostatic and gravitational forces for transportation and subsequent deposition. The wind-tunnel experiment was conducted for electrostatically charged sprays on artificial plants. 'TotalStat' electrostatic atomizer was used for charged spray application and two aluminium bars (grounded) 50 cm long and 2 cm O.D. were placed along each side of the atomizer to intensify electric field. The air pressure was maintained at 70 kPa and droplet size was measured with the help of Malvern 2600C Particle size analyzer with 300 mm lens. The charge to mass ratio was obtained from constructed Faraday's cage consisting of two metal pans and concentric rings. Spray cloud current was measured with Keithley Electrometer (Model-220 equipped with decade shunt). Charged spray applications were conducted with three charging voltages as 20, 25, 30 kV and resulting CMR was observed in the range of 0.4 to 8.0 $mC.kg^{-1}$. WSPs were used for studying deposition density and deposition pattern analyzed with microscope and calculated by software program FLUENT. The results showed that, CMR decreased with increase in droplet size (VMD) and liquid flow rate. The optimum droplet size was observed in the range of 100 to 278 µm.

Bouse (1994) analyzed the droplet size for different types of aerial spray nozzles in an air-stream to simulate the operation on an aircraft. A laser imaging spray droplet spectrometer probe was used to measure the droplet size and determined the effects of spray pressure, air velocity and nozzle orientation on droplet size for solid stream, disc core, hollow cone, swirl type hollow cone, elliptical orifice fan type and deflector fan type nozzles. He concluded that, the spray pressure for solid stream nozzles oriented to the air-stream reduced the relative velocity and increased the droplet size.

Sidahmed (1996a) developed theory of predicting size and velocity of droplets from pressure nozzles. It was postulated that atomization can be explained by energy balance equation for small mass 'Δm' of liquid separated from liquid sheet into a single droplet. When the viscosity is negligible, the minimum droplet size diameter ($df_{min}$) is associated with the Weber's number ($N_{we}$) and Bond's number ($N_{bo}$). Whereas, if the surface tension is negligible $df_{min}$ is associated with Reynold's number ($N_{re}$) and $df_{max}$ is associated with '$N_{bo} \times N_{re}/N_{we}$'.

Sidahmed (1996b) developed a mathematical model predicting the droplet size (D) from the flat liquid sheet with velocity ($U_L$) sprayed in an air-stream of velocity ($U_A$). Two empirical equations were developed, when $U_L$ was constant as well as $U_A$ was variable at a water spray pressure 276 kPa. The equation was represented by a regression line with a coefficient of determination $R^2$ of 0.9977 and a standard error of estimate (SEE) of 8.89.

For constant $U_L$ and varying $U_A$,

$$D = D_{max} e^{|1-\frac{1}{U}|^n Ln\,(\frac{Do}{Dmax})}$$

For constant $U_A$ and varying $U_L$,

$$D = D_{max} e^{|1-\frac{1}{U}|^m Ln\,(D_{Lo}/Dmax)}$$

The results showed good fit between experimental data and developed equations.

Johannama *et al.* (1999) conducted experiments on a two fluid concentric internal mixing induction charging nozzle suitable for electrostatic spraying. Droplet size measurement was done with the help of Malvern 2600 Laser Scattering instrument at horizontal as well as vertical traverse. Volume Median Diameters were determined for both charged and uncharged sprays. The results showed larger VMD in charged spray as compared to uncharged one, at three distinct operating pressures 0.14, 0.21 and 0.28 MPa and at spray liquid velocity 3 $m.s^{-1}$ and air velocity 30 $m.s^{-1}$. For charged sprays VMD obtained was in the

range of 40 to 75 µm, while for uncharged spray it was in between 12 to 32 µm. The experiment also confirmed that there was a negative pressure created near centre of the nozzle which siphoned out spray liquid and helped for atomization too.

Fritz *et al.* (2009) evaluated a series of flat fan spray nozzles at different speeds and pressure combinations in a laboratory to study the deposition and droplet sizing characterization. The nozzle operating pressure was regulated and could be varied between 0 to 830 kPa at a nozzle traverse speed between 0.5 to 7.0 $m.s^{-1}$. A photoelectric Sensor system was used for positioning of nozzle and speed calculations. A three-way solenoid valve and photorefractive micro-sensor controlled the traverse of the nozzle. Desktop computer with CIO-DIO24-CTR3 interface card (Norton, Mass.) was used to control spray table operation. Depositional characteristics were evaluated using WSPs (Spraying Systems, Wheaton, Ill.) of 26 x 76 mm size arranged on a suspended table surface. The treated WSPs were then scanned under Droplet-ScanR (Version 2.2) software to determine droplet spectra (VMD and NMD). The results showed that there was increase in the droplet size (from 249 µm to 602 µm VMD) at higher application rates due to overlapping in the range of 47 – 87 per cent.

## 2.5 DEPOSITIONAL PHYSIOGNOMIES OF ELECTROSTATICALLY CHARGED SPRAYS

Law and Michael (1981) conducted chargeability evaluation in laboratory with a field sprayer simulator, which dispensed charged spray as it passed over stationary plants. The plant morphologies tested were mature cabbage, broccoli, mature cotton plants and corn plants. Three embedded-electrode spray charging nozzles were used for evaluation with 73 $mL.min^{-1}$ flow rate per nozzle, which corresponded to 9.4 L $ha^{-1}$. The area density values of tracer particles deposited on foliar target was observed between 150 to 200 $ng.cm^{-2}$, with cloud current ranging from 6 to 8 µA for electrostatic sprayer. The depositional density for conventional sprayer was observed in the range of 50 to 75 $ng.cm^{-2}$ only.

Lake and Merchant (1984) conducted wind tunnel experiments for the development of a mathematical model for spray deposition in barley crop with an electrostatic sprayer. They reported that charging increased deposits on vertical target and tended to decrease deposits on upper surface of horizontal targets. Both the effects were significant with the smaller nozzles and was independent of nozzle height.

Law and Cooper (1988) investigated on mass transfer of fluorescent tracer onto front and back sides of the target deployed through a large scale grid. Mass transfer was determined for comparison between charged and uncharged spray from air-atomizing electrostatic nozzles and conventional hydraulic nozzles. Depending on target location, electrostatically charged spray achieved higher deposition (1.5 to 2.4 fold over uncharged spray). The highest electro-deposition benefit was achieved on target back surfaces. Deposition of charged droplets did not surpass that achieved with 370 µm VMD droplets from conventional hydraulic orchard spraying nozzles.

Gupta *et al.* (1989) conducted experiments on a prototype of hand held electrostatic spray charging unit with spinning disc atomizer. Charging system consisted of Venus C-30 power supply unit having maximum output of 3 kV and 500 µA current with 5 to 12 V DC input. The spray liquid used was deionized water with 2 g $L^{-1}$ of fluorescent tracer (Fluorescent Sodium). The standard solvent of 2 per cent ethanol was used to wash-off the tracer from targets. Air gap of 1.8 mm was kept between spinning disc and Aluminium ring electrode. A two-fold increase in deposition was found with charged spray than compared to uncharged one.

Khadir *et al.* (1994) conducted studies on spray penetration through plant canopy and deposition characteristics of an air-jet assisted charged spray in wind tunnel. Air-jets with velocities of 0, 10, 13 and 16 $m.s^{-1}$ through a long 5.1 cm wide slot were used with 119 µm charged sprays. 'TotalStat' electrostatic atomizer was used to atomize the spray with 36 kV voltage potential. The charged

spray conveyed with an air-jet velocity of 16 $m.s^{-1}$, deposited significantly more spray on the targets than the charged spray without air assistance.

Wang *et al.* (1995) investigated the effects of operating pressure and nozzle height on uniformity of spray distribution pattern under laboratory conditions using five types of 'TeeJetR 11004' nozzles. Nozzles were operated over three different heights (45.7 cm, 38.1 cm and 30.5 cm) and three different operating pressures (138 kPa, 276 kPa and 414 kPa). The results showed that effect of nozzle height on distribution uniformity was significant for nozzle height 30.5 cm to 45.7 cm. The results seemed to agree with manufacturer's recommended nozzle heights i.e. 38.1 cm to 45.7 cm with test data. However, effect of operating pressure was found to be insignificant on distribution uniformity.

Laryea and No (2002) investigated the spray characteristics of charge injected electrostatic pressure swirl nozzles for oil burner for agricultural product drying. Experiments were conducted with direct nozzle charging of hydrocarbon fuel with negative polarity. A point sharpened tungsten wire with 1.0 mm diameter was used as an electrode and placed concentrically inside fuel supply pipe. Fuel injection pressures ranging between 0.7 to 0.9 MPa with flow rates between 69.0 to 77.6 $ml.min^{-1}$ were used. The electrode was connected to variable DC high voltage from -4 to -12 kV and Faraday pile connected with digital electrometer was used to collect spray charge. Experiments reported that electrical breakdown occurred at -10 kV at injection pressure lower than 0.9 MPa; while at injection pressure equal to 0.9 MPa electrical breakdown of fuel occurred at -12 kV.

Tong-Xian *et al.* (2004) conducted experiments on spray deposition over plant foliage with self-adhesive paper targets. Self-adhesive paper micro-slide labels were used as the targets to evaluate spray coverage on tomato and citrus plant foliage. On both, upper and under leaf surfaces, self-adhesive papers were pasted randomly throughout the plant canopy before spray application. The spray

solution consisted of Brilliant blue dye (FD & C No.1) as a tracer in aqueous base. The tracer dye deposited on labels was then subsequently eluted into vials of water (20 mL) after spray application and the concentration of the rinsate obtained therefore was determined by spectrophotometry. Also the spray coverage was evaluated for comparison with same sized WSPs stapled onto the leaves. Comparatively more dye was recovered from labels than the actual plant leaves and recovery by two methods was correlated using yellow WSPs i.e. R-value = 0.83 to 0.99. Dye recovery was also correlated with the coverage measured using WSPs i.e. R-value = 0.72 to 0.95.

Latheef *et al.* (2008) conducted experiments on aerial electrostatically charged sprays to find its efficacy against fruit fly on cotton. 'Cessna AgHusky' Agricultural aircraft equipped with spray boom was used for the application with 1.5 to 2.0 m boom height above the crop canopy. The spray boom was engineered to achieve application rate of 4.68 L $ha^{-1}$ and assembled with 82 and 32 nozzles at 482.7 kPa and 193 kPa operating pressure respectively, with bipolar charging system of +5 kV potential. Six leaf samples were collected after application from top and mid-canopy locations randomly from the plot and tracer deposition was measured with Turner Digital Fluorometer (Abbott Diagnostics, C.A.) in terms of $ng.cm^{-2}$. They observed that there was no significant difference between charged and uncharged sprays.

Barbosa *et al.* (2009) conducted study on deposition and canopy penetration of different sprays in soybean (Glycine Max-L). Artificial mylar cards and tartazine tracer were used to quantify the distribution and penetration performance. The equation used for converting sample concentration results in units of volume per unit area was,

$$Deposit = \frac{(C \times V)}{(\rho \times A)}$$

Where, 'Deposit' is the final concentration, 'C' is the tracer concentration obtained through laboratory analysis (ng $L^{-1}$), 'V' is the solvent volume, 'ρ' is the original concentration of solution (mass per unit volume) and 'A' is the target

surface area. Multiple comparisons on means were made using Fisher's Test of Least Significant Difference (LSD).

Celen *et al.* (2009) studied the effect of air assistance on deposition characteristics of tunnel type electrostatic sprayer. The sprayer was attached to a 55 kW tractor and having 0 to 17 kV power supply unit with 12 V DC input. Vineyard sprayer having 50 L $min^{-1}$ discharge rate at 2 bar pressure was operated on crop position of 3 m × 1.5 m and 1.2 m height. Air support system having 710 mm diameter fan and air flow rate of 600 L $min^{-1}$ at 36 $m.s^{-1}$ air velocity was used. Tetrazine food dye was used as a tracer. Deposition was increased by 7.8 per cent with air support and 23.5 per cent reduction in drift.

Jaworek *et al.* (2009) studied electrostatic spraying of nano-thin films on metal surfaces. The electro-spray system was consisted of stainless steel capillary nozzle and heated stainless steel table of 120 mm diameter. The distance between nozzle tip and the table was kept 15 mm and 25 mm. The substrate was SS rectangular plate of 500 µm thickness and 25 mm x 30 mm dimensions. The solvent was evaporated from the spray solution by providing an electric heater placed beneath the table. The nozzle was connected to the HVAC-DC generator Model-P04015 TREK, switched to positive polarity while plate and the extractor were grounded. The spray plume was recorded using 'CCD Camera Model-NG-VS400', Panasonic Inc. Methanol ($CH_3OH$) was used as the solvent and Magnesium oxide (MgO) particulates of size 100 nm as solute. The DC bias was in the range of 5.7 to 6.3 kV and AC in 1.5 to 4.0 kV at liquid flow rate of 1.5 $ml.h^{-1}$. The results showed homogenous metal-oxide films on substrate of thickness 1 – 2 µm.

## 2.6 PERFORMANCE EVALUATION OF ELECTROSTATIC SPRAYING SYSTEMS

Arnold *et al.* (1984) studied the effectiveness of different pesticide spray treatments over three situations as pea and bean weevil (*Sitonaliniatus*) on field beans (*Viciafaba*), black bean aphid (*Aphis fabae*) on field beans and

powderymildew (*Erysiphegraminis*) on spring barley. A 0.1 per cent solution of the fluorescent tracer, 'Uvitex', was applied to the beans (as a 10 per cent solution of Uvitex concentrate, 1 per cent active ingredient in water) at the application rate of 3.7 L $ha^{-1}$ using charged or uncharged APE 80 sprayers. For biological trials against *S. lineatus*, oil-based formulations of permethrin and dimethoate were made and for water-based sprays standard emulsifiable concentrate formulations of permethrin (Ambush, Plant Protection) and dimethoate (Rogor E, FBC) were used. Insecticides were applied with the electrostatically charged rotary atomizers at the rate of 3.7 L $ha^{-1}$ and with a hydraulic sprayer fitted with 110º fan jets and delivering 440 L $ha^{-1}$. The plant samples were collected within 30 minutes after pesticide application and were chemically extracted for gas chromatography. Electrostatically charged sprays increased the overall deposition by 60 per cent compared to uncharged sprays.

Walker *et al.* (1989) conducted field evaluation of different pesticide spray atomizers for weed control in soybean cultivation. Research plots consisted of 4 rows of soybean spaced at 102 cm and 18.3 m long under study period of 6 years. The spray atomizers taken into the study were rotary atomizer from Micron Corp., Sprayrite Mfg. Inc., Spraying Systems Co., Electrostatic prototype by FMC Corp., Air-atomizing nozzle by Spraying Systems Co. and Air-atomizing electrostatic prototype by Parker-Hamifin Corp. These different nozzles were compared with the conventional fan-type spray nozzle. They observed that non-conventional atomizers did not out-perform significantly as compared to conventional hydraulic sprayers based on broad leaf weed control over foliar applied chemicals.

Gupta *et al.* (1992) conducted field experiments to compare the deposition pattern of charged and uncharged sprays. The charged spray was applied with a hand-held electrostatic spinning disc sprayer and uncharged spray with spinning disc sprayer and standard knapsack sprayer with hydraulic nozzle. Fluorometric analysis was followed for quantifying tracer deposition at different elevations of the plant. Droplet density was observed with WSPs placed at different elevations of plant canopy. Electrostatic charged spray application was done with 3kV

charging potential, 3500 – 4500 rpm spinning disc speed and 50 ml.min-1 flow rate. The charging system provided CMR of 2.5 $mC.kg^{-1}$ approximately, with droplet size in the range of 115 – 140 µm measured by collecting droplet on MgO glass slide and analyzer. The result showed the deposition of tracer increased 3.5 to 4.9 folds in rice crop with electrostatic spraying and 1.1 to 1.19 in soybean.

Bayat *et al.* (1994) conducted field experiment on comparison of spray depositions with conventional and electrostatically charged spraying in citrus trees for pest control. Investigations were conducted with code M1 and M4 with different configurations of spray application setups. The air carrier sprayer operated by standard PTO speed (540±10 rpm) was used with 2.3 mm orifice diameter nozzles with electrostatic charging system of 17 kV tension. The spraying was done at 3.5 $km.h^{-1}$ travel speed and deposition analysis was carried through fluorescent tracer, WSPs and fluorometric analysis. The relative deposition was calculated by equation,

$$RD = \left[\frac{MS}{\left(\frac{AS}{LAI}\right)}\right] \times 100$$

Where,

RD = Relative Deposition (%),

AS = Ideal Deposition ($\mu g.cm^{-2}$),

MS = Mean Stardust deposition determined by filter papers ($\mu g.cm^{-2}$),

LAI = Leaf Area Index (dimensionless).

The results showed that, the electrostatic application reduces losses in citrus trees by 11.6 per cent to 29.5 per cent, than the conventional spray application.

John *et al.* (1995) conducted a long term study on performance and efficacy of electrostatic spraying system for greenhouse agriculture. The electrostatic sprayer used in their evaluations (Electrostatic Spraying Systems, Inc., Watkinsville, GA) employed an air atomizing induction charging nozzle,

which produced droplets in the range of 30 to 60 µ. Within the nozzle, air pressure was maintained within 2.0 to 3.0 kg $cm^{-2}$, and the liquid pressure was kept around 1 $kg.cm^{-2}$. The high voltage module consisting two 9 V batteries imparted a negative charge (approximately -6 $mC.kg^{-1}$) on the droplets as they left the nozzle. Their study revealed that for controlling aphids on chrysanthemums, electrostatic spraying system given similar or gave better control as compared to conventional uncharged spray. In addition, electrostatic spraying method (50 L $ha^{-1}$) enabled them to reduce the water requirement in spray solution by 50 folds (2500 L $ha^{-1}$).

Sumner *et al.* (2000) conducted field experiments for comparing different spray techniques for pest management in cotton. Experiments included spray methods as air assisted spray, over the top hydraulic nozzle plus drop nozzles, electrostatic air assisted spray, over the top hydraulic nozzles and over the top plus shielded drop nozzles. Water sensitive cards and leaf-wash method was used to quantify the droplet deposition in various techniques. WSPs were placed into the canopy, top side and middle portion of canopy on both upper and undersides of leaves. Results have shown that electrostatic air assisted spray technique provided better coverage and lowest standard deviation in spot diameter (77 µm and 60 µm for top and underside resp.) than other methods.

Kirk *et al.* (2001) evaluated performance characteristics of aerial electrostatic spray system with different fields of cotton for control and management of ball weevil and white fly. The prototype was studied at laboratory on the basis of commercial version of aerial electrostatic spraying system. Charge to mass ratio was assessed for corresponding flow rates, spray mixture and pest mortality. The prototype aerial electrostatic spray charging nozzle system was mounted on Cessna T1888C Ag-Husky, agricultural aircraft (231 kW, 12.74 m wingspan), calibrated for 9.4 L $ha^{-1}$ at 483 kPa and conventional spray system calibrated for 46.8 L $ha^{-1}$ at 193 kPa. Spray droplet deposits with Caracid brilliant flavine dye were collected with six water sensitive papers per plant at random locations and quantified by dye fluorometry. They found higher pest mortality in

electrostatic aerial spray as 96.60 per cent compared to conventional spraying with 76.60 percent pest mortality.

Esehaghbeygi *et al.* (2010) assessed the efficacy of electrostatic charge and spinning-discs spraying for the application of 2, 4-D to control weeds in irrigated wheat. They evaluated sprayer nozzle performance in terms of wheat grain yield (Ghods variety), weed shoot biomass, and wheat residual (straw) at the research farm of Shahrekord University in 2007 and 2008. Spray penetration through dense weeds was enhanced with electrostatic charging and gave better weed control. They concluded that, spinning disc nozzle decreased water use and was cheaper to operate, however it did not significantly improve herbicide efficacy, especially in dense canopies compared with the electrostatically charged spray.

Antuniassi *et al.* (2011) evaluated the performance of aerial application equipment for soybean rust control. They evaluated field performance of different spraying systems as Micronair AU 5000 at 10 L $ha^{-1}$ (with oil) and at 20 L $ha^{-1}$ (without oil); Stol® ARD atomizer at 10 and 20 L $ha^{-1}$ (both with oil) and Spectrum (electrostatic) at 10 L $ha^{-1}$ (without oil). They used cotton oil (1.0 L $ha^{-1}$) as an adjuvant with emulsifier (BR 455) at 0.025 L $ha^{-1}$. The field trials were set up at the 3$^{rd}$ fungicide application, with four replications of each treatment. There were no statistical differences among treatments related to fungicide deposits at a confidence level of 95%. It was observed that the best results were obtained with Micronair® (10 L $ha^{-1}$ with oil), Stol® (20 L $ha^{-1}$ with oil) and electrostatic system at 10 L $ha^{-1}$.

Mishra *et al.* (2014) conducted performance evaluation of electrostatic spraying in orchards with USA made ESS®-MBP90 electrostatic sprayer. Tests were carried out with various experimental combinations of WSPs mounted on leaf top and leaf underside at distinct portions of plant canopy as top, middle, bottom and dense parts. Droplet density and uniformity coefficient for corresponding portions were obtained with the help of PC-assisted Stereo zoom

microscope CCD camera and compared between electrostatic (single and twin nozzle) spray and conventional non-electrostatic spray. They found that average droplet density on upper and underside of leaves was substantially higher in charged spray i.e. 57.53 per cent and 59.60 per cent respectively than uncharged spray method.

# MATERIALS AND METHODS

# CHAPTER III

# MATERIALS AND METHODS

The methodology adopted for the development of a prototype battery operated electrostatic sprayer including the procedures and setup to assess the performance of the developed system are described in this chapter.

## 3.1 DESIGN CONSIDERATIONS FOR THE DEVELOPMENT OF ELECTROSTATIC INDUCTION SPRAY CHARGING SYSTEM

The method of electrostatic induction spray charging was adopted for this study by considering its known advantages over other charging methods such as high charge transferability, less hazardous to life and simplicity in construction (Law, 1975). The engineering administration of tiny airborne particulates can often be improved by exposing them to electric force fields. The airborne particles those can be significantly guided by dielectrophoretic forces of spatially divergent fields, necessarily should have the essential condition for electrical force management is,

$$F_p = q_p E$$

….. Eq. 3.1

Where, $F_p$ is the electrical force (N) experienced by an individual particulate, $q_p$ is the net unipolar charge (C) on the particulate, and E is the electric-potential gradient ($V.m^{-1}$) existing at the location of the particle formation zone. This driving electric field may commonly result from: (a) conveniently positioned high-voltage electrodes; (b) induced image charges in nearby grounded boundaries; and from (c) electric space-charge fields generated by nearby airborne assemblies of other charged particles, including the charged cloud in which the individual charged particulate resides.

### 3.1.1 Criteria for introducing an electric field to liquid droplets

While the numerous technical applications of electrostatic force management of airborne particulates often dictate which of the above types of

electric field (E) is advantageous, a common requirement for successful use is the imparting of an adequate particulate charge ($q_p$). The objective of the work reported herein was the engineering design and development of a compact and reliable electrostatic-induction charging nozzle for imparting a significant percentage of the theoretical limit of unipolar charge to individual droplets of spray liquid in the electrical resistivity range of $2\times10^1$ to $2\times10^2$ Ω·m.

In theory, the level of droplet charge imparted by the electrostatic induction process should depend profoundly upon the relative time rate of charge transfer to the droplet-formation zone as compared with the time required for droplet formation. In terms of the liquid's dielectric constant κ, permittivity of air $\varepsilon_0$ and resistivity ϱ, the time constant becomes,

$$\tau = \kappa \times \varepsilon_0 \times \varrho = 76.546 \times 8.85 \times 10^{-12} \times 2 \times 10^2 = 1.3548 \times 10^{-7}$$

….. Eq. 3.2

(For water κ = 76.546 $F.m^{-1}$ at 30ºC, for air $\varepsilon_0 = 8.85\times10^{-12}$ $C^2.N^{-1}.m^{-2}$ and ϱ = $2\times10^2$ Ω-m)

Theoretically a spray liquid having charge transfer time constant (τ) is less than the length of time $t_f$ (s) which characterizes droplet formation, should be compatible with the electrostatic induction charging process. Whereas, the liquids having $\tau > t_f$ could not be satisfactorily charged by the method of electrostatic induction (Law, 1975).

The generalized schematics of electrostatic induction charger as shown in Fig. 3.1 illustrates geometric arrangement of components, for which the characteristic expression for droplet-formation time is,

$$t_f = \frac{l_c}{v}$$

….. Eq. 3.3

Where, $l_c$ (m) is the horizontal length of liquid sheet cylindroid and v is the velocity of flow ($m.s^{-1}$). At operating pressure of 6 $kg.cm^{-2}$, nozzle orifice

diameter of 0.5 mm and measured discharge rate (Q) of 2 mL.s$^{-1}$, velocity of flow (v) was found to be 10.19 m.s$^{-1}$. Therefore, the characteristic droplet formation time or phase transition time was calculated as,

$$t_f = \frac{1.2 \times 10^{-2}}{10.19} = 1.1776 \times 10^{-3}\ s$$

….. Eq. 3.4

Therefore, the essential theoretical requirement to impart the unipolar charge on liquid particulates by electrostatic induction, $\tau << t_f$ was satisfied.

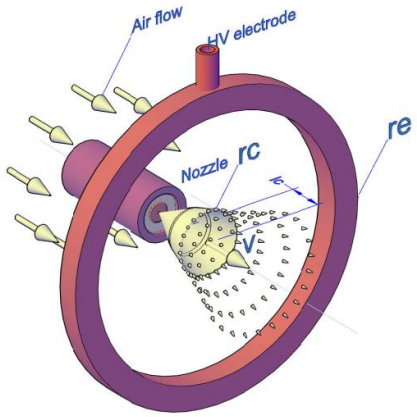


**Fig. 3.1 Comprehensive electrostatic induction spray charging system**

### 3.1.2 Prediction of spray cloud current

For $\tau << t_f$ the electrostatic induction charging system as illustrated in Fig. 3.1 could be approximated by two coaxial conducting cylinders in order to predict the electric field strength at the droplet formation zone, the charge density on the liquid sheet surface and the total droplet current. The electric field intensity (Ej) just off the surface of the liquid sheet cylindroid of radius $r_c$ (m) where droplet formation commenced. This could be approached as a function of outer cylinder (charging electrode) radius $r_e$ (m) and applied potential difference V (V) by the field equation for concentric conducting cylinders of infinite length (Attwood, 1932 cited by Law, 1975) as,

$$E_j = \frac{V}{r_c \ln(\frac{r_e}{r_c})} V.m^{-1}$$

….. Eq. 3.5

By Gauss' law the free surface charge density $\rho_s$ (C-m$^{-2}$) on the liquid sheet cylindroid would be,

$$\rho_s = \varepsilon_0 \times E_j \qquad C.m^{-2}$$

….. Eq. 3.6

Thus, the expected spray-cloud current $i_c$ (A) carried by the charged liquid would be,

$$i_c = 2\pi r_c \times \varrho_s \times v$$

….. Eq. 3.7

In terms of the applied charging voltage (V) and the liquid flow velocity (v, m.s$^{-1}$) this prediction equation for spray-cloud current becomes,

$$i_c = \frac{2\pi\varepsilon_0 V v}{\ln(\frac{r_e}{r_c})}$$

….. Eq. 3.8

From the observed Volume Median Diameter (VMD or $D_{V50}$), the droplet charge could be predicted theoretically by,

$$q_p = \frac{30\varepsilon_0 r_p V}{\ln(\frac{2r_e}{r_p})} \quad C$$

….. Eq. 3.9

From the value of $D_{V50}$, volume ($V_{DV50}$) and thereby mass ($m_p$) of the spherical particle could be calculated,

$$V_{DV50} = \frac{4}{3} \times 3.14 \times (r_p)^3 \ m^3$$

….. Eq. 3.10

Since, the mass density of water ($\rho_w$) is 997 kg.m$^{-3}$, mass of the droplet could be estimated as,

$$m_p = \rho_w \times V_{DV50} \quad kg$$

….. Eq. 3.11

Therefore, charge-to-mass ratio (CMR, mC.kg$^{-1}$) could be predicted by,

$$CMR_{theoretical} = \frac{q_p}{m_p} \quad mC.kg^{-1}$$

….. Eq. 3.12

### 3.1.3 Charging efficiency of electrostatic induction charger

The performance of an electrostatic particulate charging system in terms of charging efficiency can be determined by comparison of the imparted particulate charge to the maximum theoretical charge limit. For the agricultural airborne liquid particles having surface tension values ($\Gamma$, N.m$^{-1}$) typical of water ($\Gamma$=71.99×10$^{-3}$ N.m$^{-1}$) and common pesticides, this limit is influenced by hydrodynamic instability and rupture of the surface of the droplets due to repulsive force between unipolar charges, called Rayleigh limit. Therefore, for any given liquid particle a maximum surface charge density value ($\rho_s$) exists such that the outward expanding electrical force (due to repulsive nature of unipolar charges) on the liquid surface is just balanced by the restraining force of surface tension (Rayleigh, 1896 cited by Law, 1975). The value of maximum droplet charge limit ($q_{max}$) could be calculated as,

$$q_{max} = 8\pi\sqrt{\varepsilon_0 \times \Gamma} \times (r_p)^{3/2}$$

….. Eq. 3.13

In practical operation, the spray cloud current was measured using charge collector device coupled with digital multimeter, at different (1 kV to 12 kV) charging electrode potentials. The CMR values practically achieved were determined by taking ratio of the measured constant spray cloud current and the collected mass of spray liquid with respect to time.

The performance (charging efficiency) of an electrostatic induction spray charging system is defined as the percentage of maximum droplet charge or CMR achieved. The ratio of the charge imparted practically on a droplet to the maximum droplet charge or maximum CMR at Rayleigh limit is given by the equation (Law, 1975):

$$Charging\ efficiency\ (\%) = \frac{CMR_{Achieved}}{CMR_{Rayleigh\ limit}} \times 100$$

….. Eq. 3.14

## 3.2 PROCEDURE FOR DEVELOPMENT OF VARIABLE HIGH VOLTAGE POWER SUPPLY

A high voltage DC power supply is essential for charging an aqueous spray electrostatically. The basic voltage amplification unit mainly consists of a diode pump voltage multiplier. It has a special arrangement of P-N junction diodes and capacitors (Cockroft-Walton voltage multiplier) with an alternating current input. The voltage amplification depends upon the number of stages of diode and capacitor ladder and the capacitance value. However, these circuits are vulnerable to failure under load conditions. Moreover, detection of fault becomes challenging as these circuits consist of large number of electronic components.

In order to eliminate the need of high voltage cascade multiplier circuit and for longer operational duty, a flyback or Line Output Transformer (LOT) driven by a Horizontal Output Transistor (HOT) was developed as shown in Fig. 3.2. The flyback transformer is an integrated transformer which has built in rectifiers and divider networks and several isolated windings to output different voltages. The primary winding of the flyback transformer was driven by a switch from a DC supply (HOT). When the circuit is closed, the primary inductance caused the current to build up in a ramp. An integral diode connected in series with the secondary winding prevented the formation of secondary current that would eventually oppose the primary current gradient.

When the circuit was closed, the current in the primary dropped to zero. The energy stored in the magnetic core was released to the secondary as the magnetic field in the core collapsed. The voltage in the output winding rose instantaneously until it was limited by the load conditions. Once the voltage reached such a level as to allow the secondary current to flow, then the current in the secondary winding began to flow in the form of a descending ramp. The pulse train coming from the flyback transformer windings was converted into direct current by a simple half wave rectifier. A full wave rectifier was not essential in the circuit design as there were no corresponding pulses of opposite polarity.

In construction, windings of the primary were wound first over a ferrite rod, and then the secondary windings were wound around the primary. This arrangement minimized the leakage inductance of the primary. Finally, a ferrite frame was wrapped around the primary/secondary assembly, closing the magnetic field lines. Between the rod and the frame was an air gap, which increased the reluctance. The secondary was wound layer by layer with enameled wire, and Mylar film between the layers. In this way parts of the wire with higher voltage between them have more dielectric material between them. Unlike a transformer which uses an alternating current of 50 or 60 hertz frequency, a flyback transformer typically operates with switched currents at much higher frequencies in the range of 15 kHz to 50 kHz.

The switched DC power supply essentially requires HOTs like IRFZ44N power transistor to energize the primary of LOT at a high frequency. Due to higher switching frequency, usually power transistors become very hot and a heat sink was essential to prevent high temperature damage to the transistor. In order to generate a variable high voltage output, the voltage input to the primary side was adjusted using Pulse Width Modulation (PWM) circuit. The developed circuitry was driven by lithium ion battery (3.7 V DC, 3000 mAh) capable of generating variable high voltage output in the range of 1kV to 12kV with maximum current output of 30 µA corresponding to the power rating of around 360 mW.

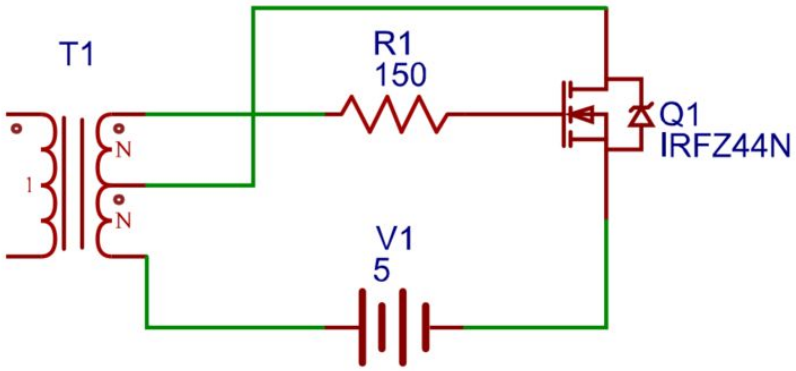


**Fig. 3.2 HVDC generator circuit**

## 3.3 SELECTION OF HIGH SPEED AIR BLOWER

A ducted fan is more efficient in producing thrust than a conventional propeller of similar diameter, due to reduced propeller blade tip losses. The ducted fan offers a smaller diameter than a free propeller to accommodate within smaller equipment. In addition, these fans are quieter than propellers; they shield the blade noise and reduce the intensity of the tip vortices which contribute to noise production.

An Electric Ducted Fan (EDF) was selected as the main component for the high speed air blower (Fig 3.3). The internal diameter of the ducted fan was 70 mm with 12 blades mounted on a DC synchronous permanent magnet motor with KV1850 rpm rating. The motor was driven by the Universal Battery Eliminator Circuit (UBEC) integrated with Electronic Speed Controller (ESC) which could be operated with 7.5 to 25 V DC power supply. The driver module was coupled with a Servo Consistency Master (SCM) to control the rotor speed manually for obtaining a variable speed.

## 3.4 LIQUID DELIVERY AND ATOMIZATION

Selection of liquid delivery and atomization system was based on the power supply (12 V DC battery), air assistance compatible and a desirable droplet spectrum. Two battery compatible mechanisms available were rotary cup/disc atomizer with a low pressure delivery and a hydraulic spray nozzle with a high pressure diaphragm pump.

The rotary atomizer could be operated on 12 V DC power supply with a low pressure low discharge pump and offer a fine droplet spectrum (30 to 100µm) depending on rotary speed and rotor shape. However, the rotor size and shape could greatly hinder the assisting air flow which in turn could affect the atomization process undesirably. Also the application of electrostatic induction charging was complicated. Whereas, the hydraulic pressure swirl nozzle with lesser disturbance to the assisting airflow and atomization (50 to 150 µm) in the direction of air flow could be advantageous in successful application of electrostatic charge. Hence, the hydraulic pressure swirl nozzle with high pressure low discharge diaphragm pump (12V DC, 6.5 A max. current) was selected for the liquid delivery and atomization.

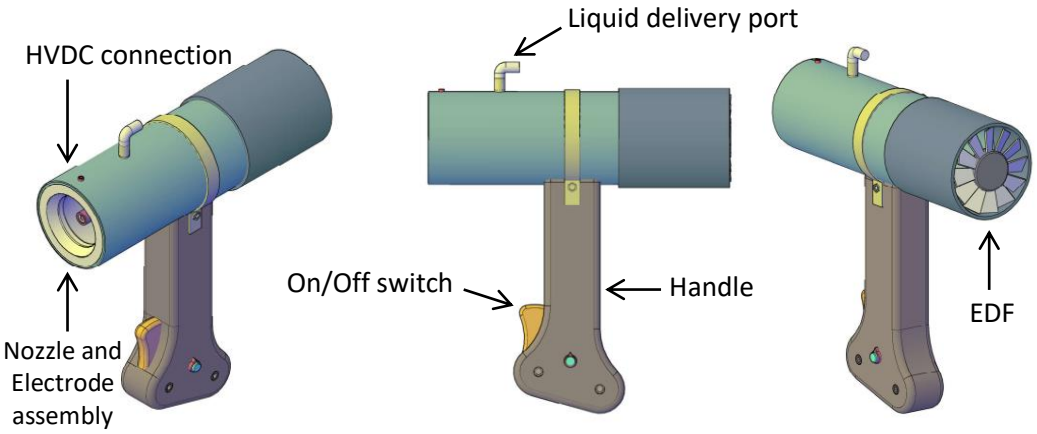


**Fig. 3.3 Conceptual design of handheld electrostatic spray gun**

## 3.5 ASSESSMENT OF NOZZLE CHARACTERISTICS

The spray nozzle selected was evaluated to assess the nozzle characteristics in terms of half-cone angle, spatial distribution pattern and discharge rate subjected to varying operating pressures and nozzle heights. Instead of conventional spray patternator (inclined triangular channel type), a grid patternator approach was employed for better understanding of spray characteristics. A catch can grid of odd number of rows was laid on a platform under the frame on which spray nozzle was held and vertically pointed towards grid center point. The 9×9 grid of plastic catch cans each of volumetric capacity

of 150 ml and opening diameter of 70 mm was used to collect the spray volume at different operating pressures and nozzle heights. The effect of blower speed and electrostatic charge induction on spatial distribution of spray was also quantified at the optimum operating pressure and at a fixed nozzle height.

## 3.6 CONCEPTUAL DESIGN OF BACKPACK FRAME

A back frame accommodating major weight contributing components such as spray solution tank, battery and pump was conceptualized. The dimensions of the backpack frame were depended on the space required for the components and design of commercially available knapsack sprayers.

Selection of material for fabrication of the backpack frame was based on overall weight, reliability and corrosion resistance. In order to keep the overall weight of the sprayer as low as possible, a compact backpack frame plastic tubes with three horizontal compartments as shown in Fig. 3.4 and Fig. 3.5. The compartments were made using PVC board of 3 mm thickness. The lower compartment accommodated the battery, diaphragm pump and the pressure control system.

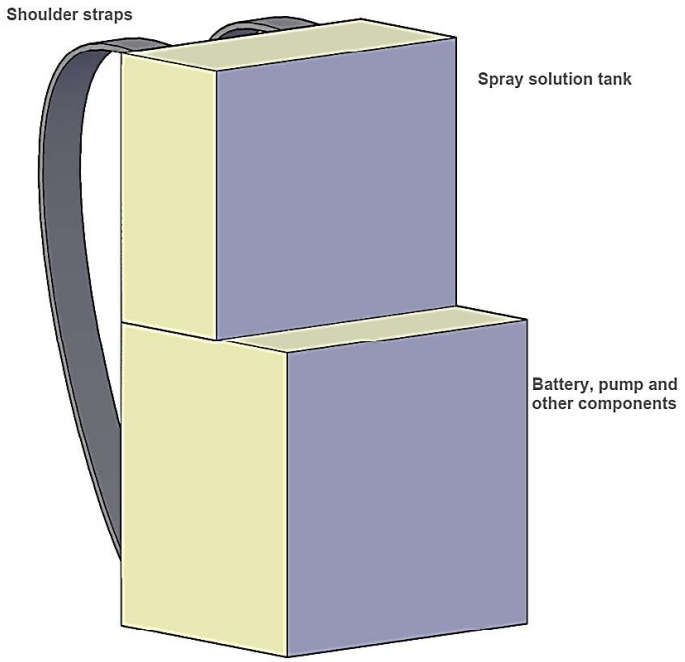


**Fig. 3.4 Block diagram of backpack assembly**

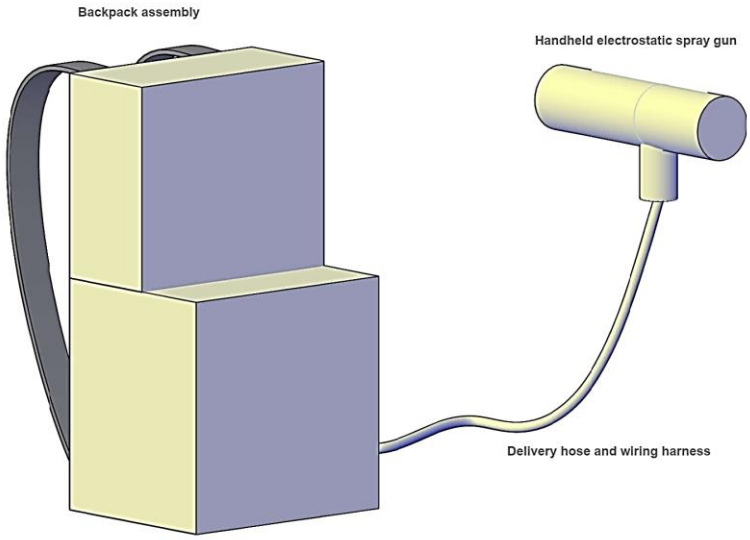


**Fig. 3.5 Block diagram of conceptual battery powered electrostatic sprayer**

## 3.7 SPRAY DROPLET SIZE AND DEPOSITION ANALYSIS

The assessment and analysis of droplet spectrum generated from the concerned spray nozzle was important to determine charging efficiency of developed electrostatic induction spray charger. Also the deposition characteristics were primarily dependent on effective droplet diameter (VMD). The droplet spectra were captured on the white glossy photography papers using methylene blue dye (10% w/w) in aqueous spray solution. The air blower was operated on lower speed (1.0 m $s^{-1}$) to minimize droplet spread due to high velocity impact on the photography paper. The spray nozzle was operated with three different pressures (4.0, 5.0 and 6.0 kg·$cm^{-2}$) to determine the optimum working pressure to produce finer droplet spectra. Also the effect of electrostatic charging on droplet size and distribution was accounted and compared with the developed spray system without electrostatic charge.

The spray impinged photography papers were allowed to dry and then scanned using flatbed scanner with 600 dpi resolution in the Greyscale JPEG file format. These scanned images were then analyzed for droplet size using 'DepositScan' Program in ImageJ image processing computer software. DepositScan is a portable scanning system for spray deposit qualification

developed by USDA-ARS Application Technology Research unit, Wooster (USA).

The image processing software readily analyzed the scanned image and displayed the results in terms of droplet size distribution ($DV_{10}$, $DV_{50}$ and $DV_{90}$), droplets per unit area, and per cent coverage of deposits within the selected image area, total number of droplets count, individual spot area and actual droplet diameter. DepositScan converted the individual spot area into actual droplet diameter using following equation,

$$D_d = 1.06\, A_s^{0.455}$$

….. Eq. 3.15

$DV_{10}$, $DV_{50}$ and $DV_{90}$ represented the distribution of the droplet diameters such that the droplets with a diameter smaller than $DV_{10}$, $DV_{50}$ and $DV_{90}$, composed 10, 50 and 90 per cent of the total spray volume analyzed.

### 3.7.1 Number Median Diameter (NMD)

NMD is the average diameter of the droplet, which divides the number of droplets into two equal halves. In other words, it is the diameter of the spray droplet, which divides the droplet spectrum into two halves whereas, the total number of spray droplets which are smaller in size will equal to the number of spray droplets which are larger in size (Matthews, 1988 cited by Balachand, 2014).

### 3.7.2 Volume Median Diameter (VMD or $DV_{50}$)

It is the diameter of the droplet that divides the volume of the spray into two equal halves. A representative sample of droplet of a spectrum is divided into two equal parts by volume, so that one half of the spray volume contains smaller droplets than a droplet whose diameter is the volume median diameter (VMD) and the other half of the volume contains larger droplets (Matthews, 1988 cited by Balachand, 2014).

### 3.7.3 Uniformity coefficient ($U_C$)

Uniformity coefficient is the ratio of VMD to NMD, a factor used for indicating the uniformity of the spectra. The VMD is affected by relatively few

large droplets whereas the NMD is more influenced by small droplets. The more uniform the spray spectra, the closer the ratio of VMD and NMD approaches to unity.

$$U_C = \frac{VMD}{NMD}$$

….. Eq. 3.16

### 3.7.4 Relative span ($R_S$)

Relative span refers to a spray quality indicator determined by subtracting the $DV_{10}$ value from the $DV_{90}$ value and dividing by the $DV_{50}$. The numerical value of $R_S$ describes the width of the particle size distribution curve plotted against the frequency of occurrence. The smaller $R_S$, lesser is the variation between the sizes of the droplets in the spray spectrum.

$$R_S = \frac{DV_{90} - DV_{10}}{DV_{50}}$$

….. Eq. 3.17

### 3.7.5 Depositional characteristics

Depositional characteristics of developed sprayer were assessed by performing field experiments on the brinjal plants. The similar technique of image processing was followed to capture and analyze the stained glossy photography paper strips mounted onto upper, middle and lower plant canopy, above and underneath leaf surface. The paper strips of size 4.0 cm × 1.5 cm were used for the assessment of spray deposits in both the abaxial and adaxial leaf surfaces. The developed spray system was operated with and without electrostatic charge induction, to verify the existence of electrostatic wrap-around effect. The spray impinged paper strips were analyzed especially to account the droplet density on both sides (above and underneath) of the leaf surfaces. The deposit population per unit area of leaf with the developed electrostatic system was compared with those when operated without charge and manually operated knapsack sprayer.

The developed system was also evaluated for spray deposit distribution in terms of on-target, ground and drift. The photography sheets of required size

(A4) were laid under the plant canopy to assess the spray deposition on ground. The spread of ground deposition along and across the crop rows were measured. The spray impinged photography sheets and strips were analyzed to account the total volume deposited on the ground and the plant. Total applied spray volume could be calculated by multiplying spray duration (s) and nozzle discharge rate ($ml \cdot s^{-1}$). The difference between total spray volume applied and the sum of on-target and ground deposition volume revealed the amount of spray volume lost in the form of drift.

## 3.8 DETERMINATION OF LEAF AREA INDEX (LAI) FOR SPRAYER CALIBRATION

Leaf area index is an important parameter that characterizes plant canopy. It is defined as the total one-sided green leaf area of a plant per unit ground surface area in broadleaf canopy crops. In the field evaluation of the developed spraying system, Brinjal (Variety: Haritha) was taken as the study crop, the average LAI of the crop was estimated using image processing computer software. Leaf samples of various representative sizes (very small, small, medium, medium large, large and extra-large) were collected randomly with their corresponding leaf count per plant. These leaf samples were scanned and analyzed using EasyLeaf software to calculate average leaf surface area per plant.

Canopy area was the other parameter essential to find LAI, which was measured by combined used of plant overhead photography and EasyLeaf image processing software. In order calibrate the software against the photographic scale distortion, a square piece (20 mm × 20 mm) of reflective red paper was placed nearby the plant perpendicular to the direction of camera lens and captured along with plant canopy in the frame. The captured images were fed to EasyLeaf software and processed to measure the canopy area by setting the area calibration scale to 4 $cm^2$. Hence, the LAI was calculated using equation,

$$LAI\ (dimensionless) = \frac{Total\ leaf\ area\ of\ plant, m^2}{Canopy\ area, m^2}$$

….. Eq. 3.18

The developed spraying system could be calibrated for given crop with respect to corresponding LAI value. A known flat land area was sprayed to know the spray volume utilized per unit area, which was then multiplied by the known value of LAI to determine actual spray volume required to spray the particular crop. Also the concentrations of different agricultural chemicals to be used with the developed spraying system could readily be calculated.

## 3.9 MEASUREMENT OF SPRAY CLOUD CURRENT

Spray cloud current measurement was essential to validate and quantify the performance of the developed spray charging system. The charge collector device was fabricated using an internal stainless steel cylinder of diameter 300 mm and length 310 mm, closed at rear end with a small opening to collect the spray liquid was insulated on external surface with PVC sheet of thickness 1.5 mm. The internal conductive charge collector cylinder was electrically isolated from any other conducting media which could leak the charge to earth. A metal cantilever frame was constructed on which the collector cylinder was hung by means of PVC pipe.

A digital multimeter was employed to measure the current generated by charge transfer from spray cloud to the collector cylinder by connecting positive terminal of DMM to the collector and negative to the earth. The spray cloud current was measured for different levels of charging by means of electrode potentials 1 kV to 12 kV in steps of 1 kV. A computer based real time data recording software was used to store the current readouts from the DMM for further analysis. The charge-to-mass ratio of charged spray was calculated taking the ratio of measured spray cloud current (μA) and mass of spray liquid (kg) collected with respect to the time of measurement (s). The electrode potential at which the maximum charge transfer occurred was determined to calculate the charging efficiency of developed system.

### 3.9.1 Digital Multimeter unit

The digital multimeter Model No. KM-5040T/BM-812a of make KUSAM-MECO Brymen, Ind. Ltd. (Fig. 3.6) was used for the measurement of

voltage and current generated by the HVDC generator unit. The DMM was equipped with 5000 counts and analog bargraph screen and also enabled with RS-232 Computer Interface-Data Logging Software which can collect data from the DMM with Infrared serial bus cable at the data collection speed of one reading per second. Fig. 3.6 shows the face window of the Computer Interface-Data Logging Software. The general specifications of the DMM used were,

| | | |
|---|---|---|
| Make | : | Kusam-Meco Brymen Industries Ltd. |
| Model | : | KM-5040T/BM-812a |
| Capacity | : | 1000 V, 10 A max. |
| Sensitivity | : | 0.1 µA, 10 µV |
| Accuracy | : | ± 0.5 % ( 3 Digits) |

### 3.9.2 High Voltage Probe

In order to measure the high voltage potential at the charging electrode in the range of kilovolts, a high voltage probe model PD-28 of make KUSAM-MECO Brymen, Ind. Ltd. was used (Fig. 3.6), in compatibility with the DMM. High voltage probe was basically a voltage divider network consisting high resistances in series form. The high voltage was applied to the voltage divider network and the corresponding current flowing through the low resistance was measured by the DMM, which has been calibrated to show corresponding high voltage.

The high voltage probe used in the present study had the specifications as,

| | | |
|---|---|---|
| Make | : | Kusam-Meco Brymen Industries Ltd. |
| Model | : | PD-28 |
| Capacity | : | 40 kV DC or 28 kV AC max. |
| Input Impedance | : | 1000 MΩ |
| Attenuation Ratio | | 1000 : 1 |
| Accuracy | : | ± 1 % |

The HV-probe has an insulated hollow body with slender shape inside which, a voltage divider network of series high resistances have been connected. The tip of probe was pointed and made of brass, served as the contact point to the

high voltage terminal. At the base, insulated handle has been provided with the surge protector shield which assures the operator safety during measurement of such high voltages. Out of the three cables emanating from the probe, one served as the earth and the other two for connecting DMM.

(High Voltage Probe)

(Digital Multimeter)

**Fig. 3.6 High voltage measurement system**

## 3.10 CHEMICAL ANALYSIS AND BIOLOGICAL EFFICACY

The developed electrostatic sprayer was evaluated for its bio-efficacy by analyzing the pesticide residues in brinjal fruits and by assessing the bio-efficacy against brinjal fruit and shoot borer (*Leucinodes orbonalis*). Pest infested crop of brinjal var. Haritha in the farm of Krishi Vigyan Kendra (KVK), Malappuram was treated with the recommended pesticide (Dimethoate, Tata Tafgor®). The brinjal crop was sprayed with different treatments with the developed spraying system and also with the conventional manually operated knapsack sprayer. Table 3.1 illustrates the spray treatments followed for pest management. All the treatments were replicated 5 times and the design followed was Randomized Block Design (RBD).

The five treatments performed were Conventional high volume spraying ($T_1$), Electrostatic standard dose spraying ($T_2$), Non-electrostatic standard dose

spraying ($T_3$), Electrostatic reduced dose spraying ($T_4$), Non-electrostatic reduced dose spraying ($T_5$) and Conventional high volume spraying ($T_6$).

The fruit samples from the treated plants were collected on zeroth, third, fifth and seventh day of spray application. QuEChERS method (Anastassiades *et al.* 2003) was followed for the extraction of pesticide residues in the fruits using GC-ECD (Gas Chromatograph-Electron Capture Detector), model Agilent 7890 B, available at the Pesticide Residue Testing Laboratory, College of Horticulture, Vellanikkara. The results were compared between the above spray treatments to quantify the field performance of the developed spraying system.

**Table 3.1 Treatment details**

| Crop | Pesticide (a.i.) | Dosage | Spraying method |
|---|---|---|---|
| Brinjal var. Haritha | Dimethoate | 750 mL $ha^{-1}$ | Conventional high volume |
| | | 450 mL $ha^{-1}$ | Developed prototype – ECS* |
| | | | Developed prototype – WEC** |

`Replications - 5

* Electrostatically charged spray, ** Without electrostatic charge

Total number of treatments = 1×2×3 = 6

The biological efficacies of the spray treatments were determined in terms of number of fruit bore holes before and one week after pesticide application and were calculated using the following formula (Abbott, 1925),

$$\text{Biological efficacy (\%)} = \frac{\text{Pest avtivity on treated plants} - \text{Pest activity on the check}}{\text{Pest activity on the check}} \times 100$$

….. Eq. 3.19

### 3.10.1 QuEChERS method

Quick, Easy, Cheap, Effective, Rugged, and Safe (QuEChERS) method of extracting pesticide residues from treated plant body samples was validated in 2005, with subsequent amendments in 2007 by Association of Analytical Communities (AOAC - 2007.01) and European Method (EN 15662).

The well-organized approach of the method makes it efficient and economical to inspect the pesticide residues in the study samples and is being adopted globally over the existing methods such as Liquid-Liquid Extraction (LLE) and Gel Permeation Chromatography (GPC). The method employed in the present pesticide residue study is explained in detail as given below,

*3.10.1.1 Solvents and Reagents*

Sample extraction is defined as the procedure or step adopted to isolate the pesticide from the sample. This was accomplished by employing suitable solvents which remain in contact with the sample for a specific time. The chemical process to extract the representative samples include acetone – $(CH_3)_2CO$ and methyl cyanide (MeCN) – $CH_3CN$ as solvents and deionized water – $H_2O$, magnesium sulfate (Anhydrous powdered form) – $MgSO_4$, Sodium chloride (Anhydrous powdered form) – NaCl as reagents. The stock solutions of 1000 µg $mL^{-1}$ were used to prepare working standard pesticide mixtures of 50 and 10 µg $mL^{-1}$ were in MeCN solvent.

*3.10.1.2 Apparatus and instruments*

The preparation of representative samples from treated leaves and fruits, separation of solids, handling of solvents and reagents, storage of extracts and analysis of pesticide residues was accomplished using the apparatus and instruments are detailed as given below,

a. Blender or Homogenizer (high volume)

A 1 L volume MG 218 Zodiac (Preethi Pvt. Ltd., Chennai) chopper cum mixer-grinder was used to comminute fruit and vegetable samples. A Vortex-Genie-2 apparatus from Scientific Industries (Bohemia, NY) was used for initial extraction and for cleanup by dispersive Solid Phase Extraction (SPE).

b. Centrifuges

A Sorvall RT6000B (Newtown, CT) centrifuge was used for 2 mL, 10-15 mL and 50 mL centrifuge tubes and a Hill Scientific MV13 (Derby, CT) mini-centrifuge was used for 1.5 mL micro-centrifuge tubes.

c. Liquid dispensers

An adjustable-volume solvent dispenser with 10 mL capacity to transfer reagents from bottle to samples. An adjustable repeating pipet was used to transfer 1 mL and 0.5 mL aliquots of extract.

d. Analytical balances

Top-loading balances with digital displays were used to weigh chopped samples, bulk salts, and smaller portions of SPE sorbents and MgSO4. Scoops of 50 µL for primary secondary amine (PSA) and 0.77 mL for NaCl could be substituted for measurement of 25 mg and 1 g portions, respectively. Since the volume of MgSO4 powder was not consistent, weighing was needed for reasonably accurate measurement of the 4 g portion; however, a scoop of 275 µL could be used to provide ≈ 150 mg.

e. Vials and vessels

For initial extraction, 40 mL Teflon centrifuge tubes (Nalgene, Rochester, NY) were used, and 1.5 mL flip-top micro-centrifuge tubes were used for dispersive SPE. Standard 1.8 mL glass auto-sampler vials for GC were used to contain the final extracts after passing through 0.45 µm Teflon filters.

f. Vortex shaker

For achieving a uniform mixing of the reagents with the comminuted test sample, vortex shaker (Tarson® Spinix™ C-01) was used.

f. Gas Chromatography (GC) instrument

Extracts were analyzed with a Hewlett-Packard (Agilent, Little Falls, DE) Model 5890 Series-II Plus GC coupled to an Electron Capture Detector (ECD). The system was equipped with a split/splitless injection inlet, electronic pressure control (EPC), and a 7673A autosampler. Chemstation software was used for instrument control and data analysis.

*3.10.1.3 Procedure*

a. Sample weight

Weigh 10 g previously homogenized sample into 50 mL Teflon centrifuge tube for the analysis.

b. Extraction/Partitioning

Add 5 mL of distilled water, wait for 30 minutes, then add 10 mL of 1 per cent acetic acid in ethyl acetate and 10 g anhydrous sodium sulfate (activated at 500° C for 5 hours) fix the screw cap, and shake sample vigorously for 1 min by using Vortex mixer at maximum speed.

c. Homogenization

Homogenize the comminuted sample mixture at 13000 to 14000 rpm for 3 minutes.

d. Centrifugation

Centrifuge the content at 3000 rpm for 5 minutes at 10° C temperature.

e. Dispersive Solid Phase Extraction (D-SPE) Cleanup

Transfer 6-8 mL of extract to a 15 mL centrifuge tube containing 50 mg primary secondary amine (PSA), 150 mg anhydrous magnesium sulfate ($MgSO_4$) per mL of supernatant extract. Add graphitized carbon black if colour impurities are present (optional) and mix on a vortex mixer immediately for 1 minute and centrifuge extract for ≈ 5 min at 5000 rpm.

f. Evaporation

Transfer 2 mL of the extract into a vial containing 200 µL of 10% diethylene glucol in methanol and evaporate the content using nitrogen concentrator at 35-40° C for LC/MS/MS. Reconstitute the residues with 2 mL solvent mixture 80 : 20 (methanol : 0.1% acetic acid in HPLC water). Sonicate mixture for 1 minute to dissolve the residues.

g. Filtration

Filter 2 mL extract through 0.2 µm PTFE membrane.

h. Sample injection

Inject 5 µL filtrate in LC/MS/MS and 2 µL in GC/MS/MS.

i. Preparation of calibration solutions

Quantitation was performed and compared by using calibration standards involving both matrix-matching (standards added to blank extracts) and non-matrix-matching (standards in solutions containing analyte protectants).

The step by step procedure followed for chemical extraction from the representative sample is given in the Fig. 3.7.

**Fig. 3.7 Flow chart for sample extraction by QuEChERS method**

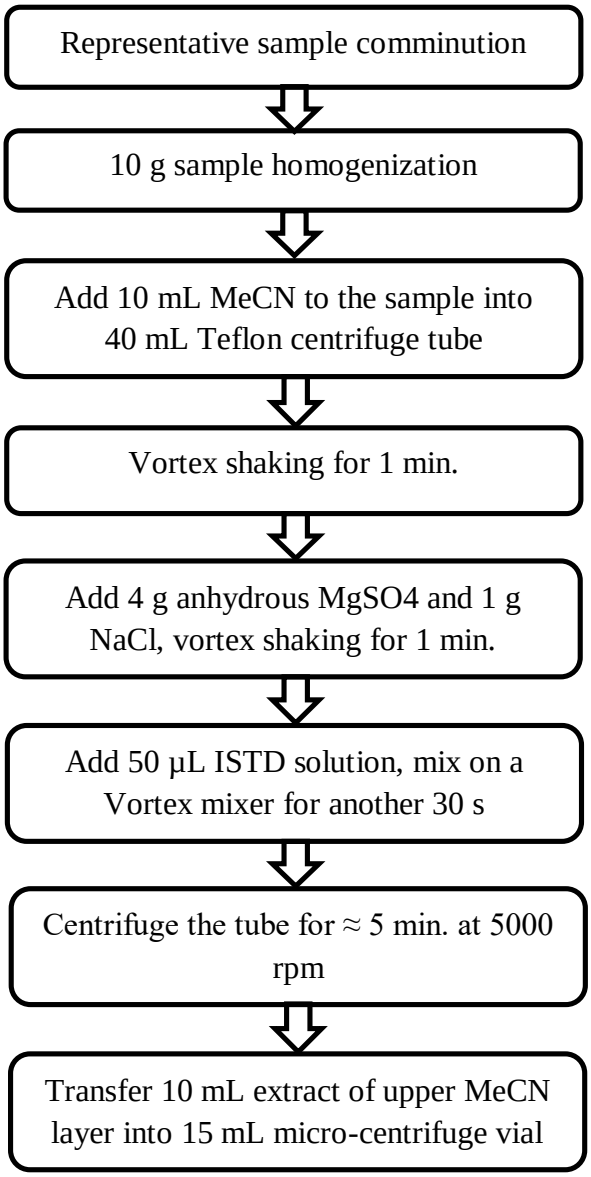

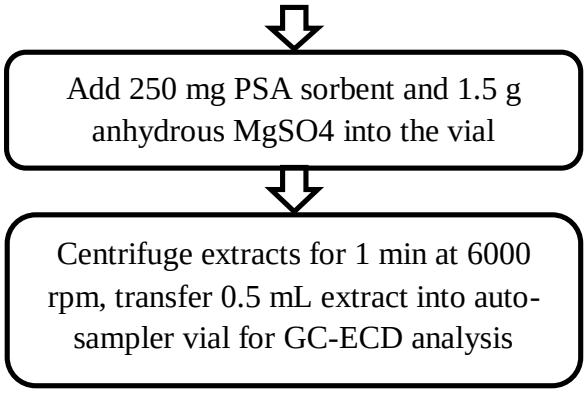


## 3.12 STATISTICAL ANALYSIS

The experimental results were analyzed statistically for the validation and significance using R-studio, an open source computer environment based on R-language using analysis of variance (ANOVA). Tukey-HSD (Honestly Significant Difference) test was also conducted for comparison of means.

## 3.12 COST ESTIMATION

The overall cost of the developed prototype was the arithmetic sum of the individual cost of each system component, machine work and labour charge incurred. The operational costs involving the fixed and variable costs were estimated using methods suggested by Indian Agricultural Statistics Research Institute (IASRI) and compared with commercially available engine powered knapsack mist-blower within the equivalent price range.

### 3.12.1 Fixed costs

The fixed costs were determined assuming the functional life of the powered knapsack sprayer to be 5 years with 250 annual working hours. The fixed costs included depreciation, interest, shelter and insurance of the machine.

#### *3.12.1.1 Depreciation*

The annual depreciation over initial investment was estimated using 'Sum of the Years Digits' method as:

$$D_{n+1} = \frac{(L - n) \cdot (P - S)}{Y_D}$$

….. Eq. 3.20

$$Y_D = \frac{L \cdot (L+1)}{2}$$

….. Eq. 3.21

Where,

$D_{n+1}$ = Depreciation at the age of machine at the ending of the year in the question, Rs. per annum

$Y_D$ = Sum of the years digits

n = Age of the machine at the beginning of year in the question, years

P = Purchase price or Initial investment, Rs.

S = Salvage value, taken as 10% of the purchase price, Rs.

L = Useful life of the machine, years

*3.12.1.2 Interest on investment*

A large portion of the fixed cost next to the depreciation for agricultural machinery is the interest on the initial investment. It is a direct expense on the borrowed capital. Though, the cash is paid for the procured machinery, the money is tied-up that might be available for use elsewhere in the business trade. Interest rates vary considerably regionally, but often in the range of 12 - 16 per cent. The annual interest is calculated on the average purchase price of the machine imposed by prevailing interest rates by the following formula:

$$I = \frac{P+S}{2} \times \frac{i}{100}$$

….. Eq. 3.22

Where,

I = Annual interest charge, Rs. per annum

i = Interest rate, per cent

*3.12.1.3 Insurance and shelter*

The annual insurance and shelter charges ($C_{IS}$) together were taken as 2 per cent of the total purchase price of the machine, calculated as:

$$C_{IS} = P \times \frac{2}{100}$$

….. Eq. 3.23

### 3.12.2 Variable costs

The variable costs include repair and maintenance, fuel, lubrication and labour charges incurred during the operating hours of the machine.

*3.12.2.1 Repair and maintenance*

Repair and maintenance costs are the important part of machine ownership. Occasional repairs and periodic maintenance are essential to keep the machine in a state of proper functionality. The causes imposing the repair and maintenance in a machine are routine wear, inadvertent breakage or damage, operator's negligence and periodic overhauls. The annual cost of repairs and maintenance ($C_{RM}$) together was taken as 5 per cent of the purchase price of the machine.

$$C_{RM} = P \times \frac{5}{100}$$

….. Eq. 3.24

*3.12.2.2 Fuel and lubrication costs (For engine powered knapsack blower)*

a. Fuel cost

The annual fuel cost ($C_{Fuel}$) for operating a gasoline engine could be calculated from its volumetric fuel consumption per hour ($F_C$, L $h^{-1}$), annual working hours (W, h) and prevailing gasoline price ($P_F$, Rs. $L^{-1}$).

$$C_{Fuel} = W \times F_C \times P_F$$

….. Eq. 3.25

b. Lubricant cost

The annual lubrication cost for a gasoline engine was taken as the 20 per cent of the estimated annual fuel cost.

*3.12.2.3 Cost of battery recharging (For battery powered sprayer)*

An electrical energy consumed in recharging the lead acid battery (sealed, maintenance-free with 4 years of useful life) from its per cent of discharged capacity could be calculated from the following formula:

$$E_{RC} = \frac{V_{battery} \times A_{battery} \times (100 - B_{capacity}) \times (100 + B_{losses})}{10^5}$$

….. Eq. 3.26

Where,

$E_{RC}$ = Electrical energy consumption per recharge cycle, kWh
$V_{battery}$ = Battery open circuit voltage, V
$A_{battery}$ = Battery capacity, Ah
$B_{capacity}$ = Battery charge potential when discharged, 20 per cent
$B_{losses}$ = Charging losses, 20 per cent

Considering the annual number of recharging cycles and the prevailing cost of electricity, the annual cost of battery recharging could be found using the following equation:

$$C_{RC} = E_{RC} \times N_{RC} \times E_{UC}$$

….. Eq. 3.27

Where,

$C_{RC}$ = Annual cost of battery recharging, Rs. per annum
$N_{RC}$ = Annual number of recharging cycles, Nos.
$E_{UC}$ = Per unit cost of electricity, Rs. per kWh

*3.12.2.3 Labour cost*

The labour cost for operating the machine could be calculated from the actual labour charge being paid (Rs. per day of 8 working hours) at a prevailing rate in the Tavanur, Kerala. The average agricultural labour charge of Rs. 750 per day was taken into consideration.

The total hourly operation costs of sprayers were calculated by dividing the sum of fixed costs and variable costs by annual working hours of the sprayer.

$$\text{Hourly operational cost, Rs. } h^{-1} = \frac{\text{Fixed costs+Variable costs}}{\text{Annual working hours}}$$

….. Eq. 3.28

# RESULTS AND DISCUSSION

# CHAPTER IV

# RESULTS AND DISCUSSION

The salient results of the investigations taken up to develop an electrostatic induction charging system and a liquid atomizer compatible to a DC power to aid electrostatic spraying is elucidated in this chapter. The results of the laboratory and field experiments conducted during the development of this battery operated electrostatic spraying system are also discussed here.

## 4.1 DEVELOPMENT OF ELECTROSTATIC INDUCTION CHARGING UNIT

The electrostatic spray charging unit (ESCU) was developed based on electrical design principles and had a variable high voltage power module, a hydraulic atomization system and a blower for the high velocity air assistance main components.

### 4.1.1 Design of electrostatic induction spray charger

The nozzle employed in the system produced infinitesimally small free jet length just off the nozzle orifice (0.5 mm) and observed to be instantaneously diverging into a hollow cylindroid liquid sheet. The length of the cylindroid liquid sheet at the operating pressure 6 $kg.cm^{-2}$ was observed to be 12 mm, measured horizontally from the centre of nozzle orifice. The diameter at the terminal point of the cylindroid was measured to be 10 mm, thereafter liquid sheet commenced to breakup into ligaments and consequently into tiny droplets due to hydrodynamic instability. The nozzle discharge (Q) measured using graduated measuring cylinder and corresponding velocity of flow (v), was found out as 1.4 $mL.s^{-1}$ and 10.19 $m.s^{-1}$ respectively.

The electric field intensity ($E_j$) induced by the charging electrode ($r_e$= 27 mm) at the liquid sheet cylindroid surface of radius $r_c$= 5 mm determined on the basis of generalized coaxial conductive cylindrical capacitor geometry, was found to be $1.0675\times10^{6}$ $V.m^{-1}$.

*4.1.1.1 Salient features of designed ESCU*

The major requirement in liquid particulate charging by induction method was $\tau < t_f$ and for the developed induction charger system, transfer time constant ($\tau = 1.3548 \times 10^{-7}$ s) was found to be much lesser than droplet formation time ($t_f = 1.1776 \times 10^{-3}$ s). This enabled the electrostatic induction spray charging system to induce a substantial image charge on the liquid spray particulates emerging through droplet formation zone successfully. The free surface charge density ($\rho_s$) on the liquid sheet cylindroid due to induced static electricity was found to be $9.4473 \times 10^{-6}$ $C.m^{-2}$ and the analogous spray-cloud current $i_c$ (A) carried by the charged liquid was mathematically predicted to be 3.0228 µA. Another prediction on the basis of applied charging potential (+9 kV) and the liquid flow velocity (10.19 $m.s^{-1}$) led the spray cloud current to the value of 3.0224 µA.

### 4.1.2 Development of variable high voltage power supply

The major components of the dc-dc variable high voltage generator module were Power MOSFET driver circuit, Pulse Width Modulator (PWM) and Line Output Transformer (LOPT or flyback) are discussed in this sub-section.

*4.1.2.1 Development of MOSFET driver based HVDC generator*

The developed voltage multiplier circuit based on a flyback transformer (Fig. 4.1) driven by IRFZ44N MOSFET (Fig. 4.2) was capable of producing the high voltage up to +12 kV DC and could be operated with an input voltage in the range of 3 to 9 V DC. Rechargeable Lithium-ion batteries (four in parallel) of standard 18650 specifications (Fig. 4.3) which had an open circuit voltage of 3.7 V at full charge and a capacity of 12000 mAh was used as the power source to the high voltage generator unit. The electrolytic aluminium axial leaded 16 V DC, 22 mF capacitor was used across the input side of the oscillator as a filter for the input battery voltage.

*4.1.2.2 Pulse width modulation for variable HVDC generator output*

The Pulse Width Modulator (PWM) of 0 to 30 V AC/DC input voltage (Fig. 4.4) was used to regulate the voltage input to the MOSFET oscillator, which in turn

enabled the system to gain variable high voltage output from 1 kV to 12 kV with maximum current output of 30 µA corresponding to the power rating of 360 mW. The high voltage polymer capacitors (2000 V DC, 10 nF) in series (7 nos.) were connected across the output high tension terminals of the LOPT as a filter the ripple and to handle the accidental loading. The standard high tension insulated cable of 3 mm core diameter was used for safe conveyance of high voltage towards the charging electrode.

**Fig. 4.1 Line Output Transformer (LOPT) or flyback transformer**

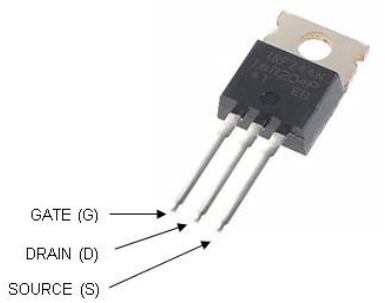


**Fig. 4.2 IRFZ44N Power MOSFET**


**Fig. 4.3 Power source of developed system: Lead acid battery (left) and Li-ion rechargeable battery (right)**

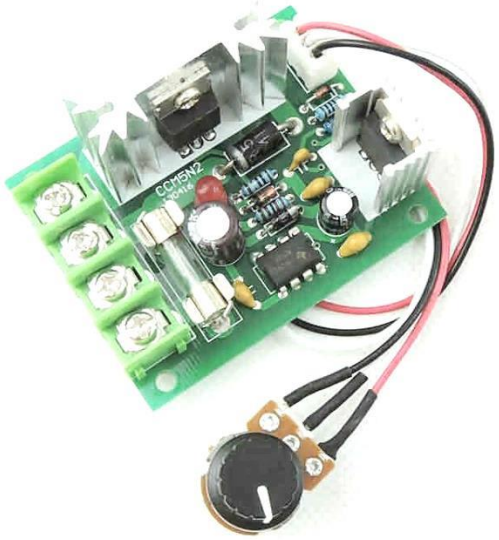

**Fig. 4.4 Pulse Width Modulator (PWM)**

*4.1.2.3 Battery monitoring and management system*

The battery monitoring system with a low voltage alarm was used to observe the instantaneous battery charge and to notify the recharging point. The low battery alarm was set to the safe value of 3.2 V below which the alarm function triggered the beeping sound. The developed portable high voltage power supply weighed about 250 g including batteries.

### 4.1.3 Development of high voltage electrode assembly

The high potential charging copper ring electrode (5 mm thickness, 54 mm diameter) was housed inside an external groove on a cylindrical sleeve fabricated using cast nylon material (Fig. 4.5 and Fig. 4.6). The outer dia. of the electrode carrier sleeve was 73 mm and a gentle gradient was given to the internal surface of the sleeve using taper turning. The converging gradient to the inner surface was provided to increase the air velocity at point where charging electrode and droplet formation zone were located. This ensured that electrode carrier assembly would not retain the tiny droplets due to electrostatic attraction and free of resultant short circuit between nozzle and charging electrode.

**Fig. 4.5 HVDC electrostatic induction charging electrode assembly**

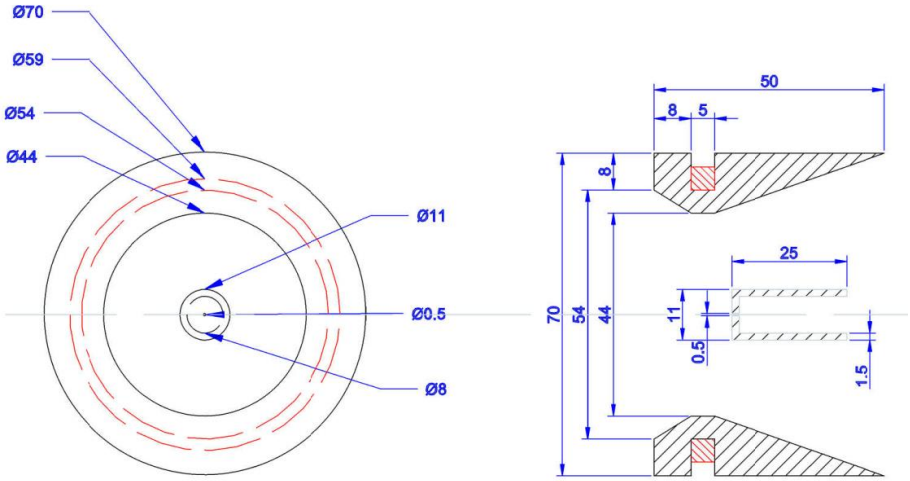


**Fig. 4.6 Constructional details of electrode carrier sleeve**

The intake side of the electrode carrier was having internal diameter of 70 mm and 51 mm on exit side. The cast nylon material with a dielectric strength of 19.7 kV $mm^{-1}$ exhibited excellent electrical insulation properties.

Since, the electrode carrier sleeve was designed and fabricated to fit inside the air blower conduit made of PVC (wall thickness = 2.5 mm, dielectric strength = 14 kV $mm^{-1}$), the high potential electrode was thus insulated from all the sides. This electrically secured geometry was meant to avoid accidental human contact with the high voltage electrode and corrosion of the electrode material due to chemical action and environmental impact.

### 4.1.4 Spray liquid atomization and nozzle characteristics

Selection of the operating pressure for the hydraulic pressure swirl nozzle was done on the basis of droplet spectrum generated. The spay nozzle was operated at (4, 5 and 6 $kg.cm^{-2}$) different pressures to observe the spray droplet spectrum. The droplet size (VMD = 91.36 µm) observed at 6 $kg.cm^{-2}$ was finest possible as compared to droplet size observed at 4 $kg.cm^{-2}$ (170.25 µm) and 5 $kg.cm^{-2}$ (135.61 µm). The droplet spectrum obtained at 6 $kg \cdot cm^{-2}$ operating pressure was the only sub-100 µm facilitating better spray chargeability longer terminal time. Hence, the hydraulic nozzle was assessed for the spray characteristics. The cone angle was found to be 60º at operating pressure of 6 $kg.cm^{-2}$ with the spray swath measured to be 650 mm, when nozzle was operated vertically downwards at an elevation of 700 mm above the flat surface. The volumetric discharge of the selected spray nozzle was measured to be 2 $mL\ s^{-1}$.

A self-priming high pressure low discharge 80 W diaphragm pump operating on 12V DC was employed for liquid delivery to the hydraulic spray nozzle. The pump had maximum discharge rate of 8 $L\ min^{-1}$ and an auto cut-off system set at a pressure of 8 $kg.cm^{-2}$ for overload protection. A solid cone hydraulic spray nozzle made of ABS (Acrylonitrile Butadiene Styrene) material was selected for liquid atomization.

The nozzle had an orifice diameter of 0.5 mm operating within a pressure range of 3.0 to 8.0 $kg.cm^{-2}$ and discharge rate between 5 to 7.5 $L\ h^{-1}$. The nozzle was installed concentrically by means of brass fittings inside a PVC conduit having internal diameter of 73 mm. The liquid delivery to the nozzle was made using compression fitting connector and high pressure flex PVC tubing from the delivery side of the diaphragm pump.

A dual channel differential valve was used to provide optimum hydraulic pressure across the nozzle and the excess flow was bypassed to the solution tank. This bypass flow could be used to agitate the spray solution continuously throughout the operation.

### 4.1.5 High speed air blower unit

An Electric Ducted Fan (EDF) was selected as the main component to develop the high-speed air blower (Fig. 4.7). The internal diameter of the ducted fan was 70 mm with 12 blades mounted on DC synchronous permanent magnet motor with KV1850 rpm rating. The motor was driven by the Universal Battery Eliminator Circuit (UBEC) integrated with Electronic Speed Controller (ESC) which could be operated with 7.5 to 25 V DC power supply. The driver module was coupled with a Servo Consistency Master (SCM) to control the rotor speed manually for variable rpm.

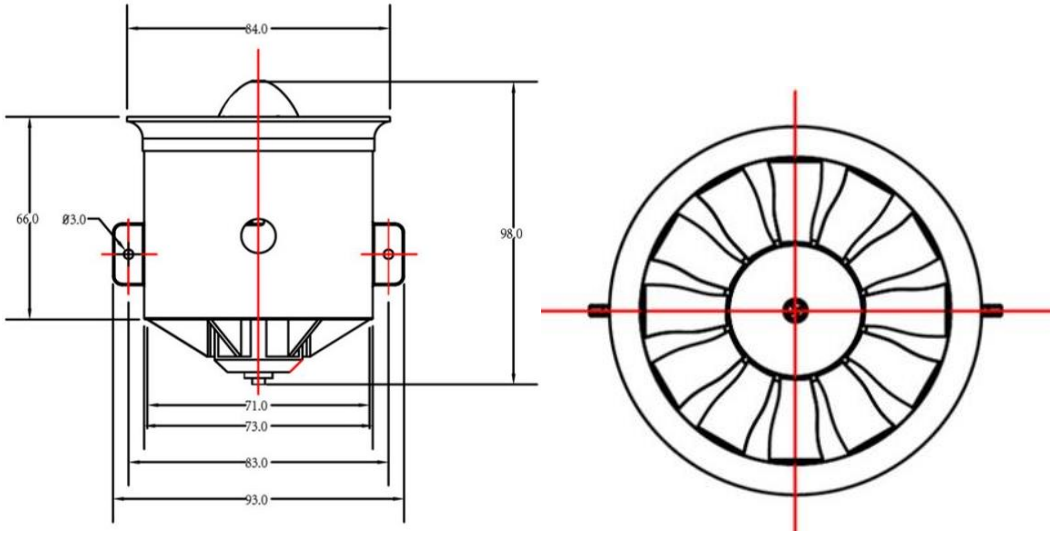


**Fig. 4.7 Constructional details of brushless DC motor mounted EDF unit**

The maximum rotary speed that could be achieved at no-load condition was the product of rotational speed rating of motor (KV1850) and voltage output (12V) from UBEC-ESC module i.e. 22200 rpm. The maximum air discharge from the EDF module at full throttle was recorded as 0.088 $m^3 s^{-1}$ with air delivery speed of 23 $m.s^{-1}$. The power source used to run the EDF was 12V 9 Ah lead acid battery and air velocity was recorded using KM908-MK1 digital anemometer.

The constructional details of the developed handheld electrostatic spray gun are illustrated in Fig. 4.8.

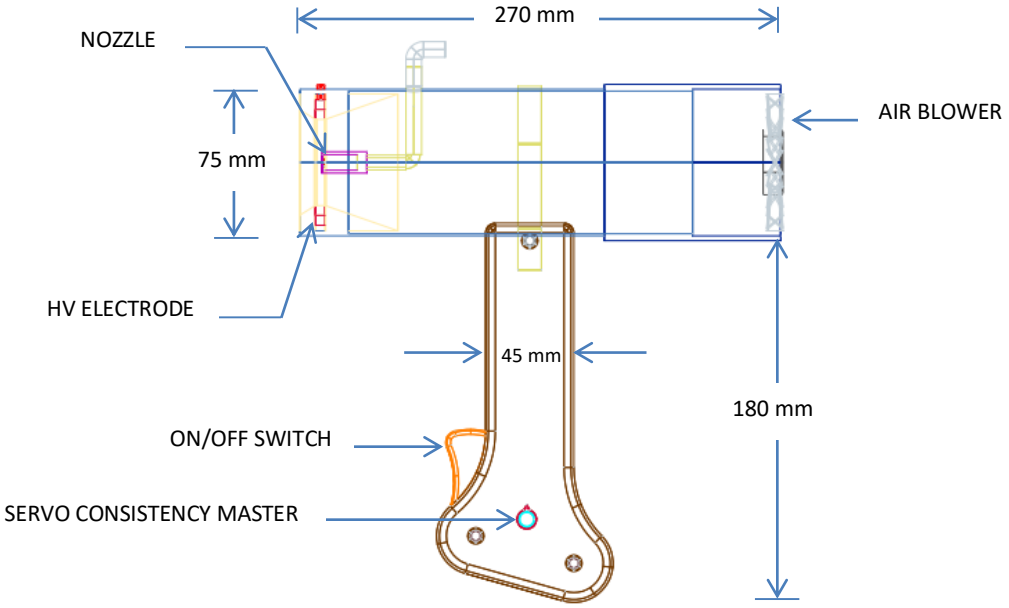


**Fig. 4.8 Constructional details of electrostatic spray gun**

## 4.2 LIGHT WEIGHT BACKPACK ASSEMBLY

In order to keep the overall weight of the sprayer as low as possible, a compact backpack frame was fabricated using 25 mm CPVC tubes with three horizontal compartments. The compartments were made using PVC board of 3 mm thickness. The lower compartment accommodated the battery, diaphragm pump and the pressure control system.

The overall dimensions of the backpack frame were 210×260×430 mm (L×B×H) as illustrated in Fig. 4.9 and weighed about 1.0 kg including straps and fittings. The high voltage circuitry was installed inside the middle compartment and the solution tank of 5 L capacity was mounted at the top compartment using velcro straps. The shoulder straps from the regular backpack were used to wear the frame as shown in Fig. 4.10.

### 4.2.1 Assembly of developed electrostatic sprayer prototype

The developed battery operated electrostatic sprayer comprised of two parts *viz.* handheld electrostatic spray gun and backpack assembly. The spray nozzle, embedded charging electrode assembly, EDF and the handle grip were the components of developed handheld electrostatic spray gun. While, the backpack assembly comprised of the spray solution tank, HVDC power supply, battery,

diaphragm pump, control valve and the pressure gauge. The developed prototype weighed about 10.00 kg (dry weight). The various components of the developed battery operated backpack type electrostatic sprayer are described in detail in Table 4.1 and Fig 4.11.

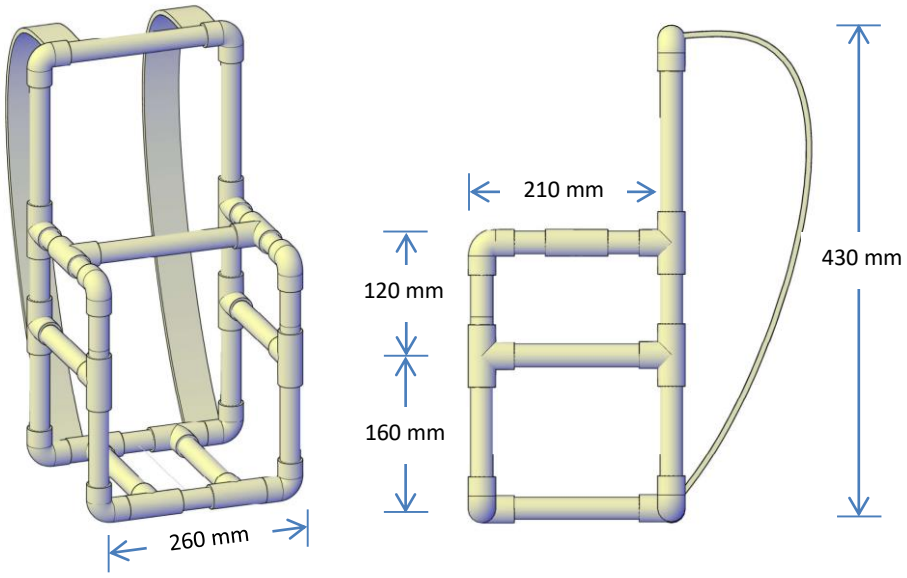


**Fig. 4.9 Light weight backpack frame**

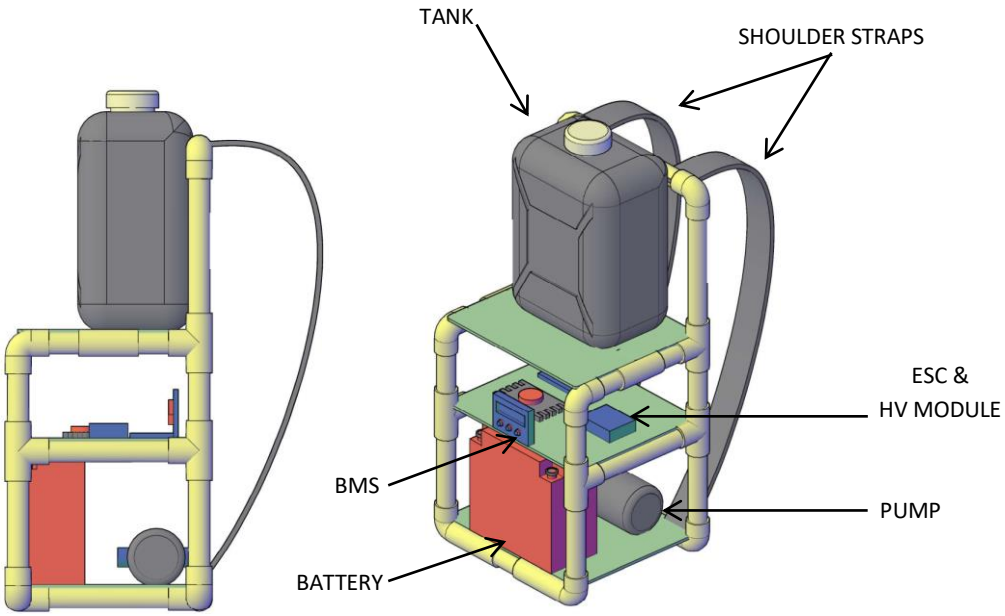


**Fig. 4.10 Design of backpack assemply**

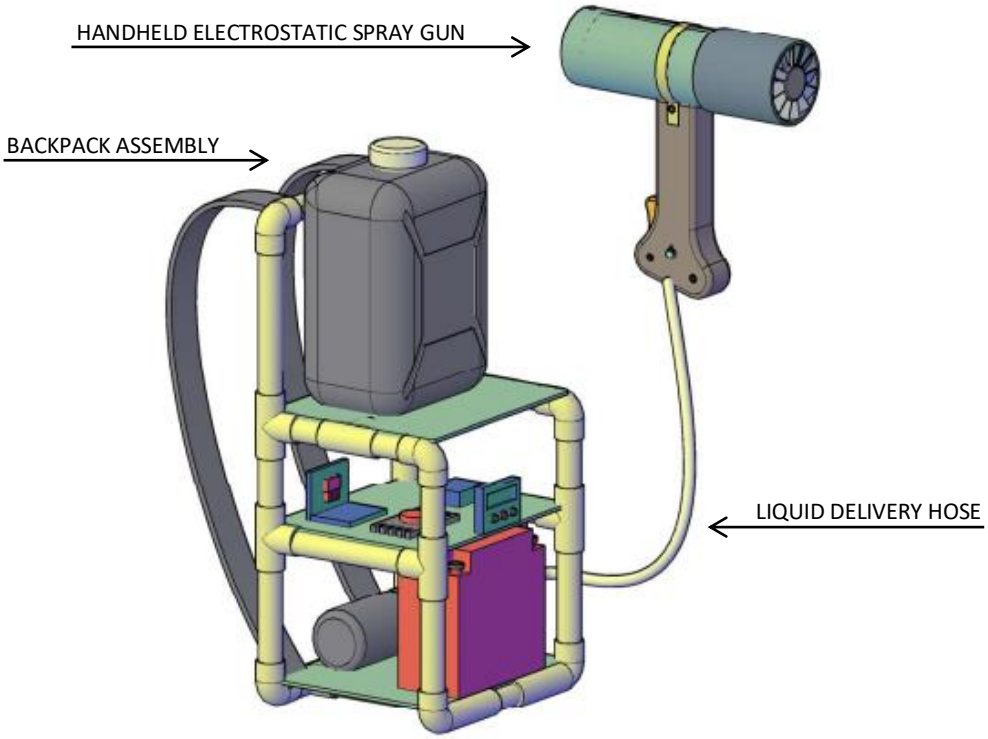


**Fig. 4.11 Conceptual design of battery operated electrostatic sprayer**

**Table 4.1 Components of the developed prototype**

| Sl. No. | Components | | Specifications |
|---|---|---|---|
| 1. | Handheld electrostatic spray gun | : | Length: 270 mm<br>Weight: 450 g |
| | a. Spray nozzle | : | Type: Hydraulic pressure swirl<br>Orifice diameter: 0.5 mm<br>Discharge: 2 mL $s^{-1}$ at 6 kg $cm^{-2}$ |
| | b. EDF unit | : | Diameter: 70 mm<br>No. of blades: 12<br>Motor type: PM-BLDC (KV1850)<br>Operating voltage: 7.5 to 25 V DC<br>ESC: UBEC 80 A |
| | c. Charging electrode | : | Material: Copper<br>Diameter: 54 mm |

| | | | |
|---|---|---|---|
| | | | Thickness: 5 mm (square cross-section) |
| | d. Electrode carrier sleeve | : | Material: Cast nylon<br>Diameter: Intake side – 70 mm,<br>Exit side – 51 mm<br>Electrode placement groove: External<br>Dielectric strength: 19.7 kV $mm^{-1}$ |
| 2. | Backpack assembly | : | Overall dry weight: 9.50 kg |
| | a. Backpack frame | : | Overall dimensions (L×B×H): 210×260×430 mm<br>Material: CPVC 25 mm pipe outer dia.<br>Weight: 1 kg |
| | b. Tank (PVC) | : | Capacity: 5 L |
| | c. HVDC power supply | : | Topology: Resonant flyback transformer<br>Oscillator: IRFZ44N Power MOSFET<br>Input voltage: 3 to 9 V DC<br>Output voltage: 1 kV to 12 kV DC<br>Max. power output: 360 mW |
| | d. Battery | : | 12V 9 Ah lead acid |
| | e. Pump | : | High pressure diaphragm (12V DC)<br>Max. current input: 6 A<br>Max. pressure: 8 kg $cm^{-2}$<br>Max. Discharge: 8 L $h^{-1}$ |
| | f. Liquid delivery hose | : | Internal diameter: 10 mm |
| | g. Pressure control valve | : | 10 m brass ball valve |
| | h. Pressure gauge | : | Graduated round dial. (14 kg $cm^{-2}$ max.) |

| | | |
|---|---|---|
| i. High tension wire | : | Silicone cable, 22 stranded,<br>3.5 mm outer dia.,<br>Max. insulation strength 30 kV.,<br>Max. operating temperature 105º C. |
| j. Battery management system | : | 3 digit LCD display,<br>3.2 V low voltage alarm |

The variable speed control of the EDF unit enabled us to select the convenient air flow rate required to achieve better level of spray conveyance for the varying crop conditions. The air blower was so light weight and smaller, so that it could be accommodated inside the handheld electrostatic spray gun (Fig. 4.12 and 4.13).

This arrangement minimized the losses that could occur in a longer air delivery duct which could have drastically reduced the efficiency of the axial air blower. Moreover, the developed air assistance system was fully battery driven ducted axial blower and triggered a little to no vibrations during the course of operation. The light weight handheld spray gun was observed to be convenient to the operator while changing the stroke (direction) of the spray during operation.

The automotive grade lead acid battery (12V, 9 Ah) housed inside the backpack frame (Fig. 4.14) offered a continuous operating time of two hours at full charge and took around three to four hours to recharge with 14.5 V DC, 1 A industrial battery charger. Whereas, the lithium-ion battery employed for powering HVDC generator unit offered a quite longer duty period of twelve hours, since there was only a little amount of current being drawn to drive the generator. The lithium battery bank took approximately two hours to reach the full charge level from 20 per cent discharged potential at the charging conditions of 5 V DC with 0.5 A current input.


**Fig. 4.12 Electric Ducted Fan (EDF)**

**Fig. 4.13 Developed air assisted electrostatic spray gun**

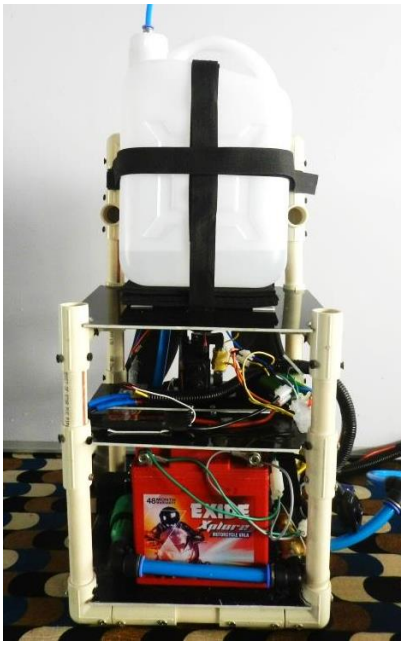

**Fig. 4.14 Backpack unit of developed electrostatic sprayer**

## 4.3 ANALYSIS OF SPRAY DROPLET SPECTRUM

The volumetric distribution of the spray droplet spectrum revealed that volume median diameter (VMD or $DV_{50}$) of the spray was 91.36 µm, while $DV_{10}$ = 60.21 µm and $DV_{90}$ = 116.21 µm as illustrated in Fig. 4.15. Also the number median diameter was (NMD) found to be 66.65 µm, which was when related to the VMD, resulted in the uniformity coefficient (UC) of 0.7299. Also, the relative span (RS) of the spray spectrum was found to be 0.6129.

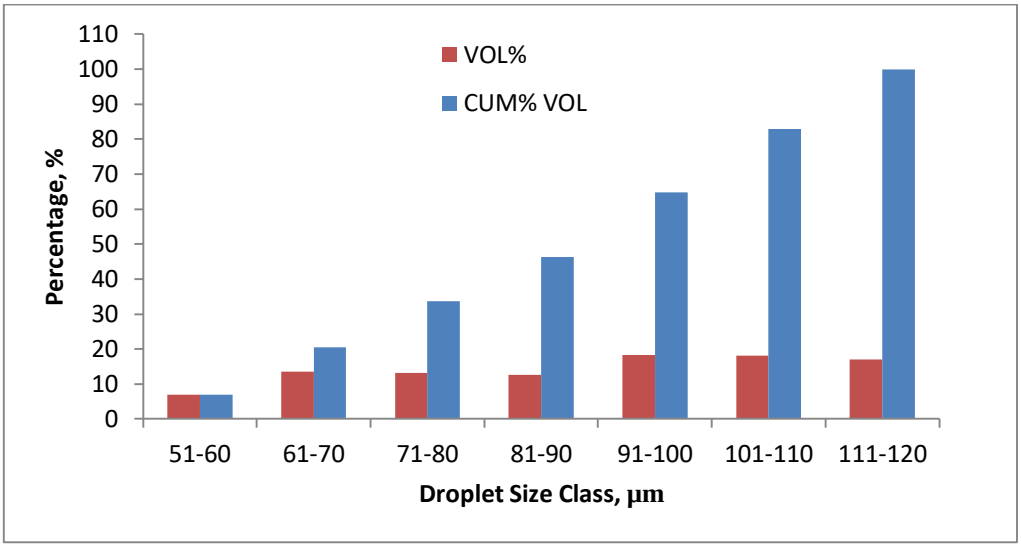


**Fig. 4.15 Volumetric distribution of spray droplet spectrum**

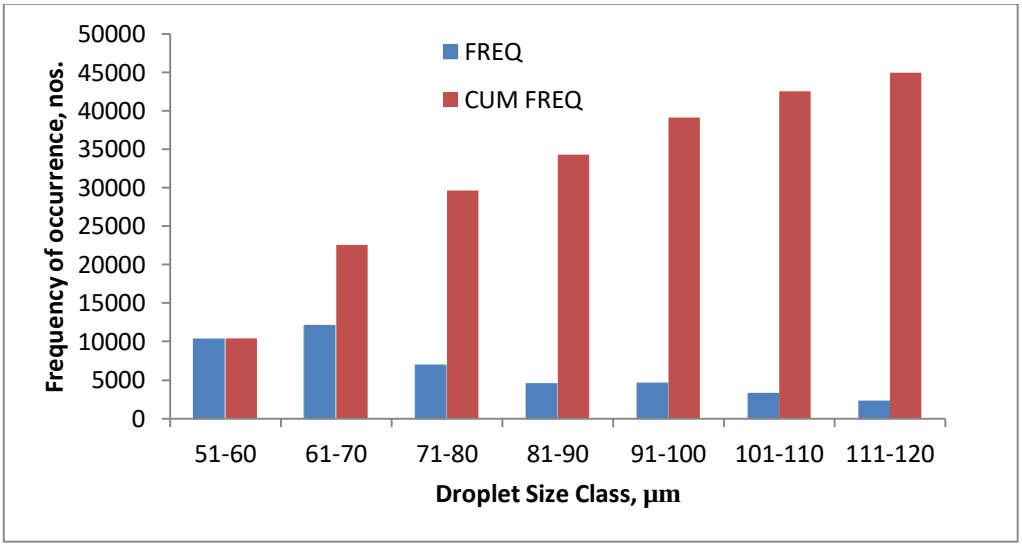


**Fig. 4.16 Frequency distribution of spray droplet spectrum**

The spray droplet spectrum was analyzed for the frequency distribution for individual class and cumulative frequency as illustrated in Fig.4.16. The maximum frequency was observed for the droplet size class of 61-70 µm, followed by class of 51-60 µm. The droplet size range from 51-80 µm covered the 2/3$^{rd}$ portion of the frequency distribution, whilst the range of droplet size 81-120 µm contributed only 1/3$^{rd}$ to the total distribution.

## 4.4 MEASUREMENT OF SPRAY CLOUD CURRENT

The developed electrostatic induction spray charging system was assessed for its effective spray chargeability with respect to different levels of charging electrode potentials and assisting air velocity at constant nozzle discharge.

### 4.4.1 Calculation of Charge to Mass Ratio (CMR)

The observed Volume Median Diameter (VMD or $D_{V50}$) was 91.36 µm and the charge carried by a droplet ($q_p$) could be predicted theoretically as $1.539\times10^{-11}$ C (Section 3.1.2). The ratio of droplet charge and mass of the droplet gave the theoretical CMR to the value of 42.90 mC kg$^{-1}$.

However, the threshold value of CMR that could be attained practically given by Rayleigh limit ($q_{max}$) was found to be 15.559 mC.kg$^{-1}$, by considering the agricultural airborne liquid particles having surface tension $71.99\times10^{-3}$ N.m$^{-1}$ and permittivity of air $8.85\times10^{-12}$ C$^2$.N$^{-1}$.m$^{-2}$ at 30ºC.

### 4.4.2 Spray chargeability of the developed electrostatic spray charger

Spray cloud current measurement was essential to validate and quantify the performance of the developed spray charging system. In the laboratory experimental setup, the spray cloud current was measured using charge collector device coupled with digital multimeter, which was recorded to the maximum value of 3.3 µA at charging electrode potential of 9 kV. The charge to mass ratio was determined by taking ratio of the measured constant spray cloud current (2.5µA) and the collected mass of spray liquid with respect to time (1.4 mL.s$^{-1}$). The maximum CMR level practically achieved was 1.79 mC.kg$^{-1}$, similar to the spray chargeability reported (2.35 mC.kg$^{-1}$) by Yu *et al.* (2011) and (0.37 mC.kg$^{-1}$) Mamidi *et al.,* (2012) respectively.

*4.4.2.1 Effect of charging electrode potential on CMR*

The spray cloud current and in turn the CMR was observed to be increasing from 0.46 mC.kg$^{-1}$ to 1.79 mC.kg$^{-1}$ with increase in electrode potential from 1 kV to 9 kV respectively at an air velocity of 10 m s$^{-1}$. However, further increment in the electrode potential from 9 kV to 12 kV resulted in abrupt fall in the CMR value from 1.79 mC.kg$^{-1}$ to 0.61 mC.kg$^{-1}$. This could be the result of reverse ionization and wetting of electrostatic spray gun due to excessive electrode potential.

The trajectory of emerging spray particles might have been so influenced due to excessive electrode potential that they were been driven back towards the electrode. The deposition of tiny spray liquid particles onto the charging electrode assembly hindered the process of electrostatic charge induction which in turn could be the cause of abrupt decline in the CMR beyond the electrode potential of 9 kV.

*4.4.2.2 Effect of assisting air velocity on CMR*

The spray assisting air velocity was observed to be influencing the spray chargeability of the electrostatic induction charger. The CMR value of charged spray followed the increasing trend with the increase in the assisting air velocity. The CMR of the charged spray at optimum charging potential (9 kV) increased respectively as 1.15 mC.kg$^{-1}$, 1.54 mC.kg$^{-1}$ and 1.79 mC.kg$^{-1}$ with respect to the air assistance velocity of 5 m s$^{-1}$, 7.5 m s$^{-1}$ and 10 m s$^{-1}$.

The gradual improvement in the CMR value at a constant electrode potential and incremental air velocity might have expedited the spray particles to escape swiftly through the strong electrostatic field inside the spray charging gun. This could be the reason behind enhanced spray chargeability without excessive wetting of charging electrode.

*4.4.2.3 Charging efficiency of the developed electrostatic spray charger*

The charging efficiency of the developed electrostatic induction spray charging system at maximum CMR of 1.79 mC.kg$^{-1}$ observed in terms of percentage of Rayleigh charge limit (15.91 mC.kg$^{-1}$) achieved was found to be 11.25 per cent at electrode potential of 9 kV.

## 4.5 DEPOSITIONAL CHARACTERISTICS OF CHARGED SPRAY

The developed electrostatic sprayer was assessed for the depositional characteristics as described in the Section 3.7. The data generated through the image processing of spray impinged photographic paper strips were analyzed for quantitative evaluation of adaxial (leaf above surface) and abaxial (leaf underneath surface) deposition. The specific methods of spray application were *viz.* the developed Air-assisted Electrostatic Spraying System (AESS), Non-electrostatic Air-assisted Spraying System (NAESS) and the conventional knapsack sprayer (CONV). Also the deposition efficiency and the effect of canopy location on spray deposits for the above mentioned spraying methods are discussed as follows:

### 4.5.1 Adaxial and abaxial deposition on plant target

The image processing analysis revealed that, there was approximately three-fold increase in the spray deposits per square centimeter of average leaf top surface area with electrostatically charged spray (327 deposits $cm^{-2}$) compared to conventional knapsack sprayer (102 deposits $cm^{-2}$). The electrostatic wrap-around effect was also observed to be spectacular (Fig. 4.17, 4.18). When charging system was turned on, a massive deposition on the underneath leaf surface was observed (Fig. 4.19). The average droplet population on the surface was observed as 250 droplets per $cm^2$. These results confirm with the findings reported by Fritz *et al.* (2009) and Mishra *et al.* (2014).

In both the cases of developed spraying system without electrostatic charging and conventional manually operated knapsack sprayer, no deposition on abaxial leaf surface was observed (Fig. 4.20 & 4.21). The conventional sprayer executed excess deposition on adaxial leaf surface which caused undesirable dripping of applied spray solution (Fig. 4.22).

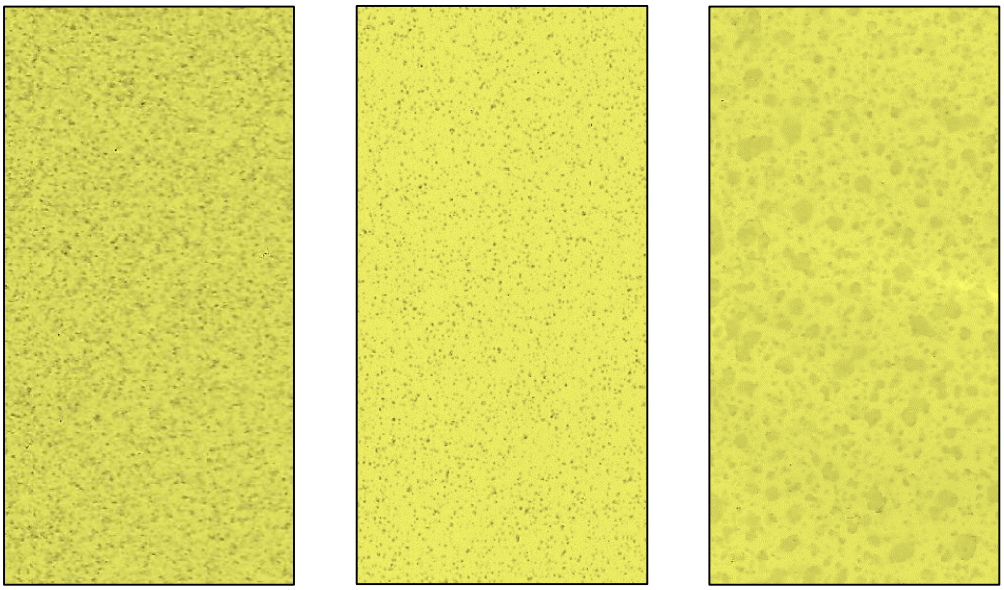

(a) (b) (c)

**Fig. 4.17 Adaxial deposition (a) Electrostatic, (b) Uncharged and (c) Conventional spray**

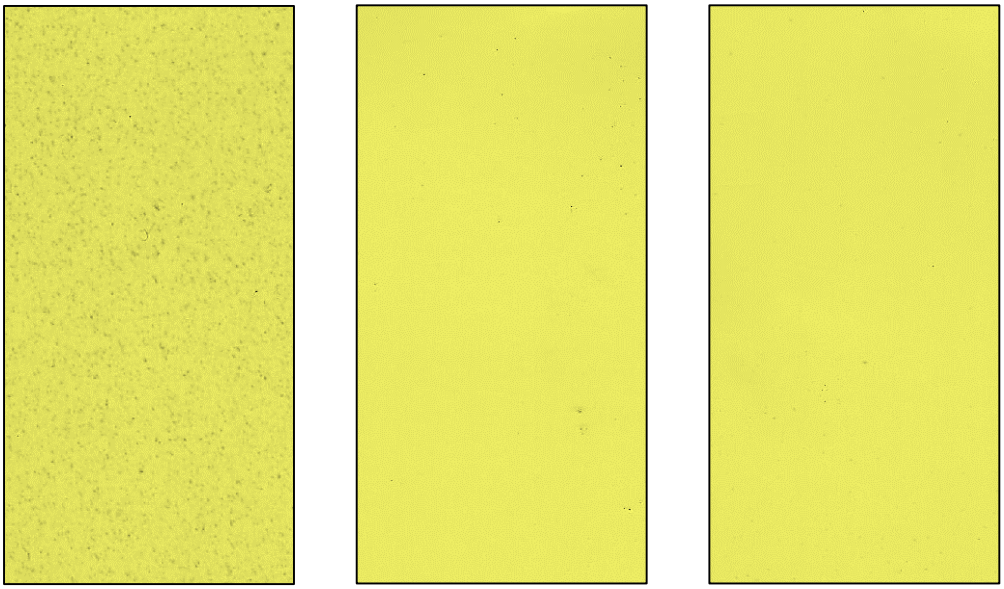

(a) (b) (c)

**Fig. 4.18 Abaxial deposition (a) Electrostatic, (b) Uncharged and (c) Conventional spray**

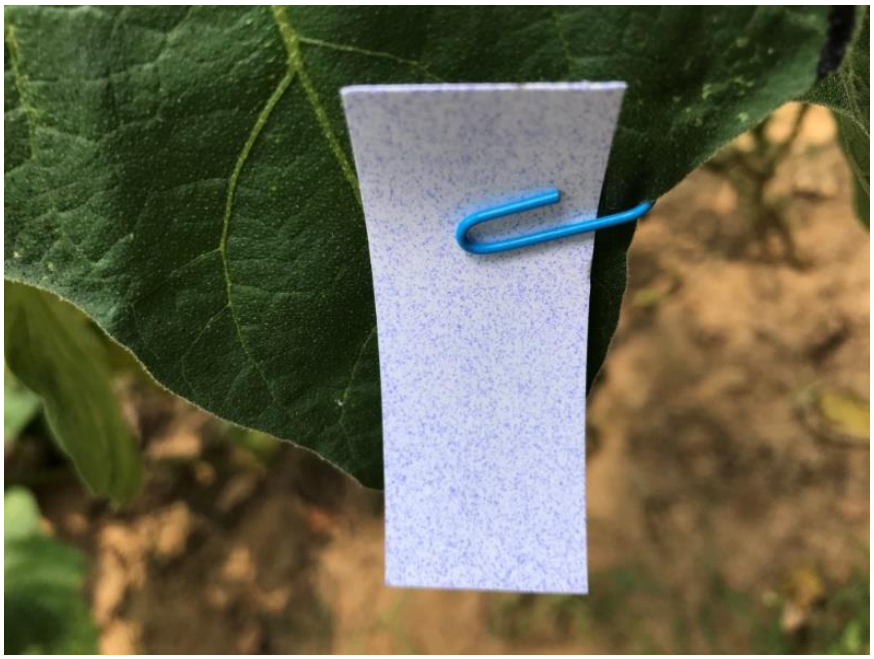

**Fig. 4.19 Adaxial deposition by electrostatic spraying**

**Fig. 4.20 Abaxial deposition by electrostatic spraying**

**Fig. 4.21 Abaxial spray deposition using uncharged spray**

**Fig. 4.22 Dripping of spray liquid using conventional sprayer**

### 4.4.2 Assessment of distribution of applied spray volume on the target

The developed system was evaluated for spray deposit distribution in terms of on-target, ground and drift in comparison with the uncharged and conventional spray application method.

*4.4.2.1 Deposition efficiency*

The spray deposit distribution of electrostatic spray was accounted in terms of percentage of total spray volume applied as 50.62 per cent on-target, 10.09 per cent on ground and 39.27 per cent in the form drift compared to the conventional knapsack sprayer with corresponding percentage distribution as 28.20, 34.81 and 36.97 per cent respectively (Fig. 4.23).

It was clearly observed that the electrostatic spray charging improved the on-target deposition by 1.8 times than that of conventional spraying. However, the developed spraying system without electrostatic charge resulted in the excess ground (15.41 per cent) and drift (56.40 per cent) losses resulted in on-target deposition of 28.19 per cent. The excess off-target movement of applied spray volume might have occurred due to finer droplet spectra which was vulnerable to wind drift in absence of directorial electrostatic force.

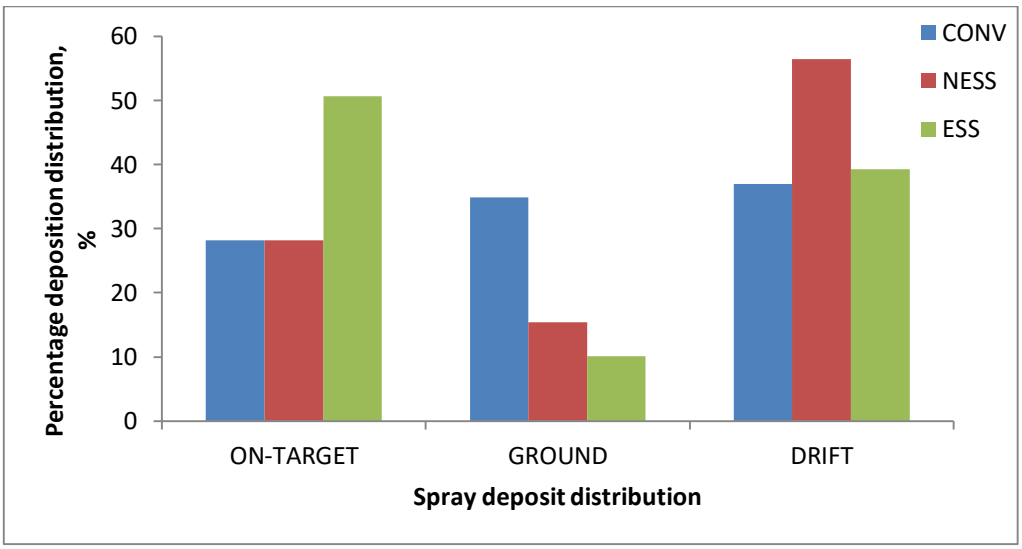


**Fig. 4.23 Comparison of applied spray volume distribution**

The environmental contamination could be narrowed down with the reduced off-target movement of the spray chemicals. It was observed that the developed electrostatic spraying system reduced the amount of spray drift and ground deposition by 31.22 per cent (from 538 g $ha^{-1}$ to 370 g $ha^{-1}$) as compared to the conventional manually operated knapsack sprayer.

*4.4.2.2 Effect of canopy location on spray deposition*

Approximately three-fold increment in upper canopy deposition was observed with electrostatically charged spray particles (350 deposits $cm^{-2}$) as compared to conventional spraying method (100 deposits $cm^{-2}$). Similar trend was observed in the cases of middle and lower canopy depositions.

However, the abaxial leaf surface deposition in case of charged spray was found to be decremented when analyzed for upper (300 - 350 deposits $cm^{-2}$), middle (200 - 250 deposits $cm^{-2}$) and lower canopy (50 - 100 deposits $cm^{-2}$) leaves respectively.

## 4.5 DETERMINATION OF LEAF AREA INDEX (LAI)

The average Total Leaf Area per Plant (TLAP) and corresponding Plant Canopy Area (PCA) were measured using 'EasyLeaf' image analysis software. These values were found to be 6425.45 $cm^2$ (Fig. 24) and 3894.21 $cm^2$ (Fig. 4.25) respectively. The average leaf area index (LAI) was observed to be 1.65 for brinjal crop and sprayer was calibrated to cover the 1 ha of the crop with 150 litres of spray solution on the basis of existing practice of applying spray solution at the rate of 500 L $ha^{-1}$. Moreover, the computer based image analysis process provided a non-destructive method to measure TLAP and PCA.

The above assessment revealed that the developed air-assisted electrostatic sprayer enabled us to cut short the water requirement for spraying per unit area by $1/3^{rd}$, which meant to save tremendous amount of water being used in conventional methods of agricultural spraying. This can be very advantageous to the farmer as it not only saves water but also the labour required.

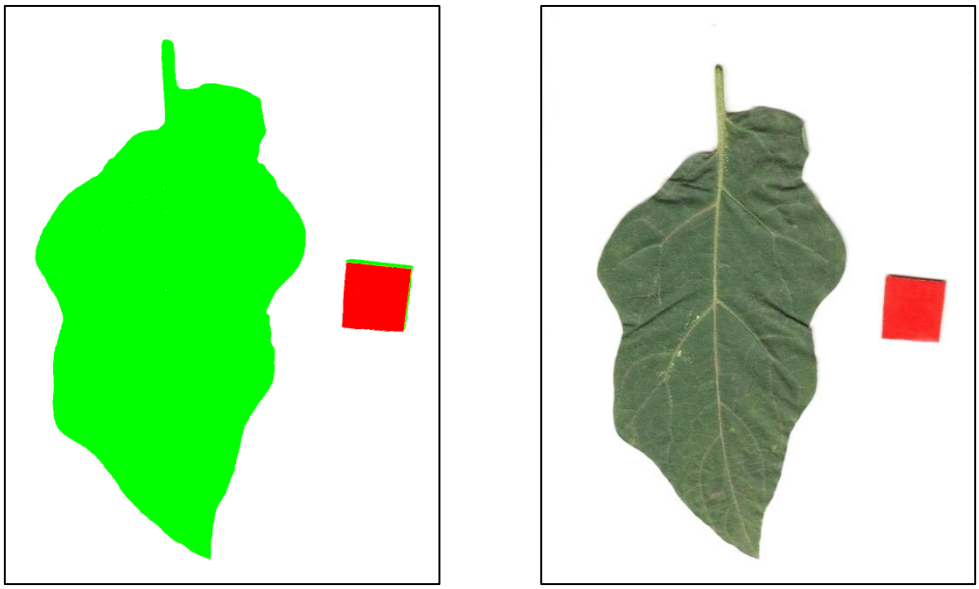

**Fig. 4.24 Image analysis for measurement of individual leaf area using EasyLeaf software**

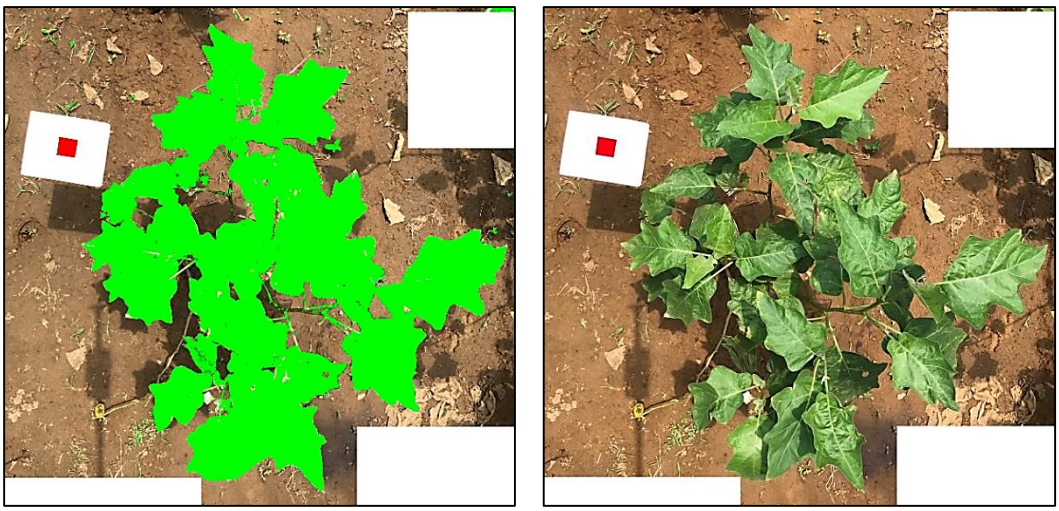

**Fig. 4.25 Image processing of plant canopy area using EasyLeaf software**

4.6 PESTICIDE RESIDUE ANALYSIS AND BIOLOGICAL EFFICACY

The fruit and leaf samples from the treated plants were collected on zeroth, third, fifth and seventh day of spray application. The standard method of chemical extraction was followed in order to determine the pesticide residues in the plant body using GC-ECD (Gas Chromatograph – Electron Capture Detector), Agilent Technologies available at the Pesticide Residue Testing Laboratory, College of

Horticulture, Vellanikkara. The results were compared between the above spray treatments to quantify the field performance of the developed spraying system.

### 4.6.1 Quantification of Active Ingredient (A.I.) deposition on plants

The results obtained from GC-ECD technique shown that, in spite of large spray volume (500 L $ha^{-1}$ @ 1.5 mL $L^{-1}$ pesticide dose) was being used to cover the crop canopies using conventional sprayer, the average content of active ingredient (47.37 ng.$\mu L^{-1}$) found in the plant body samples was much lesser than that of achieved using electrostatic spraying (147.63 ng.$\mu L^{-1}$) with the same dose of active ingredient per hectare (150 L $ha^{-1}$ @ 5 mL $L^{-1}$). The pesticide residues observed on $0^{th}$, $3^{rd}$, $5^{th}$ and $7^{th}$ day are illustrated in Fig. 4.26 to Fig.4.29.

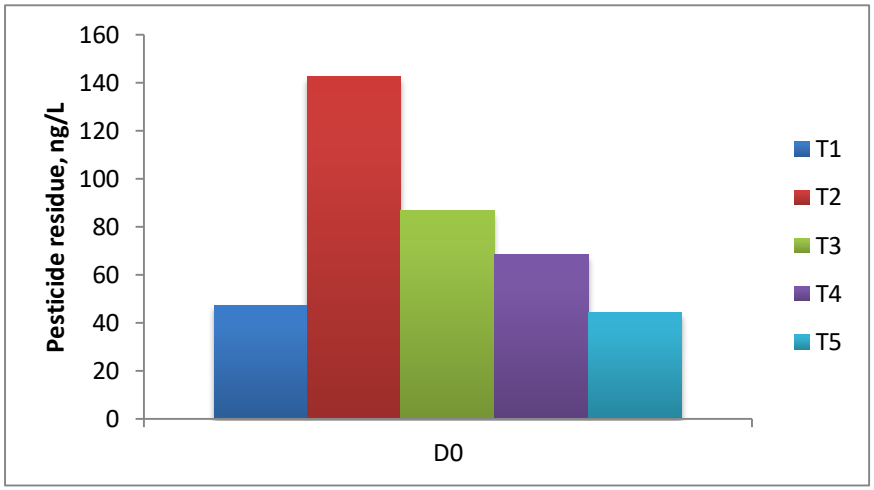


**Fig. 4.26 Pesticide residue observed on $0^{th}$ day of spraying**

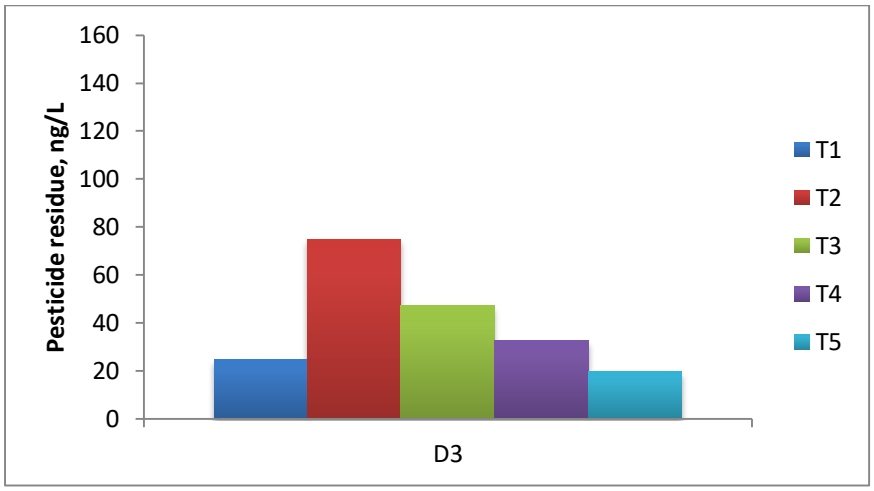


**Fig. 4.27 Pesticide residue observed on $3^{rd}$ day of spraying**

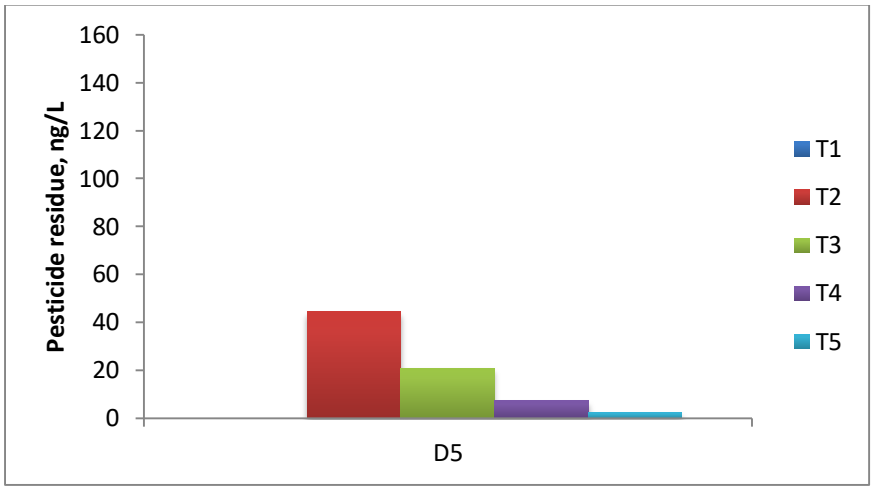


**Fig. 4.28 Pesticide residue observed on 5th day of spraying**

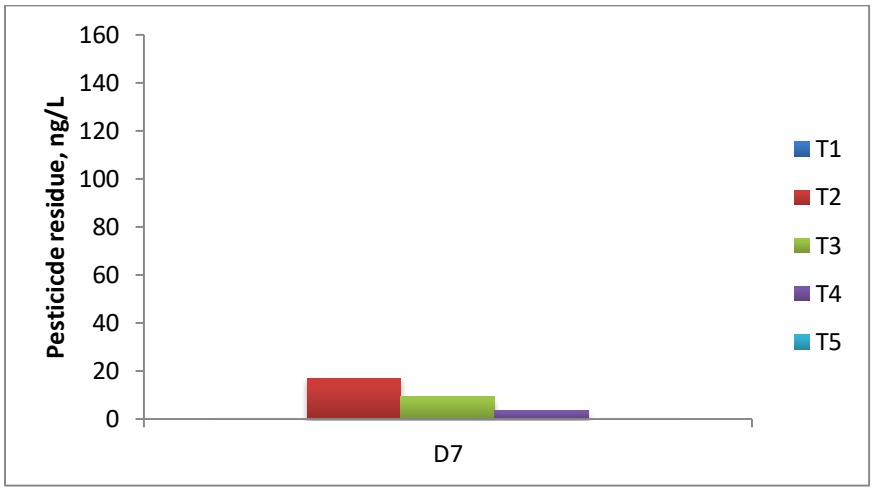


**Fig. 4.29 Pesticide residue observed on 7th day of spraying**

There was nearly about three-fold increase observed in the active ingredient (pesticide residue) present in the plant body on the day of spray application. Even with the reduced dosage of active ingredient (3 mL $L^{-1}$), developed electrostatic spraying resulted in 44.38 per cent increase of pesticide residue in the samples compared to conventional spraying method.

### 4.6.1 Biological efficacy

In the case of conventional spraying, GC-ECD analysis of the plant body samples collected on subsequent days shown that gradual reduction in the pesticide residue reached to null point on 5th day after spray application. On the other hand,

electrostatic spraying had shown 44.53 ng.µL$^{-1}$ and 16.93 ng.µL$^{-1}$ pesticide residues on 5$^{th}$ and 7$^{th}$ day respectively.

The longer residence of pesticide residue on the target plant could have helped the electrostatic spraying treatment to reduce or terminate the pest activity better than that of the conventional spraying method. The Fig. 4.30 illustrates the residual pesticide content observed for different spray treatments *viz.* $T_1$ - Conventional high volume sprayer (1.5 mL L$^{-1}$) 500 L ha$^{-1}$, $T_2$ - Electrostatic sprayer (5 mL L$^{-1}$) 150 L ha$^{-1}$, $T_3$ - Non-electrostatic sprayer (5 mL L$^{-1}$) 150 L ha$^{-1}$, $T_4$ - Electrostatic sprayer (3 mL L$^{-1}$) 150 L ha$^{-1}$ and $T_5$ - Non-electrostatic sprayer (3 mL L$^{-1}$) 150 L ha$^{-1}$.

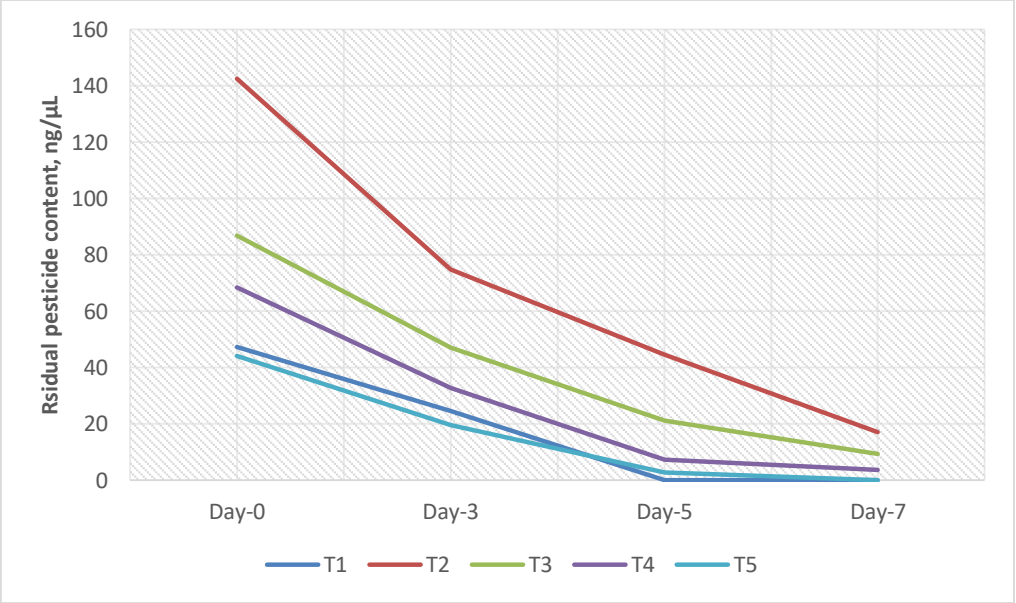


**Fig. 4.30 Residual pesticide content w.r.t. day of application**

The biological efficacies of concerned spray treatments were determined in terms of number of fruit bore holes before and one week after pesticide application. The electrostatic spraying was found to be supervened into biological efficacy of 54.62 per cent over the conventional spraying. Even the reduced dose of active ingredient with the charged spray application resulted into a superior bio-efficacy of 32 per cent as compared to the conventional spraying. The percentage increase in the fruit bore holes was taken as the biological efficacy.

## 4.7 STATISTICAL ANALYSIS

The results obtained from the experimental data were statistically analyzed and reported in terms of analysis of variance (ANOVA) using R-studio, an open source computer environment based on R-language and Tukey-HSD (Honestly Significant Difference) test was conducted for comparison of means.

### 4.7.1 Effect of electrode potential on spray chargeability

*4.7.1.1 ANOVA of CMR w.r.t. electrode potential*

The charging potential of induction electrode significantly influenced the CMR values at the constant flow rate of 1.4 mL $s^{-1}$ and the insignificance within the replications shown the validity of the experimental data as reported in the ANOVA Table. 4.2.

**Table 4.2 ANOVA for effect on CMR w.r.t. electrode potential**

| | dF | Sum Sq. | Mean Sq. | F value | P value |
|---|---|---|---|---|---|
| REP | 2 | 0.245 | 0.1223 | 14.09 | 0.1152 |
| VOLT | 11 | 6.684 | 0.6076 | 70.00 | 1.68e-14 *** |
| Residuals | 22 | 0.191 | 0.0087 | | |
| Significance codes: 0 '***' 0.001, '**' 0.01, '*' 0.05, '.' 0.1 and ' ' 1 | | | | | |

The graphical representation of the ANOVA for the effect of electrode potential on CMR of charged spray cloud describes the variation of the residual means vs. fitted trend line as illustrated in Fig. 4.31.

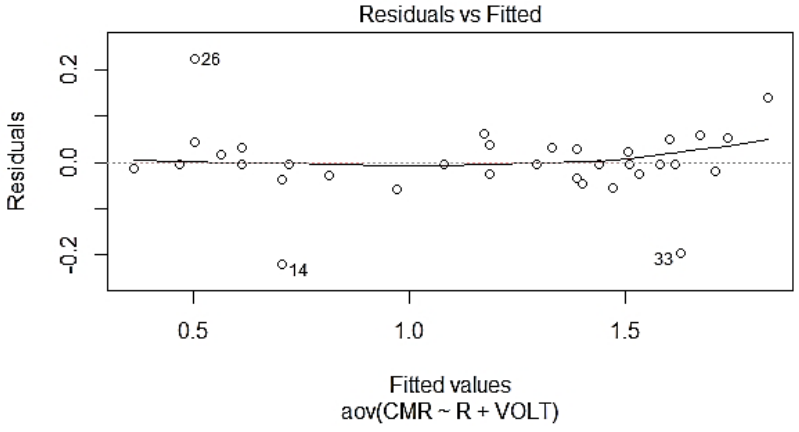


**Fig. 4.31 ANOVA Plot of effect on CMR w.r.t. electrode potential**

*4.7.1.2 Comparison of means*

The factor means obtained from ANOVA were compared using Tukey-HSD test to determine the significances of different interactions between the charging electrode potentials at 5 per cent significance level as reported in Table 4.2. The developed electrostatic spray charging system could able to generate CMR of 1.79 $mC.kg^{-1}$ maximum at a charging electrode potential of 9 kV which was significantly superior to all other electrode potential levels followed by 8 kV and 7 kV.

The mean CMR levels obtained at 7 kV, 6 kV and 10 kV were similar, but were significantly higher than 4 kV, 5 kV and 11 kV, which were significantly similar. The charging electrode potentials of 1 kV, 2 kV, 3 kV and 12 kV shown the similar levels of CMR and were significantly lower than all other electrode potential levels.

**Table 4.3 Tukey-HSD test for effect of electrode potential on CMR**

| Sl. No. | Electrode potential, kV | Mean CMR, $mC \cdot kg^{-1}$ |
|---|---|---|
| 1. | $V_9$ | $1.79^{a}$ |
| 2. | $V_8$ | $1.61^{b}$ |
| 3. | $V_7$ | $1.57^{c}$ |
| 4. | $V_6$ | $1.50^{cd}$ |
| 5. | $V_{10}$ | $1.43^{cd}$ |
| 6. | $V_5$ | $1.28^{de}$ |
| 7. | $V_{11}$ | $1.28^{de}$ |
| 8. | $V_4$ | $1.07^{e}$ |
| 9. | $V_3$ | $0.71^{f}$ |
| 10. | $V_{12}$ | $0.61^{f}$ |
| 11. | $V_2$ | $0.61^{f}$ |
| 12. | $V_1$ | $0.46^{f}$ |
| Significance level, $\alpha = 0.05$ | | |

### 4.7.2 Effect of spray treatments on pesticide residue in plant body

*4.7.2.1 ANOVA of effect of treatments on pesticide residue*

The ANOVA summary reported in Table 4.3 ensured the validity of the experimental data owing to insignificance within the replications. The interactions within the treatments were observed to be clearly significant.

**Table 4.4 ANOVA for effect of treatments on pesticide residue**

| | Df | Sum Sq. | Mean Sq. | F value | P value |
|---|---|---|---|---|---|
| REP | 4 | 395 | 99 | 0.096 | 0.984 |
| TREAT | 4 | 38403 | 9601 | 9.306 | 2.38e-06 *** |
| Residuals | 91 | 93880 | 1032 | | |
| Significance codes: 0 '***' 0.001, '**' 0.01, '*' 0.05, '.' 0.1 and ' ' 1 | | | | | |

The ANOVA plot of interactions between the treatments and the day of sampling on plant pesticide residues is illustrated in the Fig. 4.32 which describes the significant variation of the Active Ingredient (a.i.) or pesticide residues w.r.t. treatments and day of sample collection graphically.

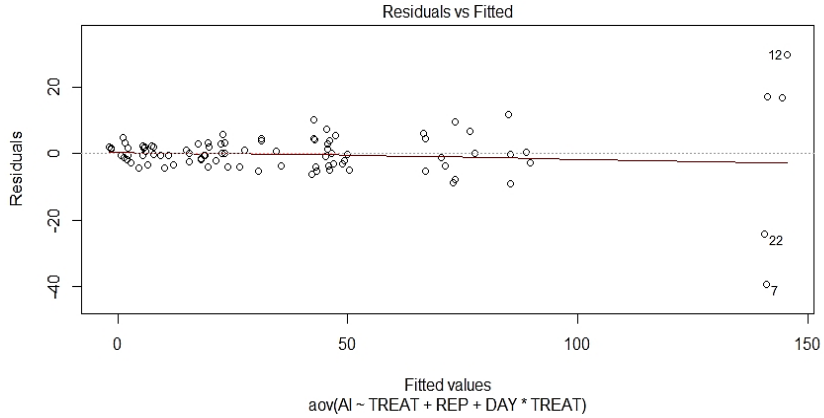


**Fig. 4.32 ANOVA Plot of effect of treatments on pesticide residue**

*4.7.2.2 Comparison of means*

The significant differences observed from ANOVA for effect of treatment on pesticide residues were compared using Tukey-HSD test to identify the significantly different treatments in particular (Table 4.4).

The test revealed that Conventional high volume spraying ($T_1$) and Non-electrostatic reduced dose spraying ($T_5$) were significantly similar. Whereas, all other interactions between Electrostatic standard dose spraying ($T_2$), Non-electrostatic standard dose spraying ($T_3$) and Electrostatic reduced dose spraying ($T_4$) were significantly different. The test results clearly indicated that $T_2$ was significantly different and superior to all other treatments followed by $T_3$ and $T_4$.

**Table 4.5 Tukey-HSD test for effect of treatments on pesticide residue**

| Sl. No. | Treatment | Mean pesticide residue, ng·µL$^{-1}$ |
|---|---|---|
| 1. | Electrostatic spraying* ($T_2$) | 142.63$^a$ |
| 2. | Non-electrostatic spraying* ($T_3$) | 86.86$^b$ |
| 3. | Electrostatic spraying** ($T_4$) | 68.35$^c$ |
| 4. | Conventional spraying*** ($T_1$) | 47.37$^d$ |
| 5. | Non-electrostatic spraying** ($T_5$) | 44.10$^d$ |

*Standard dose (5 ml·L$^{-1}$ @ 150 L·ha$^{-1}$), **Reduced dose (3 ml·L$^{-1}$ @ 150 L·ha$^{-1}$)

***Conventional dose (1.5 ml·L$^{-1}$ @ 500 L·ha$^{-1}$)

### 4.7.3 Effect of spray treatments on deposition efficiency

*4.7.3.1 ANOVA for effect of treatments on deposition efficiency*

The ANOVA (Table 4.5) clearly shown that interactions between the treatments were significantly different and insignificance within the replications validated the experimental data statistically.

**Table 4.6 ANOVA for effect of treatments on deposition efficiency**

| | *df* | SS | MS | F | P |
|---|---|---|---|---|---|
| TREAT | 2 | 91657 | 45829 | 98.95 | 0.000392 *** |
| REP | 2 | 11408 | 5704 | 12.32 | 0.19515 |
| Residuals | 4 | 1852 | 463 | | |

Significance codes: '***' significant at α = 0.001

*4.7.3.2 Comparison of means*

The comparison of factor means (Tukey-HSD test) revealed that interactions between Electrostatic ($T_3$) and Conventional spray application ($T_1$) were significantly different, whereas the developed electrostatic charged spray application (50.62 per cent) clearly superseded the conventional manually operated knapsack sprayer (28.20 per cent) in terms of deposition efficiency. However, the developed prototype without electrostatic spray charging ($T_2$) gave similar performance as compared to the conventional sprayer ($T_1$) significantly.

**Table 4.7 Tukey-HSD test for effect of treatments on deposition efficiency**

| Sl. No. | Treatment | Mean deposition efficiency, per cent |
|---|---|---|
| 1. | Developed prototype – ECS ($T_3$) | $50.62^a$ |
| 2. | Developed prototype – WESC ($T_2$) | $28.19^b$ |
| 3. | Conventional sprayer ($T_1$) | $28.20^b$ |

ECS – Electrostatic charged spray, WESC – Without electrostatic spray charging

Significance level : $\alpha = 0.05$

4.8 COST ESTIMATION

The cost of individual components and overall cost of the developed battery operated electrostatic sprayer are tabulated as shown in the Table 4.7. The major components *viz.* battery and EDF unit together accounted around 50 per cent of the total cost of the developed prototype. The cost of a commercial electrostatic (ESS® MBP90™) spraying system (Rs. 4.5 lakhs) was approximately 40 times higher than that of the developed system (Rs. 12000). The cost reduction was achieved without compromising the performance *viz.* charge induction, deposition efficiency which makes it technologically advanced yet affordable. The developed battery operated electrostatic sprayer fit into the price segment (Rs. 5000 to 50000) of commercially available engine powered knapsack mist blowers like Aspee® Bolo™ (Rs. 8000.00) and Oleamac® AM-162™ (Rs. 45000.00).

The major cost reduction was accountable to the improved mechanism of liquid atomization and air assistance. The developed electrostatic sprayer used the hydraulic nozzle driven by 12 V DC high pressure diaphragm pump for atomization in contrast to the air-blast atomization used in commercial electrostatic sprayers. This not only reduced the overall cost, but also shrunk the size and weight of the prototype making it portable and operator friendly.

**Table 4.8 Cost estimate of developed prototype**

| Sl. No. | Component details | Quantity | Approx. cost, Rs. |
|---|---|---|---|
| 1. | Lead acid storage battery, 12V 9 Ah | 1 | 2300.00 |
| 2. | Lithium-ion rechargeable battery, 3.7 V, 3000 mAh | 4 | 1000.00 |
| 3. | High pressure diaphragm pump, 12 V DC | 1 | 1200.00 |
| 4. | Electric Ducted Fan (EDF), Electronic Speed Controller (ESC) and Servo Consistency Master (SCM) | 1 set | 3000.00 |
| 5. | Line Output Transformer (LOPT) | 1 | 450.00 |
| 6. | Metal Oxide Semiconductor Field Effect Transistor (MOSFET) | 1 | 50.00 |
| 7. | Battery Charge Monitor (BCM) | 1 | 350.00 |
| 8. | PVC Tank, 5 L capacity | 1 | 200.00 |
| 9. | Hydraulic nozzle, brass fittings, pressure gauge, control valve, compression fittings and high pressure flex PVC tubing | 1 set | 1200.00 |
| 10. | CPVC Backpack frame | 1 | 500.00 |
| 11. | Electrical wiring harness and insulation | 1 set | 250.00 |
| 12. | Miscellaneous | | 1500.00 |
| | | **Total** | **12000.00** |

Since the developed prototype was fully battery powered, it could eliminate the emissions and vibrations inherent with the internal combustion engine run sprayers. The prime mover employed for the high speed air blower was brushless

direct current (BLDC) motor, which ensured longer operational life compared not only to IC engines but also to ordinary brush type motors. The requirement for maintenance also was expected to be much less in this case.

### 4.8.1 Operational cost

The cost analysis (Table 4.9 and 4.10) revealed that the developed battery operated electrostatic sprayer had a reduced annual operating cost (Rs. 28302.00) as compared to the commercial gasoline engine powered knapsack mist-blower (Rs. 44677.50). Considering the annual operational hours as 250, the hourly operating costs of the developed electrostatic sprayer and the commercial knapsack mist-blower were Rs. 114.00 and Rs. 178.00, respectively.

**Table 4.9 Parameters of cost analysis**

| Sl. No. | Particulars | Details |
|---|---|---|
| 1. | Useful life | 5 years |
| 2. | Annual operational hours | 250 h |
| 3. | Salvage value | @10% of purchase price (P) |
| 4. | Interest on investment | @12% p.a. |
| 5. | Insurance and shelter | @2% of P p.a. |
| 6. | Repair and Maintenance cost | @5% of P p.a. |
| 7. | Labor wages (per labor per day) | @Rs. 750.00 |

The major factor influencing the operating cost of engine powered mist-blower i.e. fuel and lubrication could be clearly identified from Table 4.10. The gasoline fuel and lubricating oil costs contributed about 35 per cent of the total operating cost. In contrast to the conventional mist-blower, the developed battery operated electrostatic sprayer had the advantage of being electrically powered. Since the liquid delivery, atomization system and high speed air-blower were driven by electric motors and had much higher conversion efficiencies (85 to 90 per cent)

than a gasoline engine (28 to 32 per cent), cost saving in the input energy was obvious. Considering 250 battery recharging cycles per year, the average annual electricity cost estimated was Rs. 352.50 only.

**Table 4.10 Comparison of annual operational costs (Rs. per annum)**

| Sl. No. | Particulars | Developed AESS | Conventional mistblower |
|---|---|---|---|
| 1. | Initial investment | 12000.00 | 15000.00 |
| 2. | Depreciation | 2880.00 | 3600.00 |
| 3. | Interest on investment | 792.00 | 990.00 |
| 4. | Insurance and shelter | 240.00 | 300.00 |
| 5. | Repair and Maintenance | 600.00 | 750.00 |
| 6. | Battery recharging or Fuel and lubricants | 352.50 | Gasoline: 13000.00<br>2T oil: 2600.00 |
| 7. | Labour cost | 23437.50 | 23437.50 |
| **8.** | **Total annual cost (Σ row 2 to 7)** | **28302.00** | **44677.50** |

The developed battery operated electrostatic sprayer could give an overall annual cost saving (Rs. 16376.00) of 36.65 per cent over the engine powered knapsack mist-blower. Moreover, the developed sprayer with reduced pesticide (active ingredient) dose could lessen the annual pesticide expenses by 40 per cent compared to the conventional high volume spraying. The environmental advantage was significant as a large quantity of harmful chemicals could be salvaged from spilling into the soil which eventually reach the ground water and enter into the biological system ultimately harming humans.

# SUMMARY AND CONCLUSIONS

# CHAPTER V

# SUMMARY AND CONCLUSIONS

The introduction of electrical charging of sprays for agricultural application is much advantageous over conventional systems and has been widely accepted as a superior technique for increased application efficiency due to reduced drift, resulting in lesser chemical expenditure. The development of a fully battery operated backpack type electrostatic spraying system will be a milestone in the area of indigenously developed modern plant protection equipment. Hence, the study was contemplated at Department of Farm Machinery and Power Engineering, KCAET, Tavanur, Kerala Agricultural University during 2016 to 2019.

The objectives of the study were, to develop a battery powered backpack type electrostatic induction charging sprayer including investigations on the dynamic charge acquisition, spray chargeability and depositional characteristics of the charged spray on plant targets.

A portable and light weight high voltage (HV) generator with reliable circuitry was developed. The HV generator was based on a variable output power MOSFET driven fly-back transformer and was analysed for the charge induction on spray droplet. A high capacity Electric Ducted Fan (EDF) was used for required air assistance. Experimental prototype of a backpack type rechargeable battery powered electrostatic sprayer with air blower assistance was thus developed. The deposition characteristics and field performance was tested on brinjal crop in the instructional farm of KCAET, Tavanur.

The developed electrostatic sprayer exhibited good levels of charge induction on the liquid spray particles at different levels of electrode potentials (1 kV to 12 kV). The maximum charge to mass ratio (CMR) of electrostatically charged spray was observed to be 1.79 $mC.kg^{-1}$ at a charging electrode potential of 9 kV at 1.4 mL $s^{-1}$ nozzle discharge.

The CMR levels were found to be increasing with the increase in charging electrode potential from 1 kV to 9 kV at constant nozzle discharge of 1.4 mL $s^{-1}$. The CMR level began to decline from 1.79 mC.$kg^{-1}$ to 0.61 mC.$kg^{-1}$, when the electrode potential was further increased from 9 kV to 12 kV, due to the onset of reverse ionization phenomenon.

The EDF unit used for high velocity air assistance was capable of transporting the charged spray droplets towards the distant targets such as orchard trees and longer spray throw for field crops up to a distance of 5 m.

The high pressure atomization system produced the fine droplet spectrum having volume median diameter (VMD) of 91.36 µm, which was an important factor influencing the charge transfer mechanism by electrostatic induction and thereby desired wrap-around effect. The finer droplet spectrum ensured the better coverage and improved biological efficacy. As there were very less moving mechanical components in the diaphragm pump reduction in overall noise and vibrations of the spraying system could offer better operator comfort and reduced system maintenance.

The salient conclusions drawn from the present study are as follows:

- The maximum CMR value (1.79 mC.$kg^{-1}$) was observed at 9 kV charging electrode potential with an air assistance velocity of 10 m $s^{-1}$ and nozzle discharge of 1.4 mL $s^{-1}$.
- The CMR of the charged spray at optimum charging potential (9 kV) increased as 1.15 mC.$kg^{-1}$, 1.54 mC.$kg^{-1}$ and 1.79 mC.$kg^{-1}$ with respect to the air assistance velocity of 5 m $s^{-1}$, 7.5 m $s^{-1}$ and 10 m $s^{-1}$.
- The CMR level began to decline from 1.79 mC $kg^{-1}$to 0.61 mC $kg^{-1}$, when the electrode potential was further increased from 9 kV to 12 kV due to reverse ionization and wetting of charging electrode assembly.
- The charging efficiency of the developed electrostatic induction spray charging system at maximum CMR of 1.79 mC.$kg^{-1}$ observed in terms of percentage of Rayleigh charge limit (15.91 mC.$kg^{-1}$) achieved was found to be 11.25 per cent at the electrode potential of 9 kV.

- The volumetric distribution of the spray droplet spectrum observed was VMD or $DV_{50}$ = 91.36 µm, $DV_{10}$ = 60.21 µm and $DV_{90}$ = 116.21 µm.
- The number median diameter was (NMD) found to be 66.65 µm, which was when related to the VMD, resulted in the uniformity coefficient (UC) of 0.7299 and the relative span (RS) of the spray spectrum of 0.6129.
- The droplet size range from 51-80 µm covered the $2/3^{rd}$ portion of the frequency distribution, whilst the range of droplet size 81-120 µm contributed only $1/3^{rd}$ to the total distribution.
- The spray deposit distribution of electrostatic spray was accounted in terms of percentage of total spray volume applied as 50.62 per cent on-target, 10.09 per cent on ground and 39.27 per cent in the form drift compared to the conventional knapsack sprayer with corresponding percentage distribution as 28.20, 34.81 and 36.97 per cent respectively
- There was approximately three-fold increment in overall canopy deposition with electrostatically charged spray particles (350 deposits $cm^{-2}$) as compared to conventional spraying method (100 deposits $cm^{-2}$).
- The abaxial leaf surface deposition in case of charged spray was found to be decremented from upper (300 - 350 deposits $cm^{-2}$), middle (200 - 250 deposits $cm^{-2}$) to lower canopy (50 - 100 deposits $cm^{-2}$) leaves respectively.
- The electrostatic spray charging improved the on-target deposition by 1.8 times that of conventional spraying. However, the developed spraying system without electrostatic charge resulted in the excess ground (15.41 per cent) and drift (63.97 per cent) losses.
- The average total leaf area per plant and corresponding plant canopy area measured using EasyLeaf image analysis software were found to be 6425.45 $cm^2$ and 3894.21 $cm^2$, respectively leading to the average leaf area index (LAI) of 1.65 for brinjal crop.

- The water requirement for spraying per unit area was reduced to 1/3$^{rd}$ using electrostatic spraying (150 L ha$^{-1}$) compared to conventional methods of agricultural spraying (500 L ha$^{-1}$).
- The electrostatic spraying technique increased the deposition of active ingredient (147.63 ng.µL$^{-1}$) by three fold compared to the conventional sprayer (47.37 ng.µL$^{-1}$) with the same dose of active ingredient per hectare.
- The biological efficacy of electrostatic spraying was superior over the conventional spraying with the standard dose of active ingredient (54.62 per cent higher).
- Even with the reduced dose of active ingredient, the charged spray application resulted into a bio-efficacy of 32 per cent higher to that of conventional spraying.

The cost effectiveness of the developed system was estimated in terms of annual operating cost and compared with the engine powered knapsack mist-blower commercially available as summarized below,

- The cost of developed system was much lesser than that of the commercially available electrostatic spraying systems without compromising the performance viz. charge induction, deposition efficiency and in environment friendly application.
- The cost of a commercial electrostatic (ESS® MBP90™) spraying system (Rs. 4.5 lakhs) was approximately 40 times higher than that of the developed system (Rs. 12000).
- The cost reduction was achieved without compromising the performance *viz.* charge induction, deposition efficiency which makes it technologically advanced yet affordable.
- The developed prototype being fully battery powered could eliminate the emissions and vibrations inherent with the internal combustion engine run sprayers.

- The prime mover employed for the high speed air blower was brushless direct current (BLDC) motor, which ensured longer operational life with lesser maintenance compared not only to IC engines but also to ordinary brush type motors.
- The cost analysis revealed that the developed battery operated electrostatic sprayer had a reduced annual operating cost (Rs. 28302.00) as compared to the commercial gasoline engine powered knapsack mist-blower (Rs. 44677.50).
- Considering the annual operational hours as 250, the hourly operating costs of the developed electrostatic sprayer and the commercial knapsack mist-blower were Rs. 114.00 and Rs. 178.00, respectively.
- The developed battery operated electrostatic sprayer could give an overall annual cost saving (Rs. 16376.00) of 36.65 per cent over the engine powered knapsack mist-blower.
- Moreover, the developed sprayer with reduced pesticide (active ingredient) dose could lessen the annual pesticide expenses by 40 per cent compared to the conventional high volume spraying.
- The environmental advantage was significant as a large quantity of harmful chemicals could be salvaged from spilling into the soil which eventually reach the ground water and enter into the biological system ultimately harming humans.

# DEVELOPMENT OF A BATTERY OPERATED ELECTROSTATIC SPRAYER

**by**

**DIPAK S. KHATAWKAR**

**(2016-28-002)**

## ABSTRACT

**Submitted in partial fulfilment of the requirement for the degree of**

**DOCTOR OF PHILOSOPHY**
**IN**
**AGRICULTURAL ENGINEERING**

**(Farm Power and Machinery)**

**Faculty of Agricultural Engineering and Technology**
**Kerala Agricultural University**

**DEPARTMENT OF FARM MACHINERY AND POWER ENGINEERING**

**KELAPPAJI COLLEGE OF AGRICULTURAL ENGINEERING AND TECHNOLOGY, TAVANUR – 679 573**

**KERALA, INDIA**

**2019**

# ABSTRACT

An experimental prototype of backpack type rechargeable battery powered air assisted electrostatic sprayer was developed, maintaining the commercial competence and affordability of the marginal and small farmer community in India. The developed prototype was analyzed for charge induction on spray droplet, deposition characteristics and field performance on brinjal crop at instructional farm of KCAET, Tavanur.

The developed prototype electrostatic sprayer established good levels of charge induction on the spray particles at different stages of electrode potentials (1 kV to 12 kV). The maximum Charge to Mass Ratio (CMR) of electrostatically charged spray was observed to be 1.79 mC $kg^{-1}$ at a charging electrode potential of 9 kV at 2 ml $s^{-1}$ nozzle discharge. The Electric Ducted Fan (EDF) for high velocity air assistance was capable of carrying the charged spray droplets towards the distant targets such as orchard trees and longer (up to 5 m) spray throw for field crops. The high pressure atomization system produced the fine droplet spectrum having Volume Median Diameter (VMD) of 91.36 µm which aided better charge induction and the resultant wrap-around effect. The field study revealed that the electrostatic charged spray enhanced the on-target deposition nearly about two folds than the conventional spray. Also, the biological efficacy was observed to be 54.62 per cent superior to the conventional spraying method. As there were very less moving mechanical components, reduction in overall noise and vibrations of the spraying system could offer better operator comfort and reduced system maintenance.

The cost of a commercial electrostatic (ESS® MBP90™) spraying system (Rs. 4.5 lakhs) was approximately 40 times higher than that of the developed system (Rs. 12000). The annual operating cost of the developed battery operated electrostatic sprayer was much lesser (Rs. 28302.00) than that of commercial gasoline engine powered knapsack mist-blower (Rs. 44677.50). Considering the annual operational hours as 250, the hourly operating costs of the developed electrostatic sprayer and the commercial knapsack mist-blower were Rs. 114.00

and Rs. 178.00, respectively. The developed battery operated electrostatic sprayer could give an overall annual cost saving (Rs. 16376.00) of 36.65 per cent over the engine powered knapsack mist-blower. Moreover, the developed sprayer with reduced pesticide (active ingredient) dose could lessen the annual pesticide expenses by 40 per cent compared to the conventional high volume spraying. The environmental advantage was significant as a large quantity of harmful chemicals could be salvaged from spilling into the soil which eventually reach the ground water and enter into the biological system ultimately harming humans. The overall features and cost effectiveness of the developed prototype could encourage majority of the Indian famers to upgrade with the air assisted electrostatic spraying technology leading to their socio-economic welfare.

# APPENDICES

# APPENDIX – I

**Results of Tukey-HSD test for effect of charging electrode potential on CMR**

| Compar. | Diff. | Lower mean | Upper mean | P value |
|---|---|---|---|---|
| V10-V1 | 9.681125e-01 | 0.691601390 | 1.24506528 | 0.0000000 |
| V11-V1 | 8.246688e-01 | 0.547934723 | 1.10139861 | 0.0000000 |
| V12-V1 | 1.441021e-01 | -0.132351211 | 0.42032542 | 0.7510000* |
| V2-V1 | 1.433698e-01 | -0.133675442 | 0.41912641 | 0.7590000* |
| V3-V1 | 2.511245e-01 | -0.025836133 | 0.52736589 | 0.0990000* |
| V4-V1 | 6.108569e-01 | 0.333652133 | 0.88732501 | 0.0000031 |
| V5-V1 | 8.247458e-01 | 0.547623155 | 1.10803141 | 0.0000000 |
| V6-V1 | 1.045264e+00 | 0.763478952 | 1.31703214 | 0.0000000 |
| V7-V1 | 1.112365e+00 | 0.834433215 | 1.38845016 | 0.0000000 |
| V8-V1 | 1.140012e+00 | 0.870431653 | 1.42390154 | 0.0000000 |
| V9-V1 | 1.263210e+00 | 0.990413562 | 1.54380115 | 0.0000000 |
| V11-V10 | -1.438569e-01 | -0.421336555 | 0.13340255 | 0.7540000* |
| V12-V10 | -8.242012e-01 | -1.101462323 | -0.54714528 | 0.0000000 |
| V2-V10 | -8.250213e-01 | -1.102123262 | -0.54898756 | 0.0000000 |
| V3-V10 | -7.176548e-01 | -0.994336591 | -0.44002010 | 0.0000002 |
| V4-V10 | -3.588562e-01 | -0.634121252 | -0.08112032 | 0.0040000 |
| V5-V10 | -1.433765e-01 | -0.420123234 | 0.13315487 | 0.7540000* |
| V6-V10 | 7.209863e-02 | -0.204114489 | 0.34899523 | 0.9970000* |
| V7-V10 | 1.433213e-01 | -0.133995886 | 0.41900325 | 0.7590000* |
| V8-V10 | 1.780018e-01 | -0.098558463 | 0.45544015 | 0.4740000* |
| V9-V10 | 2.980006e-01 | 0.021112542 | 0.57566230 | 0.0270000 |
| V12-V11 | -6.803386e-01 | -0.957265451 | -0.40311470 | 0.0000005 |
| V2-V11 | -6.810125e-01 | -0.958332669 | -0.40455026 | 0.0000005 |
| V3-V11 | -5.731489e-01 | -0.850787858 | -0.29633025 | 0.0000084 |
| V4-V11 | -2.149087e-01 | -0.491336545 | 0.06211450 | 0.2380000* |

| | | | | |
|---|---|---|---|---|
| V5-V11 | 2.223654e-16 | -0.276126543 | 0.27600145 | 1.0000000* |
| V6-V11 | 2.151256e-01 | -0.061325413 | 0.49299087 | 0.2314705* |
| V7-V11 | 2.861489e-01 | 0.009442545 | 0.56333026 | 0.0379528 |
| V8-V11 | 3.228563e-01 | 0.045998591 | 0.59966213 | 0.0136078 |
| V9-V11 | 4.420036e-01 | 0.165332653 | 0.71911997 | 0.0003720 |
| V2-V12 | -1.005858e-03 | -0.277778423 | 0.27530154 | 1.0000000* |
| V3-V12 | 1.071254e-01 | -0.169468796 | 0.38365214 | 0.9499659* |
| V4-V12 | 4.667614e-01 | 0.189626256 | 0.74336987 | 0.0001822 |
| V5-V12 | 6.803654e-01 | 0.403254666 | 0.95414789 | 0.0000005 |
| V6-V12 | 8.961239e-01 | 0.619154248 | 1.17365248 | 0.0000000 |
| V7-V12 | 9.676065e-01 | 0.690998587 | 1.24456325 | 0.0000000 |
| V8-V12 | 1.001790e+00 | 0.726125459 | 1.27998568 | 0.0000000 |
| V9-V12 | 1.126352e+00 | 0.846587855 | 1.39958741 | 0.0000000 |
| V3-V2 | 1.085124e-01 | -0.168125485 | 0.38423652 | 0.9468935* |
| V4-V2 | 4.670140e-01 | 0.190125472 | 0.74420310 | 0.0001768 |
| V5-V2 | 6.816667e-01 | 0.404934723 | 0.95839861 | 0.0000005 |
| V6-V2 | 8.973333e-01 | 0.620601390 | 1.17406528 | 0.0000000 |
| V7-V2 | 9.683333e-01 | 0.691601390 | 1.24506528 | 0.0000000 |
| V8-V2 | 1.004000e+00 | 0.727268056 | 1.28073194 | 0.0000000 |
| V9-V2 | 1.124000e+00 | 0.847268056 | 1.40073194 | 0.0000000 |
| V4-V3 | 3.593333e-01 | 0.082601390 | 0.63606528 | 0.0045257 |
| V5-V3 | 5.736667e-01 | 0.296934723 | 0.85039861 | 0.0000084 |
| V6-V3 | 7.893333e-01 | 0.512601390 | 1.06606528 | 0.0000000 |
| V7-V3 | 8.603333e-01 | 0.583601390 | 1.13706528 | 0.0000000 |
| V8-V3 | 8.960000e-01 | 0.619268056 | 1.17273194 | 0.0000000 |
| V9-V3 | 1.016000e+00 | 0.739268056 | 1.29273194 | 0.0000000 |
| V5-V4 | 2.143333e-01 | -.062398610 | 0.49106528 | 0.2383466* |
| V6-V4 | 4.300000e-01 | 0.153268056 | 0.70673194 | 0.0005382 |
| V7-V4 | 5.010000e-01 | 0.224268056 | 0.77773194 | 0.0000659 |

| | | | | |
|---|---|---|---|---|
| V8-V4 | 5.366667e-01 | 0.259934723 | 0.81339861 | 0.0000237 |
| V9-V4 | 6.566667e-01 | 0.379934723 | 0.93339861 | 0.0000009 |
| V6-V5 | 2.156667e-01 | -.061065277 | 0.49239861 | 0.2314705* |
| V7-V5 | 2.866667e-01 | 0.009934723 | 0.56339861 | 0.0379528 |
| V8-V5 | 3.223333e-01 | 0.045601390 | 0.59906528 | 0.0136078 |
| V9-V5 | 4.423333e-01 | 0.165601390 | 0.71906528 | 0.0003720 |
| V7-V6 | 7.100000e-02 | -0.205731944 | 0.34773194 | 0.9977954* |
| V8-V6 | 1.066667e-01 | -0.170065277 | 0.38339861 | 0.9509623* |
| V9-V6 | 2.266667e-01 | -0.050065277 | 0.50339861 | 0.1803256* |
| V8-V7 | 3.566667e-02 | -0.241065277 | 0.31239861 | 0.9999971* |
| V9-V7 | 1.556667e-01 | -0.121065277 | 0.43239861 | 0.6610082* |
| V9-V8 | 1.200000e-01 | -0.156731944 | 0.39673194 | 0.8998773* |

'*' Significant at $\alpha = 0.05$

# APPENDIX – II

**Results of Tukey-HSD test for effect of treatments on pesticide residue**

| Compar. | Diff. | Lower mean | Upper mean | P value |
|---|---|---|---|---|
| T2-T1 | 51.729806 | 44.563888 | 58.895725 | 0.0000000* |
| T3-T1 | 23.041436 | 15.875518 | 30.207354 | 0.0000000* |
| T4-T1 | 9.975540 | 2.809622 | 17.141458 | 0.0019409* |
| T5-T1 | -1.430819 | -8.596737 | 5.735099 | 0.9806195 |
| T3-T2 | -28.688370 | -35.854289 | -21.522452 | 0.0000000* |
| T4-T2 - | -41.754266 | -48.920185 | 34.588348 | 0.0000000* |
| T5-T2 | -53.160625 | -60.326544 | -45.994707 | 0.0000000* |
| T4-T3 | -13.065896 | -20.231814 | -5.899978 | 0.0000240* |
| T5-T3 | -24.472255 | -31.638173 | -17.306337 | 0.0000000* |
| T5-T4 | -11.406359 | -18.572277 | -4.240441 | 0.0002764* |

'*' Significant at $\alpha = 0.05$

# APPENDIX – III

**Results of Tukey-HSD test for effect of treatments on deposition efficiency**

| Compar. | Diff. | Lower mean | Upper mean | P |
|---|---|---|---|---|
| T2-T1 | 199.5333 | 136.90951 | 262.15715 | 0.0007640* |
| T3-T1 | 226.1333 | 163.50951 | 288.75715 | 0.0004695* |
| T3-T2 | 26.6000 - | 36.02382 | 89.22382 | 0.3768321 |

'*' Significant at $\alpha = 0.05$

# REFERENCES

# REFERENCES


Abbott, W. S. 1925. A method of computing effectiveness of an insecticide. *J. American Mosquito Control Asso*. 3(2), pp. 265-267.

Alamuhanna, E. A. and Maghirang, R. G. 2010. Measuring the electrostatic charge of airborne particles. *J. Fd., Agric. & Environ*., 8(3), pp. 1033-1036.

Almekinders, H., Ozkan, H. E., Reichard, D. L., Carpenter, T. G. and Brazee, R. D. 1992. Spray deposition patterns of an electrostatic atomizer. *Trans. ASAE*, 36(6), pp. 1361-1367.

Anantheswaran, R. C. and Law, S. E. 1979. Electrostatic spraying of turf grass. VSGA, *Green Section Project Rec*., pp. 1-4.

Anonymous. 2019. All India Report on Number and Area of Operational Holdings. *Agri. Census: 2015-16 (Phase-I)*, Agriculture Census Division, Dept. of Agri., Co-op. and Farmers Welfare, Ministry of Agri. and Farmers Welfare, Govt. of India, 88p.

Antuniassi, U. R., Velini, E. D., Oliviera, R. B., Maria, A. P. and Figueiredo, Z. N. 2011. Systems of aerial spraying for soybean rust control. *Eng. Agric.*, Jaboticabal, 31(4), pp. 695-703.

Arnold, A. J., Cayley, G. R., Dunne, Y., Etheridge, P., Griffiths, D. C., Phillips, F. T., Pye, B. J., Scott, G. C. and Vojvodic, P. R. 1984. Biological effectiveness of electrostatically charged rotary atomisers. *Ann. Appl. Biol.*, Vol. 105, pp. 353-359.

Balachand, C. H. 2014. Investigations on spray drift characteristics of motorized knapsack mist blower. M. Tech. (Agril. Eng.) thesis, Tamil Nadu Agri. University, Coimbatore, 170p.

Barbosa, R. N., Griffin, J. L. and Hollier, C. A. 2009. Effect of spray rate and method of application in spray deposition. *Appl. Eng. in Agric*., ASABE, 25(2), pp. 181-184.

Bayat, A., Zeren, Y. and Rifat, M. V. 1994. Spray deposition with conventional and electrostatically charged spraying in citrus trees. *Agric. Mech. Asia, Afr. and Latin Am.*, 25(4), pp. 35-39.

Bode, L. E. and Bowen, H. D. 1991. Spray distribution and charge-mass ratio of electrostatically charged agricultural sprays. *Trans. ASAE*, 34(5), pp. 1928-1934.

Bouse, L. F., 1994. Effect of nozzle type and operation on spray droplet size. *Trans. ASAE*, pp. 1389-1400.

Carlton, J. B. and Bouse, L. F. 1980. Electrostatic spinner-nozzle for charging. *Trans. ASAE*, 37(5), pp. 1369-1374.

Carlton, J. B., Bouse, L. F. and Kirk, I. W. 1995. Electrostatic charging of aerial spray over cotton. *Trans. ASAE*, 38(6), pp. 1641-1645.

Celen, H. I., Durgut, M. R., Gurkan, G. A. and Erdal, K. 2009. Effect of air assistance on deposition distribution of spraying by tunnel type sprayer. *Afr. J. Agric. Res*., 4(12), pp. 1392-1397.

Changqi, Y. 2018. An isolated high-voltage high-frequency pulsed power converter for plasma generation. M. Sc. (Electr. Eng.) thesis, University of Michigan-Dearborn, 52p.

Chaudhari, M., Dalvi, S., Sawant, V. and Pinjari, N. 2017. Design and simulation of high voltage dc source by using cockroft walton voltage multiplier. *Int. J. Adv. Res. Electrical, Electronics and Instru. Eng*., 6(3), pp. 1301-1304.

Choi, J. H., Byong, J. H., Park, J. S. and Kim, J. H. 2016. Development of high voltage module for an electrostatic painting robot system. *Int. J. Syst. Appl., Eng. and Dev*., Vol. 10, pp. 315-319.

Copple, E. J., 1999. High efficiency dc step-up voltage converter. United States Patent No. 5929614.
Available:https://patentimages.storage.googleapis.com/a3/4a/06/24acc7cf74c66c/US5929614.pdf [9 June 2019].

Derksen, R. C. and Bode, L. E. 1986. Droplet size comparison from rotary atomizers. *Trans. ASAE*, 29(5), pp. 1204-1207.

Dwivedi, C. K. and Daigavane, M. B. 2011. Multi-purpose low cost DC high voltage generator (60 kV output), using Cockroft-walton voltage multiplier circuit. *Int. J. Sci. & Technol. Edu. Res.*, 2(7), pp. 109-119.

Esehaghbeygi, A., Tadayyon, A. and Besharati, S. 2010. Comparison of electrostatic and spinning-discs spray nozzles on wheat weeds control. *J. Am. Sci.*, 6(12), pp. 529-533.

Fritz, B. K., Parker, C., Lopez, J. D., Hoffmann, W. C. and Schleider, P. 2009. Deposition and Droplet sizing characterization of a laboratory spray table. *Appl. Eng. in Agric*., ASABE, 25(2), pp. 175-180.

Gupta, C. P., Alamban, R. B. and Dante, E. T. 1994. Development of knapsack electrostatic spinning disc sprayer for herbicide application in rice. *Agric. Mech. Asia, Afr. and Latin Am*., 25(4), pp. 31-37.

Gupta, C. P., Singh, G., Muhamein, M. and Dante, E. T., 1992. Development of a hand-held electrostatic spinning-disc sprayer. *Trans. ASAE*, 35(6), pp. 1753-1758.

Gupta, C. P., Singh, G., Parameshwarkumar, M. and Ganapathy, S. 1989. Farmer driven electrostatic low-volume sprayer. Innovative Scient. Res. U.S.-Israel CDR program, AIT, Bangkok, pp. 1-21.

Howard, M. 1989. Power supply having combined forward converter and flyback action for high efficiency conversion from low to high voltage. United States Patent No. 4890210. Available:https://patentimages.storage.googleapis.com/ff/41/9a/4c769dd886383d/US4890210.pdf. [9 June 2019].

Jaworek, A., Sobczyk, A. J., Krupa, A., Lackowski, M. and Czech, T. 2009. Electrostatic deposition of nano-thin films on metal substrate. *Bull. Polish Sci.*, 57(1), pp. 63-70.

Johannama, M. R., Watkins, A. P. and Yule, A. J. 1999. Examination of electrostatically charged spray for agricultural spraying applications. *ILASS-Europe'99*, pp. 1-6.

John, K., Giles, D. K. and Parrella, M. P. 1995. Electrostatic sprayers improve pesticide efficacy in greenhouse. *California Agric*., 49(4), pp. 31-35.

Khadir, A. I., Carpenter, T. G. and Reichard, D. L. 1994. Effects of air jets on deposition of charged spray in plant canopies. *Trans. ASAE*, 37(5), pp. 1423-1429.

Kihm, K. D., Kim, B. H. and McFarland, A. R. 1991. Atomization, charge and deposition characteristics of bipolarly charged aircraft sprays. *Atomization and Sprays*, Vol. 2, pp. 463-481.

Kirk, I. W., Hoffmann, W. C. and Carlton, J. B. 2001. Aerial electrostatic spray system performance. *Trans. ASAE*., 44(5), pp. 1089-1092.

Krause, C. R. and Derksen, R. C. 1991. Comparison of electrostatic and cold-fog sprayers using cold-field emission scanning electron microscopy and energy dispersive X-ray microanalysis. *USDA Agric. Res. Serv*., Madison-Wooster, USA, pp. 1-7.

Kuriyama, H., Kaneko, K., Kameyama, S., Tanahashi, R. and Yamamoto, A. 1997. Dc-dc high voltage converter using flyback voltage. United States Patent No. 5621623. Available:https://patentimages.storage.googleapis.com/96/7b/d2/38755b5b789c56/US5621623.pdf [9 June 2019].

Lake, J. R. and Merchant, J. A. 1984. Wind tunnel experiments and mathematical model of electrostatic spray deposition in Barley. *J. Agric. Eng. Res*., Vol. 30, pp. 185-195.

Lane, M. D. and Law, S. E. 1982. Transient charge transfer in living plants undergoing electrostatic spraying. *Trans. ASAE*, pp. 1148-1159.

Laryea, G. N. and No, S. Y. 2002. Spray characteristics of charge injected electrostatic pressure-swirl nozzle. *ILASS-Zaragoza*, Europe, 9(11), pp. 1-6.

Latheef, M., Kirk, I. W., Carlton, J. B. and Hoffmann, W. C. 2008. Aerial electrostatic charged sprays for deposition and efficacy against sweet potato whitefly (Bemisiatabaci) on cotton. *Pest Mgmt. Sci*., Wiley Interscience. 65: 744-752., Vol. 65, pp. 744-752.

Law, S. E. 1975. Electrostatic induction instrument for tracking and charge measurement of airborne agricultural particulates. *Trans. ASAE*, pp. 40-47.

Law, S. E. and Cooper, S. C. 1988. Depositional characteristics of charged and uncharged droplets applied by an orchard air carrier sprayer. *Trans. ASAE*, 31(4), pp. 984-989.

Law, S. E. and Michael, D. L. 1981. Electrostatic deposition of pesticide spray onto foliar targets of varying morphology. *Trans. ASAE*, pp. 1441-1445.

Law, S. E. and Scherm, H. 2005. Electrostatic application of a plant disease biocontrol agent for prevention of fungal infection through the stigmatic surfaces of blueberry flowers. *J. Electrostatics*, 63(5), pp. 399-408.

Luciana, N. and Cramariuc, R. 2009. Contribution about the electrohydrodynamic spraying. *U.P.B. Sci. Bull., Ser.-C*, 71(3), pp. 205-213.

Mamidi, V., Ghanashyam, C., Patel, M. K., Reddy, V. and Kapur, P. 2012. Electrostatic hand presuure swirl nozzle for small crop growers. *Int. J. Appl. Sci. & Tech., Res. Excellence*, 2(2), pp. 164-168.

Maynagh, B., Ghobadian, B., Johannama, M. and Hashjin, T. 2009. Effect of electrostatic induction parameters on droplet charging for agricultural application. *J. Agric. Sci. & Tech.*, 11(1), pp. 249-257.

Mishra, P. K., Singh, M., Sharma, A., Sharma, K. and Singh, B. 2014. Studies on effect of electrostatic spraying in orchards. *Agric. Eng. Int., J. CIGR*, 16(3), pp. 60-69.

Oerke, C. N., 2006. Crop losses to pests. *J. Agric. Sci.* Cambridge University Press, 144(1), pp. 31-43.

Patel, B. M., Devmurari, S. H. and Rathod, M. P. 2014. Development of high voltage solid state marx generator for liquid applications. *Int. J. Eng. Res. & Tech.*, 3(12), pp. 755-758.

Patel, M. K., Sahoo, H. K., Nayak, M. K., Kumar, A., Ghanashyam, C. and Amod, K. 2015. Electrostatic nozzle: new trends in agricultural pesticide spraying. *Int. J. Electr. & Electronics Eng*., pp. 6-11.

Petersen, A. 1989. High power flyback, variable input-output voltage, decoupled power supply. United States Patent No. 4814965. Available: https://patentimages.storage.googleapis.com/89/55/64/69ea52e2c933b9/US4814965.pdf [9 June 2019].

Robson, S., Mauri, M. T., Fernandes, H. C., Monteiro, P. M., Rodrigues, M. and Cleyton, B. A. 2013. Parameters of electrostatic spraying and its influence on the application efficiency. *Rev. Ceres*, Vicosa-Brazil, 60(4), pp. 474-479.

Santelmann, W. F. 1986. Method of and apparatus for efficient high voltage generation by resonant flyback. United States Patent No. 4616300. Available:https://patentimages.storage.googleapis.com/d8/cf/61/e0b6cea099034d/US4616300.pdf [9 June 2019].

Sharma, C., Jhala, A. K. and Prajapati, M. 2015. Low cost high voltage generation: a technique. *Int. J. Sci., Eng. & Tech. Res.*, 4(12), pp. 4026-4030.

Sidahamed, M. M. 1996a. Theory of predicting the size and velocity of droplets from pressure nozzles. *Trans. ASAE*, 35(5), pp. 385-391.

Sidahmed, M. M. 1996b. Theory of predicting the size and velocity of droplets from pressure nozzles. *Trans. ASAE*, 35(5), pp. 1651-1655.

Smith, D. B., Goering, C. E., Liljeldahl, L. A. and Reichard, D. L. 1977. AC charging of Agricultural sprays. *Trans. ASAE*, 34(6), pp. 1002-1007.

State wise chemical pesticide consumption. 2019. Statistical database, Directorate of Plant Protection, Quarantine and Storage (DPPQS), Ministry of Agri. and Farmers Welfare, Govt. of India. Available: http://ppqs.gov.in/statistical-database?page=1

Sumner, H. R., Herzog, G. A., Sumner, P. E., Bader, M. and Mullinix, B. G. 2000. Chemical application equipment for improved deposition in cotton. *J. Cott.Sci.*, Vol. 4, pp. 19-27.

Sundaraaj, R., Amuthavalli, T. and Vimala, D. 2018. Invasion and establishment of the solanum whitefly *Aleurothrixus trachoides* (Back) (Hemiptera: Aleyrodidae) in South India, *Current Science*, 115(1), pp. 29-31.

Sushil, S. N. (2016). Emerging issues of plant protection in India. *Int. Conf. on Natural Res. Management: Ecol. Perspectives*, SKUAST, Jammu.

Tong-Xian, L., Philip, A. S. and Conner, J. M. 2004. Evaluation of spray deposition on plant foliage with self-adhesive paper targets. *Subtropical Plant Sci*., Vol. 36, pp. 39-43.

Walker, T. J., Dennis, R. G. and Gary, W. H. 1989. Field testing of several pesticide spray atomizers. *Trans. ASAE*, 5(3), pp. 319-323.

Waluyo, S., Nugraha, S. and Permana, Y. 2015. Miniature prototype design and implementation of modified multiplier circuit DC high voltage generator. *Int. J. Electr. Eng. & Tech*., 6(1), pp. 1-12.

Wang, L., Zhang, N., Slocombe, J. W., Thierstein, G. E. and Kuhlman, D. K. 1995. Experimental analysis of spray distribution pattern uniformity for agricultural nozzles. *Appl. Eng. in Agric*., 25(2), pp. 50-55.

Yu, R., Zhou, H. and Zheng, J. 2011. Design and experiments on droplet charging device for high range electrostatic sprayer. *Pesticides in Modern Wld. - Pesticide Use & Mgmt.*, pp. 137-148.